

(e,e'p) and Nuclear Structure

Paul Ulmer

Old Dominion University

Hampton University Graduate Studies 2003

Thanks to:

W. Boeglin

T.W. Donnelly (Nuclear physics course at MIT)

J. Gilfoyle

R. Gilman

R. Niyazov

J. Kelly (Adv. Nucl. Phys. 23, 75 (1996))

B. Reitz

A. Saha

S. Strauch

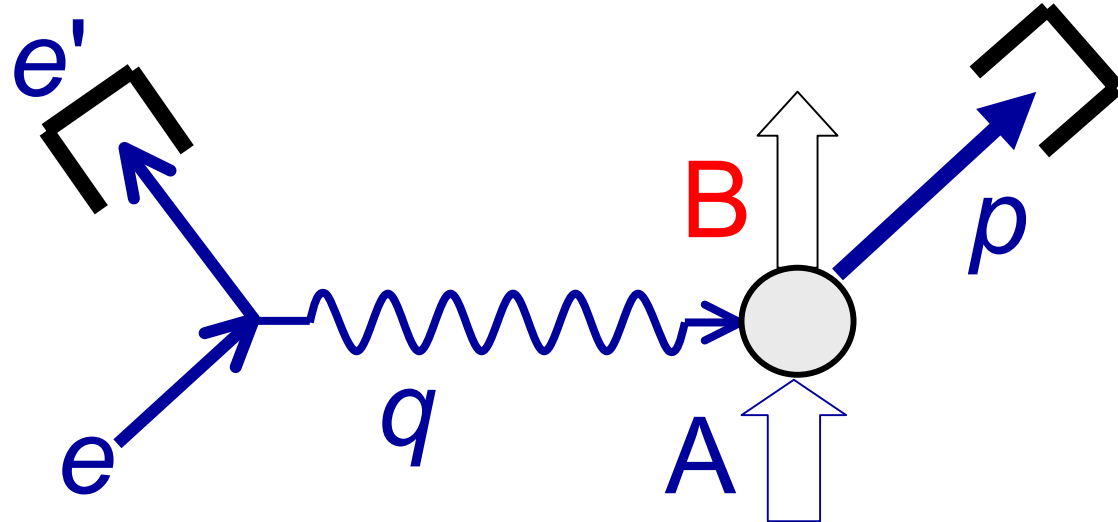
E. Voutier

L. Weinstein

Outline

- Introduction
- Background
 - Experimental
 - Theoretical
- Nuclear Structure
- Medium-modified nucleons
 - Cross sections
 - Polarization transfer
- Studies of the reaction mechanism
- Few-body nuclei
 - The deuteron
 - $^{3,4}\text{He}$

A(e,e'p)B

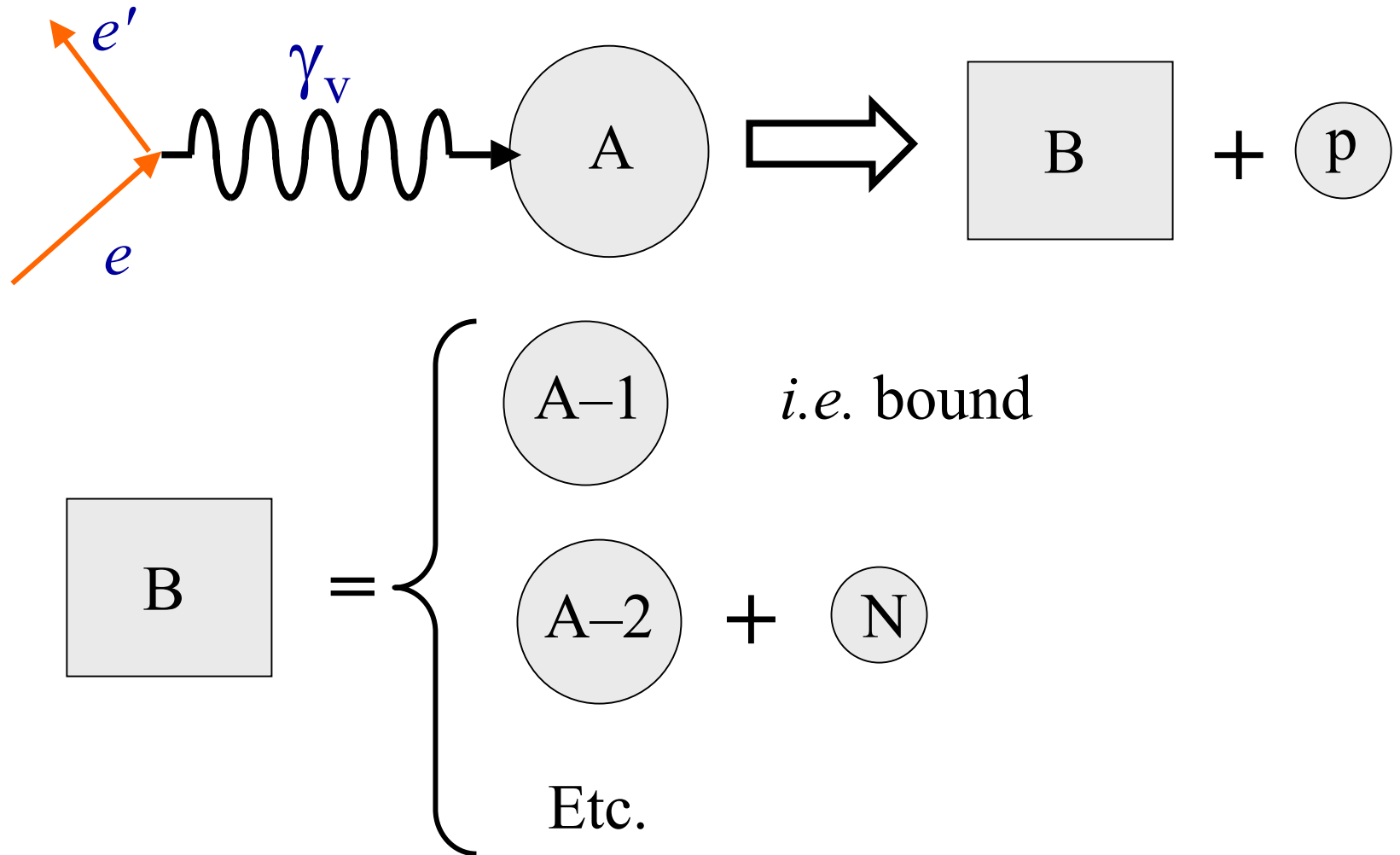


Known: e and A

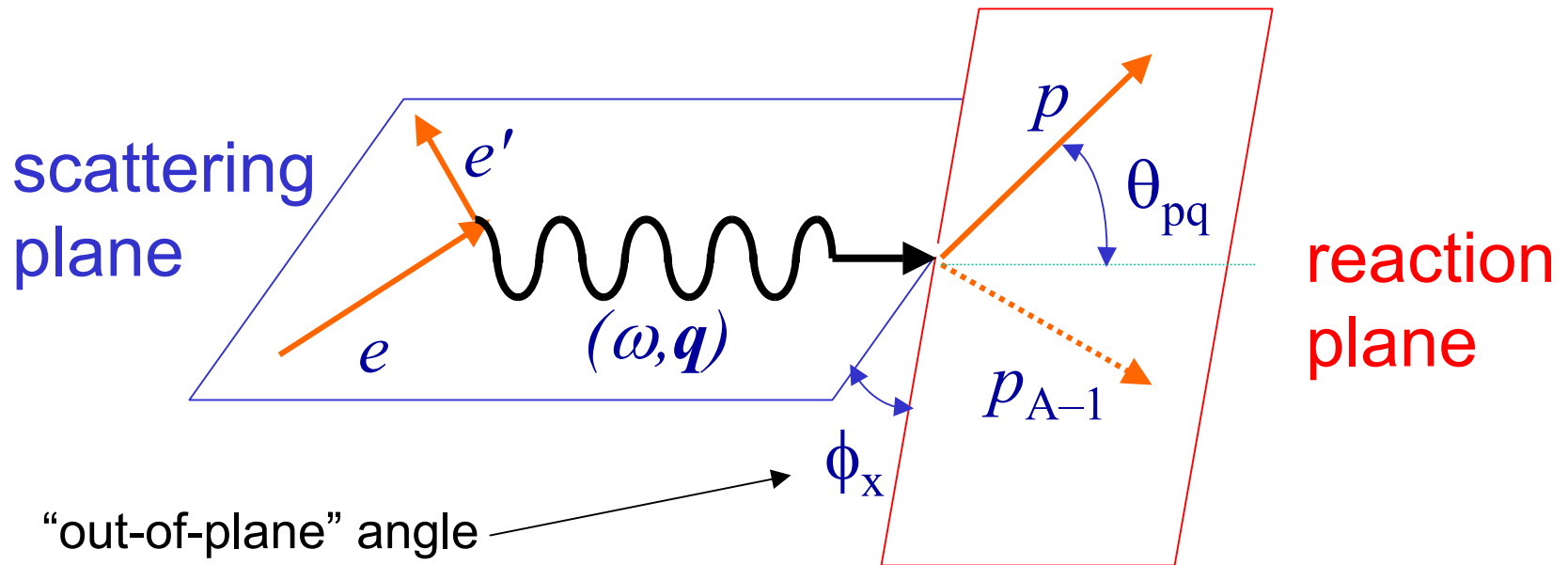
Detect: e' and p

Infer: $p_m = q - p = p_B$

(e,e'p) - Schematically



Kinematics



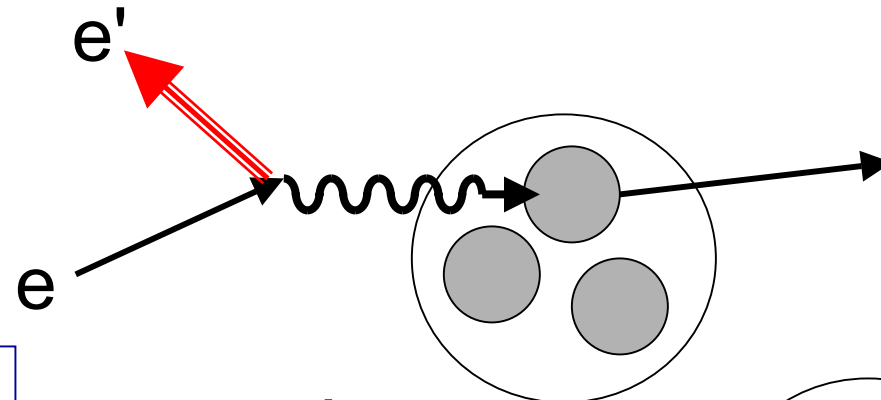
In ERL_e: $Q^2 \equiv -q_\mu q^\mu = \mathbf{q}^2 - \omega^2 = 4ee' \sin^2\theta/2$

Missing momentum: $\mathbf{p}_m = \mathbf{q} - \mathbf{p} = \mathbf{p}_{A-1}$

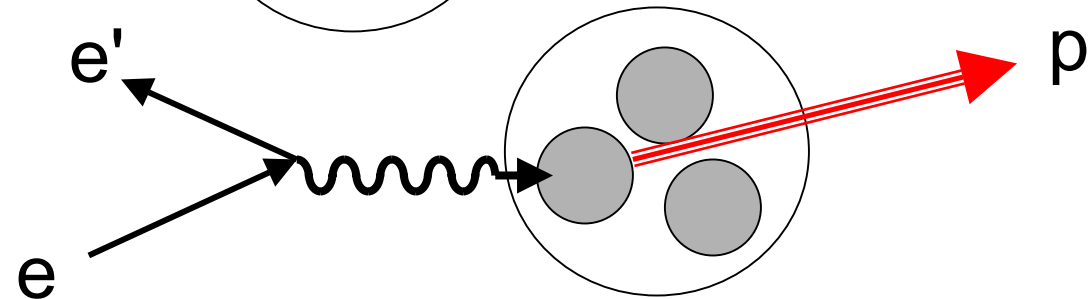
Missing mass: $\varepsilon_m = \omega - T_p - T_{A-1}$

Some (Very Few)
Experimental Details ...

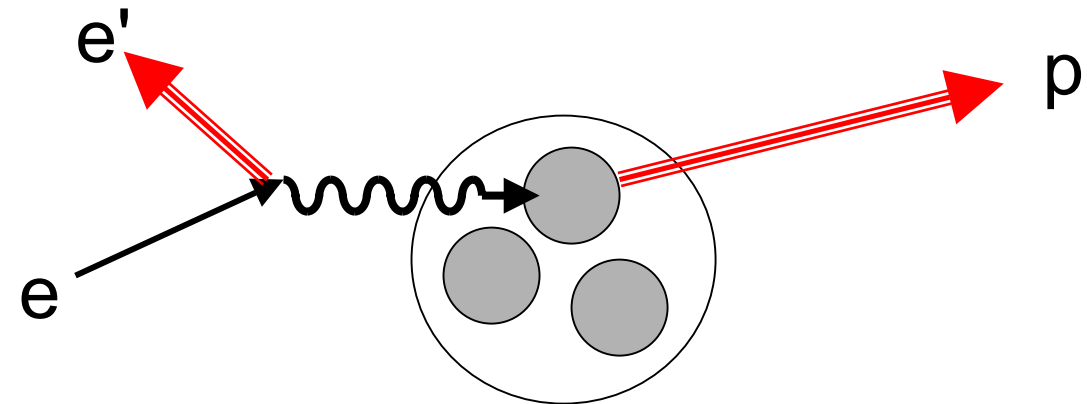

Detected

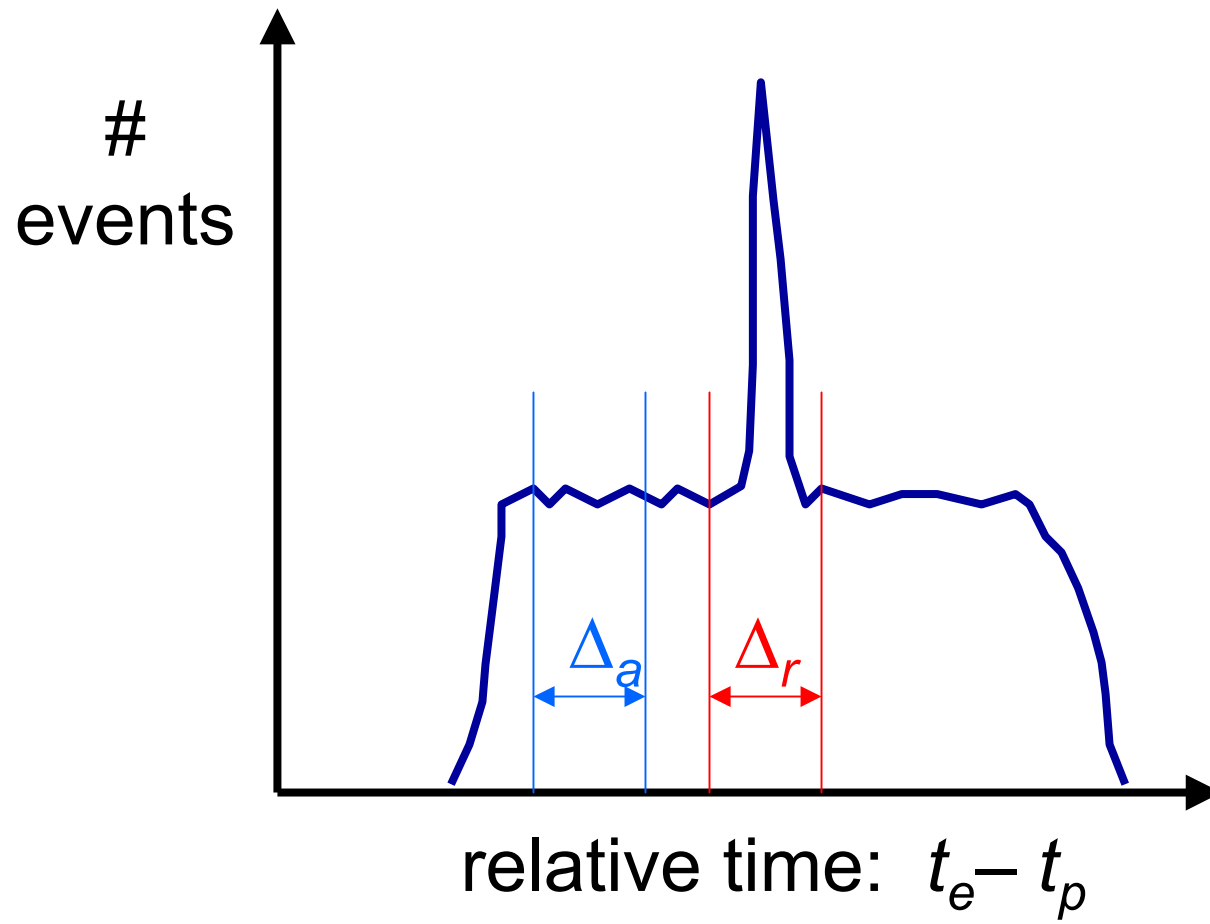


**“accidental”
(uncorrelated)**



**“real”
(correlated)**





$$C(x) = [C(x) \cap \text{Real}] - \frac{\Delta_r}{\Delta_a} \times [C(x) \cap \text{Accidental}]$$

$$\begin{aligned}\text{Accidentals Rate} &= R_e \times R_p \times \Delta\tau/\text{DF} \\ &\propto I^2 \Delta\tau/\text{DF}\end{aligned}$$

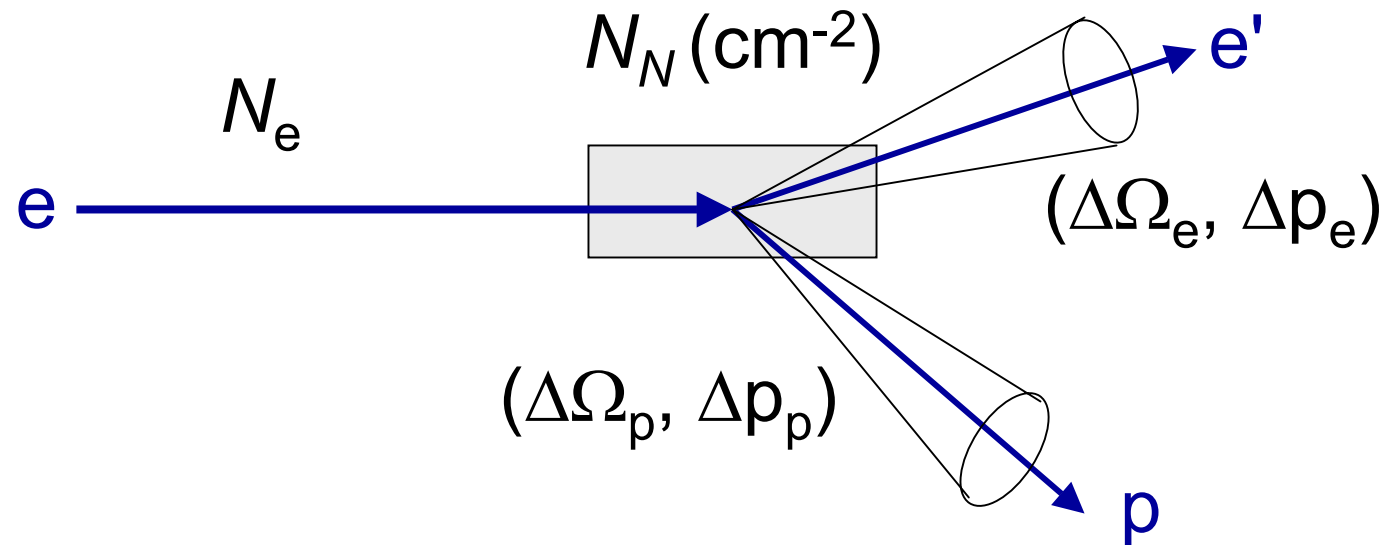
$$\begin{aligned}\text{Reals Rate} &= R_{eep} \\ &\propto I\end{aligned}$$

$$S:N = \text{Reals/Accidentals} \propto \text{DF } / (\Delta\tau * I)$$

Compromise:

Optimize $S:N$ and R_{eep}

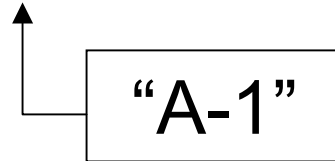
Extracting the cross section



$$\left\langle \frac{d^6\sigma}{d\Omega_e d\Omega_p dp_e dp_p} \right\rangle = \frac{\text{Counts}}{N_e N_N \Delta\Omega_e \Delta\Omega_p \Delta p_e \Delta p_p}$$

Some Theory ...

Cross Section for A(e,e'p)B in OPEA



$$d\sigma_{\text{lab}} = \frac{1}{\beta} \frac{m_e}{e} \sum_{if} \left| M_{fi} \right|^2 \left[\frac{m_e}{e'} \frac{d^3 k'}{(2\pi)^3} \right] \left[\frac{m}{E} \frac{d^3 p}{(2\pi)^3} \right]$$
$$\times (2\pi)^4 \delta^4(P + P_{A-1} - Q - P_A)$$

where

$$M_{fi} = \frac{4\pi\alpha}{Q^2} \langle k' \lambda' | j_\mu | k \lambda \rangle \langle Bp | J^\mu | A \rangle$$

Current-Current Interaction

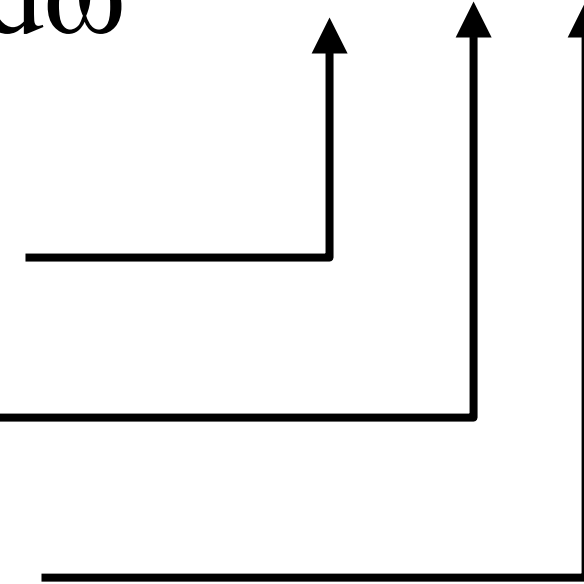
Square of Matrix Element

$$\sum_{if} \left| M_{fi} \right|^2 = \left(\frac{4\pi\alpha}{Q^2} \right)^2 \underbrace{\sum_{if} \left\langle k' \lambda' | j_\mu | k \lambda \right\rangle^* \left\langle k' \lambda' | j_\nu | k \lambda \right\rangle}_{W^{\mu\nu}} \eta_{\mu\nu}$$

Cross Section in terms of Tensors

$$\frac{d^6\sigma}{d\Omega_e d\Omega_p dp d\omega} = \sigma_M \eta_{\mu\nu} W^{\mu\nu}$$

Mott cross section



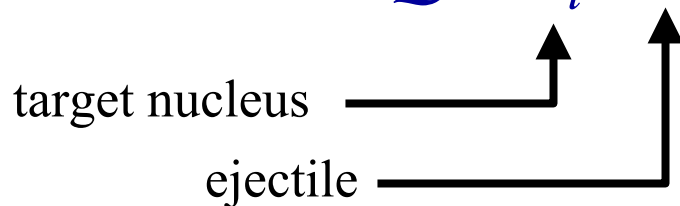
Electron tensor

Nuclear tensor

Consider Unpolarized Case

Lorentz Vectors/Scalars

3 indep. momenta: Q, P_i, P ($P_{A-1} = Q + P_i - P$)



6 indep. scalars: $\cancel{P_i^2}, \cancel{P^2}, Q^2, Q \cdot P_i, Q \cdot P, P \cdot P_i$

$$= M_A^2 = m^2$$

Nuclear Response Tensor

$$\begin{aligned} W^{\mu\nu} = & X_1 g_{\mu\nu} + X_2 q^\mu q^\nu + X_3 p_i^\mu p_i^\nu \\ & + X_4 p^\mu p^\nu + X_5 q^\mu p_i^\nu + X_6 p_i^\mu q^\nu \\ & + X_7 q^\mu p^\nu + X_8 p^\mu q^\nu + X_9 p^\mu p_i^\nu \\ & + X_{10} p_i^\mu p^\nu \\ & + (\text{PV terms like } \epsilon_{\mu\nu\rho\sigma} q_\rho p_\sigma) \end{aligned}$$

X_i are the response functions

Impose Current Conservation

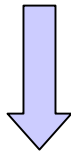
$$S^\nu \equiv q_\mu W^{\mu\nu} = 0$$

$$T^\mu \equiv q_\nu W^{\mu\nu} = 0$$

Then $q_\nu S^\nu = 0$, $p_\nu S^\nu = 0$, $p_{i\nu} S^\nu = 0$

$q_\mu T^\mu = 0$, $p_\mu T^\mu = 0$, $p_{i\mu} T^\mu = 0$

Get 6 equations in 10 unknowns



4 independent response functions

Putting it all together ...

$$\left(\frac{d^6\sigma}{d\Omega_e d\Omega_p dp d\omega} \right)_{LAB} = \frac{pE}{(2\pi)^3} \sigma_M [v_L R_L + v_T R_T + v_{LT} R_{LT} \cos \varphi_x + v_{TT} R_{TT} \cos 2\varphi_x]$$

with

$$\sigma_M = \frac{\alpha^2 \cos^2 \theta/2}{4e^2 \sin^4 \theta/2}$$

$$v_L = \left(\frac{Q^2}{q^2} \right)^2 \quad v_T = \frac{Q^2}{2q^2} + \tan^2 \theta/2$$

$$v_{TT} = \frac{Q^2}{2q^2} \quad v_{LT} = \frac{Q^2}{q^2} \sqrt{\frac{Q^2}{q^2} + \tan^2 \theta/2}$$

The Response Functions

Use spherical basis with z-axis along \mathbf{q} :

Nuclear 4-current

$$\left\{ \begin{array}{l} J_{fi}^0 \equiv J_{fi}^z = \frac{\omega}{q} \rho_{fi} \\ J_{fi}^{\pm 1} \equiv \mp \frac{1}{\sqrt{2}} (J_{fi}^x \pm i J_{fi}^y) \end{array} \right.$$

$$R_L = |\rho_{fi}(\vec{q})|^2 = \left(\frac{\vec{q}}{\omega} \right)^2 |J_{fi}^0(\vec{q})|^2$$

$$R_T = |J_{fi}^{+1}(\vec{q})|^2 + |J_{fi}^{-1}(\vec{q})|^2$$

$$R_{TT} = 2 \operatorname{Re} \{ J_{fi}^{+1}(\vec{q}) J_{fi}^{-1}(\vec{q}) \}$$

$$R_{LT} = -2 \operatorname{Re} \{ \rho_{fi}(\vec{q}) (J_{fi}^{+1}(\vec{q}) - J_{fi}^{-1}(\vec{q})) \}$$

Response functions depend on scalar quantities

In lab:

$$\left\{ \begin{array}{l} Q \cdot P_i = \omega M_A \\ P \cdot P_i = E M_A \\ Q \cdot P = \omega E - q p \cos \theta_{pq} \end{array} \right.$$

Can choose:

$$Q^2, \omega, \varepsilon_m, p_m$$

Note: no ϕ_x dependence in response functions

Including electron and recoil proton polarizations

$$\begin{aligned}
 \left(\frac{d^6\sigma}{d\Omega_e d\Omega_p dp d\omega} \right)_{LAB} = & \frac{pE}{(2\pi)^3} \sigma_M \{ v_L (R_L + R_L^n S_n) + v_T (R_T + R_T^n S_n) \} \\
 & + v_{LT} [(R_{LT} + R_{LT}^n S_n) \cos \varphi_x + (R_{LT}^l S_l + R_{LT}^t S_t) \sin \varphi_x] \\
 & + v_{TT} [(R_{TT} + R_{TT}^n S_n) \cos 2\varphi_x + (R_{TT}^l S_l + R_{TT}^t S_t) \sin 2\varphi_x] \\
 & + h v_{LT'} [(R_{LT'} + R_{LT'}^n S_n) \sin \varphi_x + (R_{LT'}^l S_l + R_{LT'}^t S_t) \cos \varphi_x] \\
 & + h v_{TT'} (R_{TT'}^l S_l + R_{TT'}^t S_t) \}
 \end{aligned}$$

with $v_{LT'} = \frac{Q^2}{q^2} \tan \theta/2$ $v_{TT'} = \tan \theta/2 \sqrt{\frac{Q^2}{q^2} + \tan^2 \theta/2}$

and other v 's defined as before

Extracting Response Functions

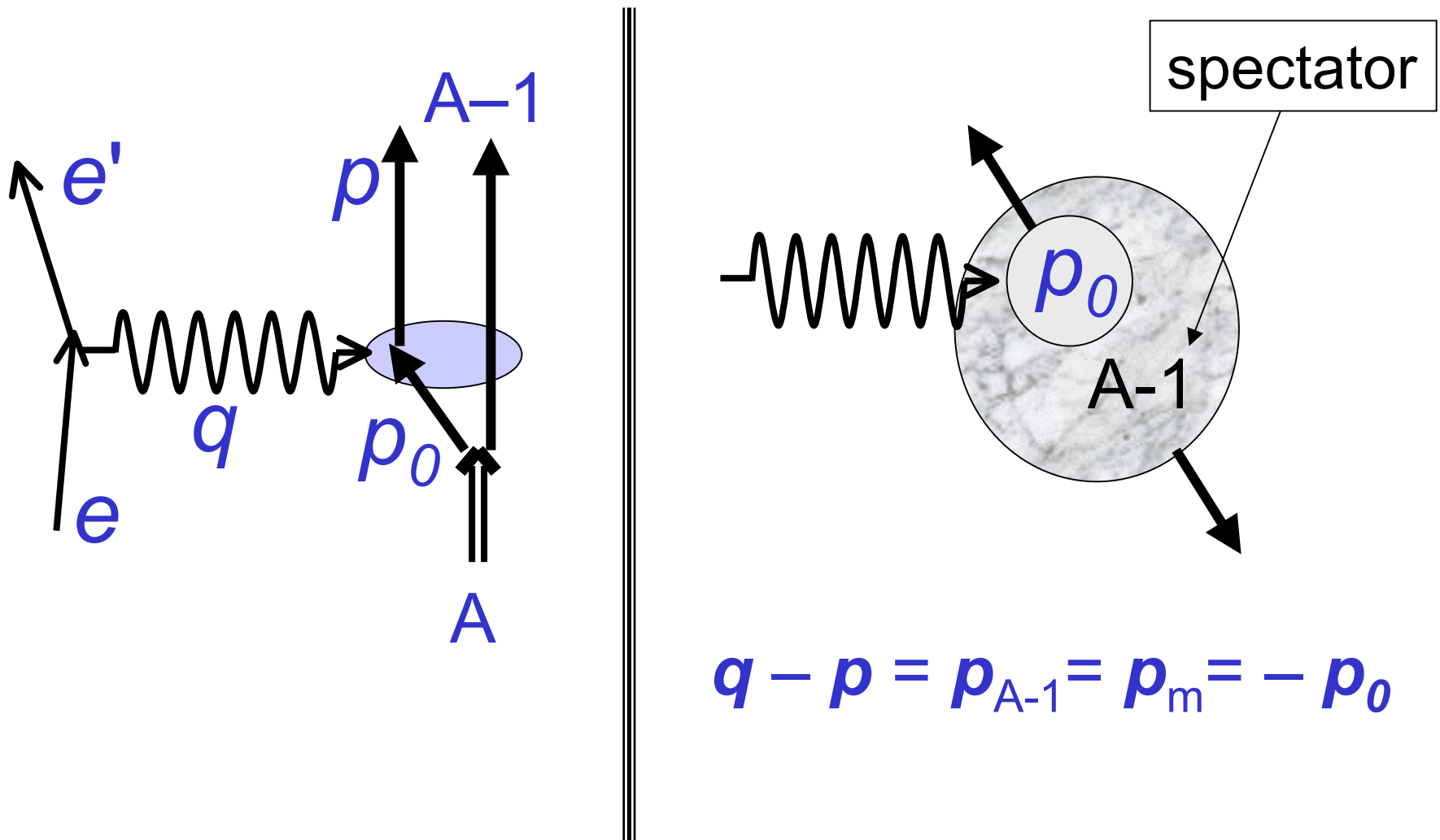
For instance: R_{LT} and A_ϕ ($= A_{LT}$)

$$\sigma_{eep} = K\sigma_M [v_L R_L + v_T R_T + v_{LT} R_{LT} \cos \varphi_x + v_{TT} R_{TT} \cos 2\varphi_x]$$

$$R_{LT} = \frac{\sigma_{eep}(\varphi_x = 0) - \sigma_{eep}(\varphi_x = \pi)}{2K\sigma_M v_{LT}}$$

$$A_\phi = \frac{\sigma_{eep}(\varphi_x = 0) - \sigma_{eep}(\varphi_x = \pi)}{\sigma_{eep}(\varphi_x = 0) + \sigma_{eep}(\varphi_x = \pi)}$$

Plane Wave Impulse Approximation (PWIA)



The Spectral Function

In nonrelativistic PWIA:

$$\frac{d^6\sigma}{d\omega d\Omega_e dp d\Omega_p} = K \sigma_{ep} S(p_m, \varepsilon_m)$$



For bound state of recoil system:

$$\rightarrow \frac{d^5\sigma}{d\omega d\Omega_e d\Omega_p} = K' \sigma_{ep} |\Phi(p_m)|^2$$

proton momentum distribution

The Spectral Function, cont'd.

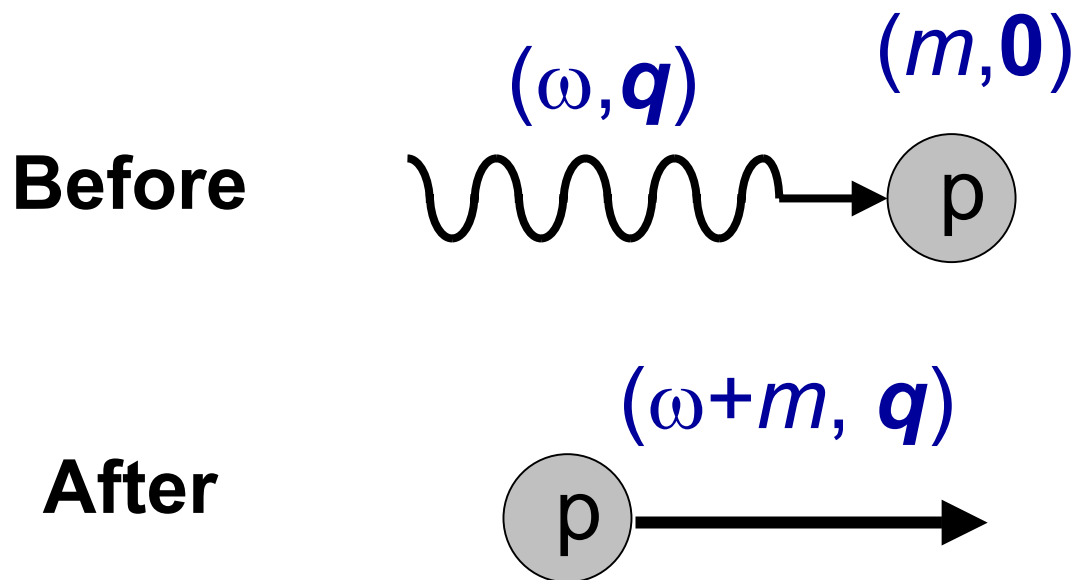
$$S(\vec{p}_0, E_0) = \sum_f \left| \langle B_f | a(\vec{p}_0) | A \rangle \right|^2 \delta(E_0 - \varepsilon_m)$$

where $\vec{p}_0 = -\vec{p}_m$ = initial momentum

$E_0 = E - \omega$ = initial energy

Note: S is not an observable!

Elastic Scattering from a Proton at Rest



Proton is on-shell \Rightarrow $(\omega + m)^2 - \mathbf{q}^2 = m^2$

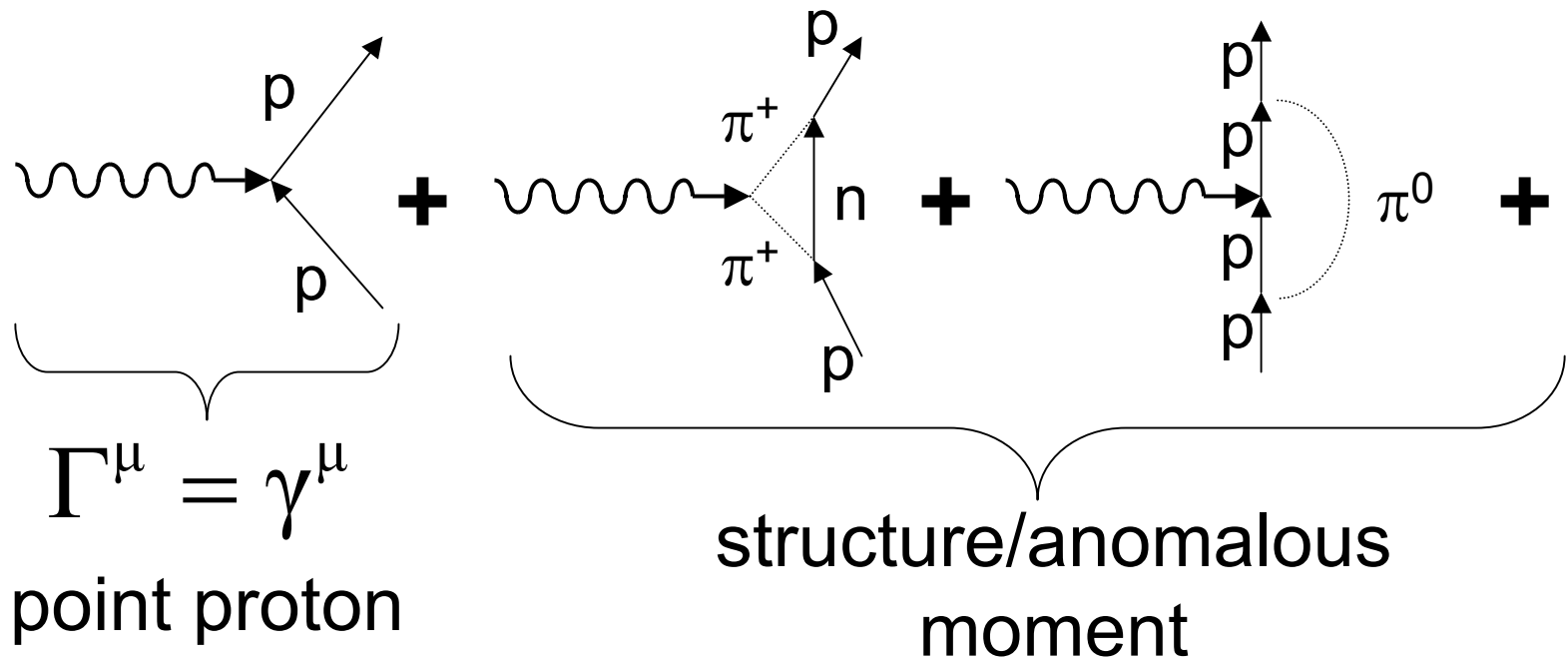
$$\omega^2 + 2m\omega + m^2 - \mathbf{q}^2 = m^2$$

$$\omega = Q^2 / 2m$$

Scattering from a Proton , cont'd.

$$\left\langle p, s_f \middle| J^\mu \middle| p - q, s_i \right\rangle = \bar{U}_f \Gamma^\mu U_i$$

Vertex fcn



Scattering from a Proton , cont'd.

Vertex fcn:

$$\Gamma^\mu = \gamma^\mu F_1(Q^2) + i\sigma^{\mu\nu} \frac{q_\nu}{2m} \kappa F_2(Q^2)$$

Dirac FF  Pauli FF 

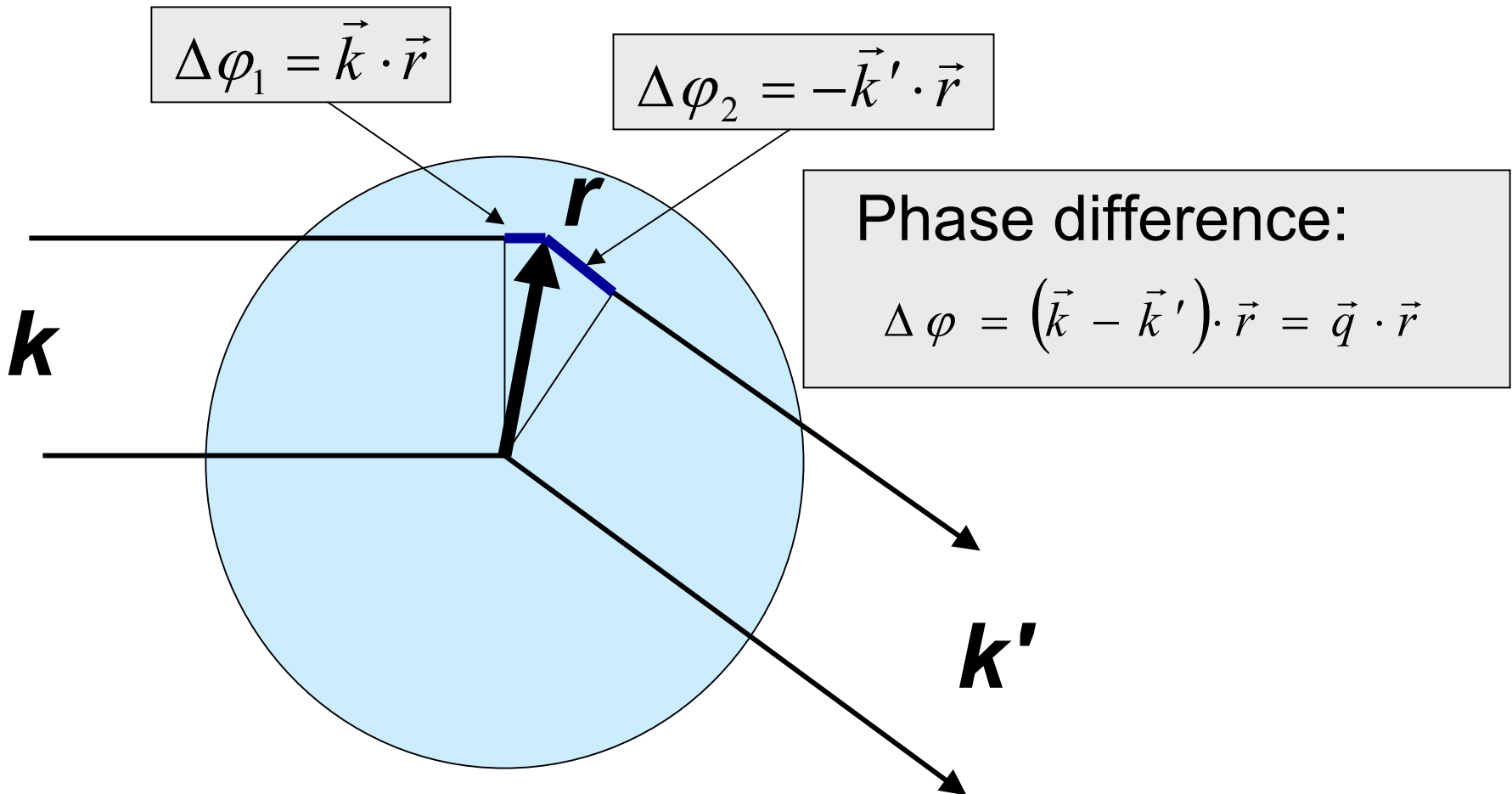
Sachs FF's

$$\left. \begin{array}{l} G_E(Q^2) = F_1(Q^2) - \tau \kappa F_2(Q^2) \\ G_M(Q^2) = F_1(Q^2) + \kappa F_2(Q^2) \end{array} \right\}$$

with $\tau = \frac{Q^2}{4m^2}$

G_E and G_M are the Fourier transforms of the charge and magnetization densities in the Breit frame.

Form Factor



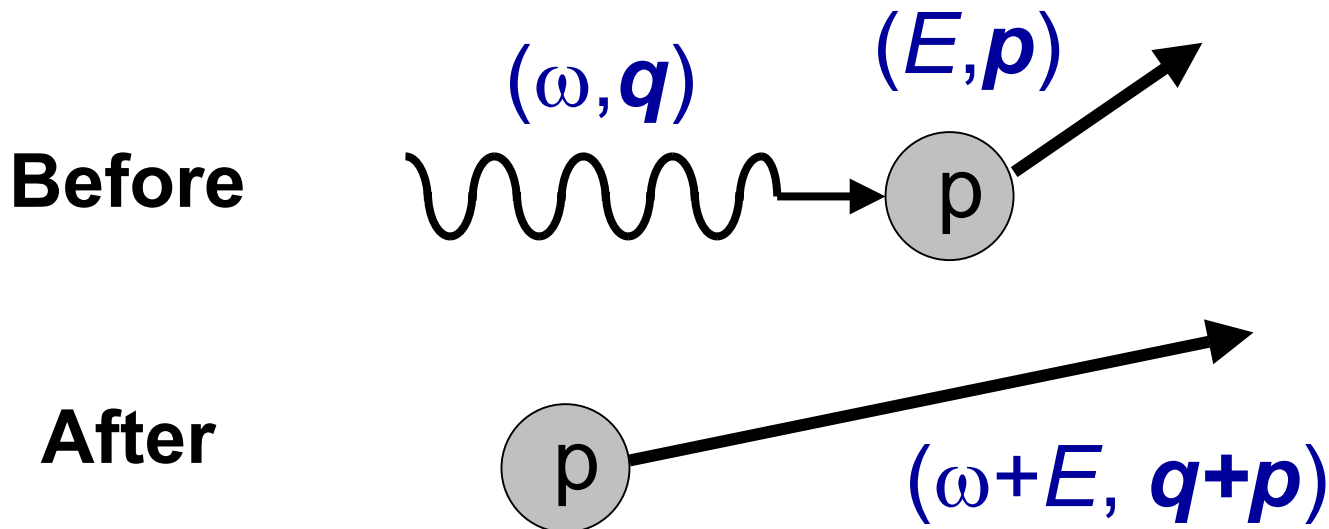
Amplitude at \mathbf{q} : $F(\mathbf{q}) = \int d\vec{r} A(\vec{r}) e^{i\vec{q} \cdot \vec{r}}$

Cross section for ep elastic

$$\frac{d\sigma}{d\Omega} = f_{rec} \sigma_M \left[\frac{G_E^2 + \tau G_M^2}{1 + \tau} + 2\tau \tan^2 \frac{\theta}{2} G_M^2 \right]$$

However, $(e, e'p)$ on a **nucleus** involves scattering from **moving** protons, *i.e.* Fermi motion.

Elastic Scattering from a Moving Proton



$$(\omega + E)^2 - (\mathbf{q} + \mathbf{p})^2 = m^2$$

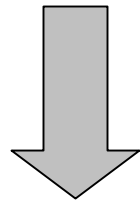
$$\omega^2 + 2E\omega + E^2 - \mathbf{q}^2 - 2\mathbf{p} \cdot \mathbf{q} - \mathbf{p}^2 = m^2$$

$$Q^2 = 2E\omega - 2\mathbf{p} \cdot \mathbf{q}$$

$$\omega (E/m) = (Q^2/2m) + \mathbf{p} \cdot \mathbf{q} / m$$

Cross section for ep elastic scattering off moving protons

Follow same procedure as for unpolarized ($e,e'p$) from nucleus



We get same form for cross section, with 4 response functions ...

Response functions for ep elastic scattering off moving protons

$$R_L = \left[\frac{(E_0 + E)}{2m} \right]^2 W_1 - \frac{\vec{q}^2}{4m^2} W_2$$

$$R_T = 2\tau W_2 + \frac{\vec{p}^2 \sin^2 \theta_{pq}}{m^2} W_1$$

$$R_{LT} = - \frac{(E_0 + E) |\vec{p}| \sin \theta_{pq}}{m^2} W_1$$

$$R_{TT} = \frac{\vec{p}^2 \sin^2 \theta_{pq}}{m^2} W_1$$

with

$$W_1 = F_1^2 + \tau(\kappa F_2)^2 \quad W_2 = (F_1 + \kappa F_2)^2$$

Quasielastic Scattering

For $E \approx m$:

$$\omega \approx (Q^2/2m) + \mathbf{p} \cdot \mathbf{q} / m$$

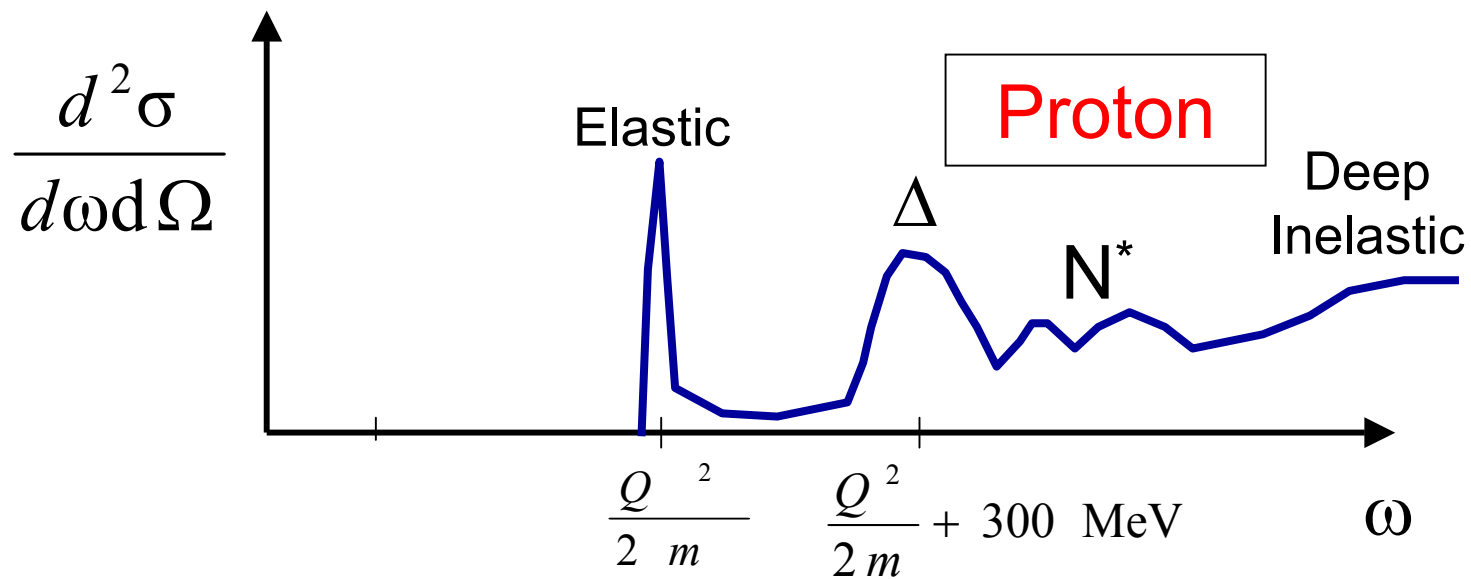
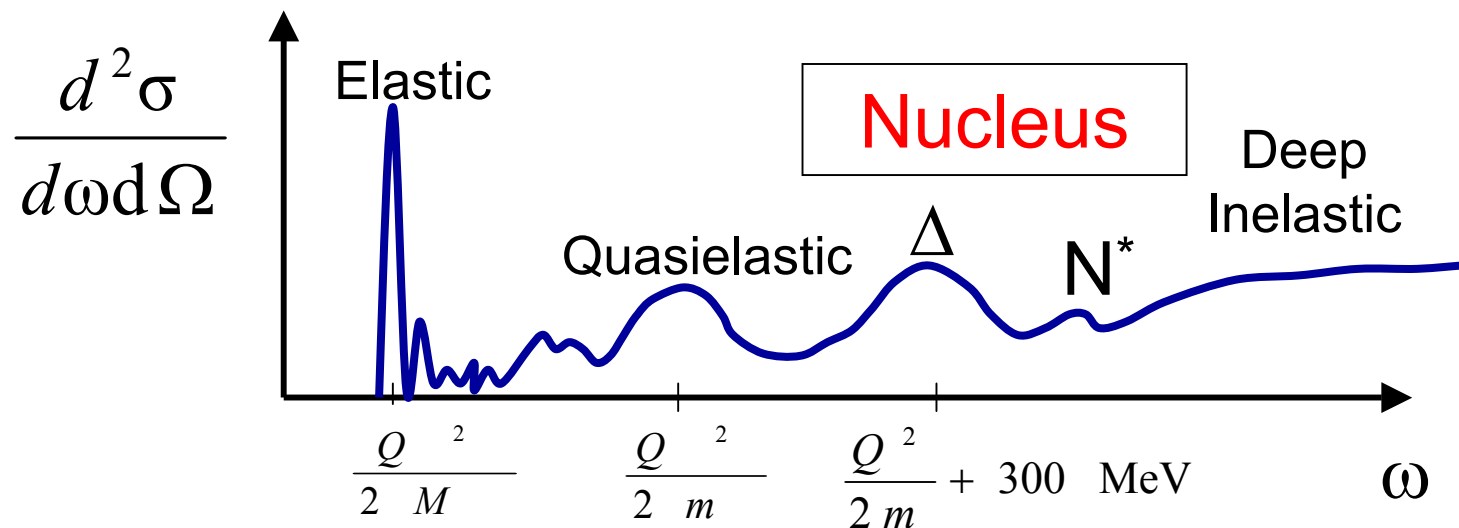
If we “quasielastically” scatter from nucleons within nucleus:

Expect peak at:

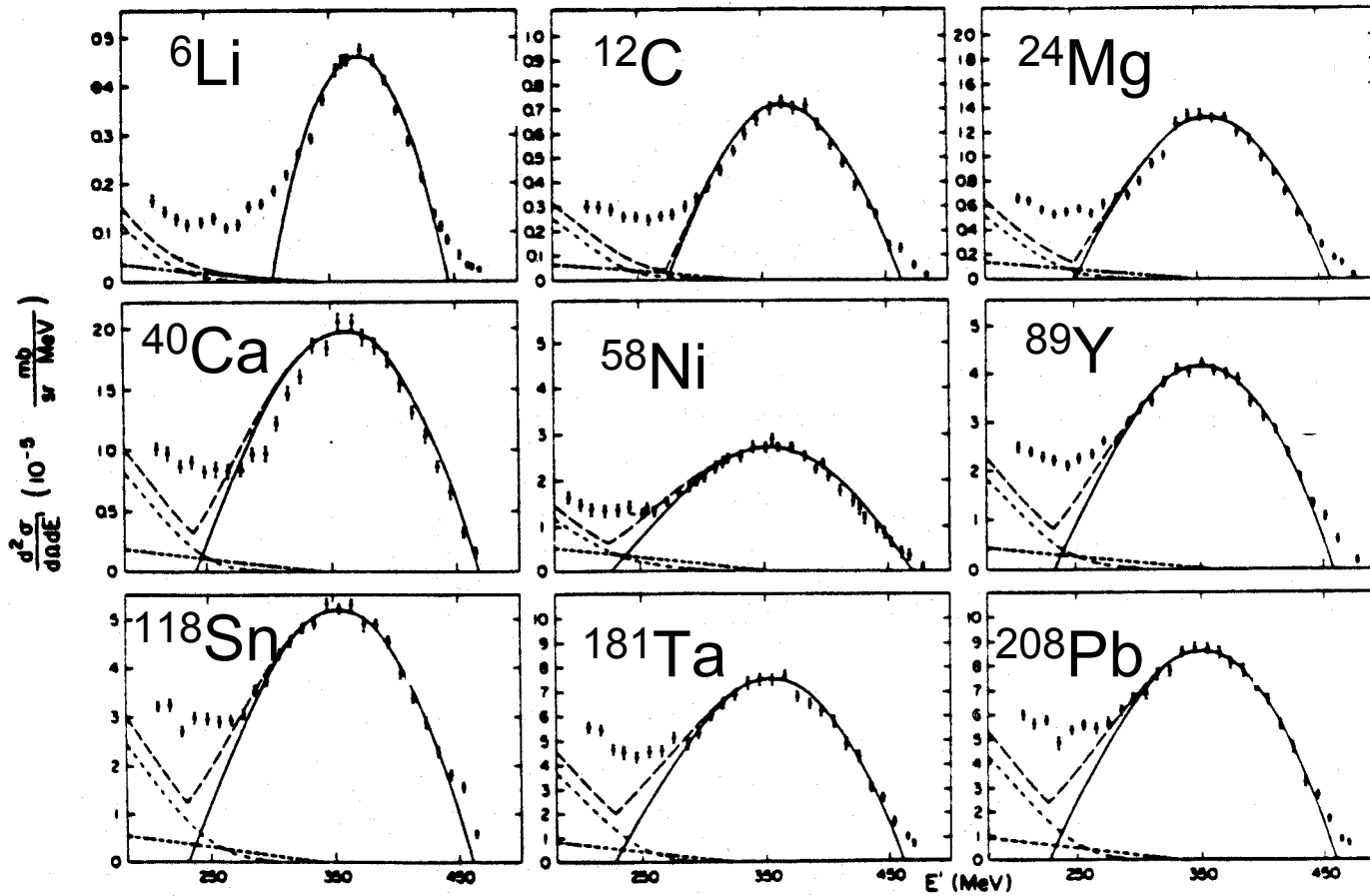
$$\omega \approx (Q^2/2m)$$

Broadened by Fermi motion: $\mathbf{p} \cdot \mathbf{q} / m$

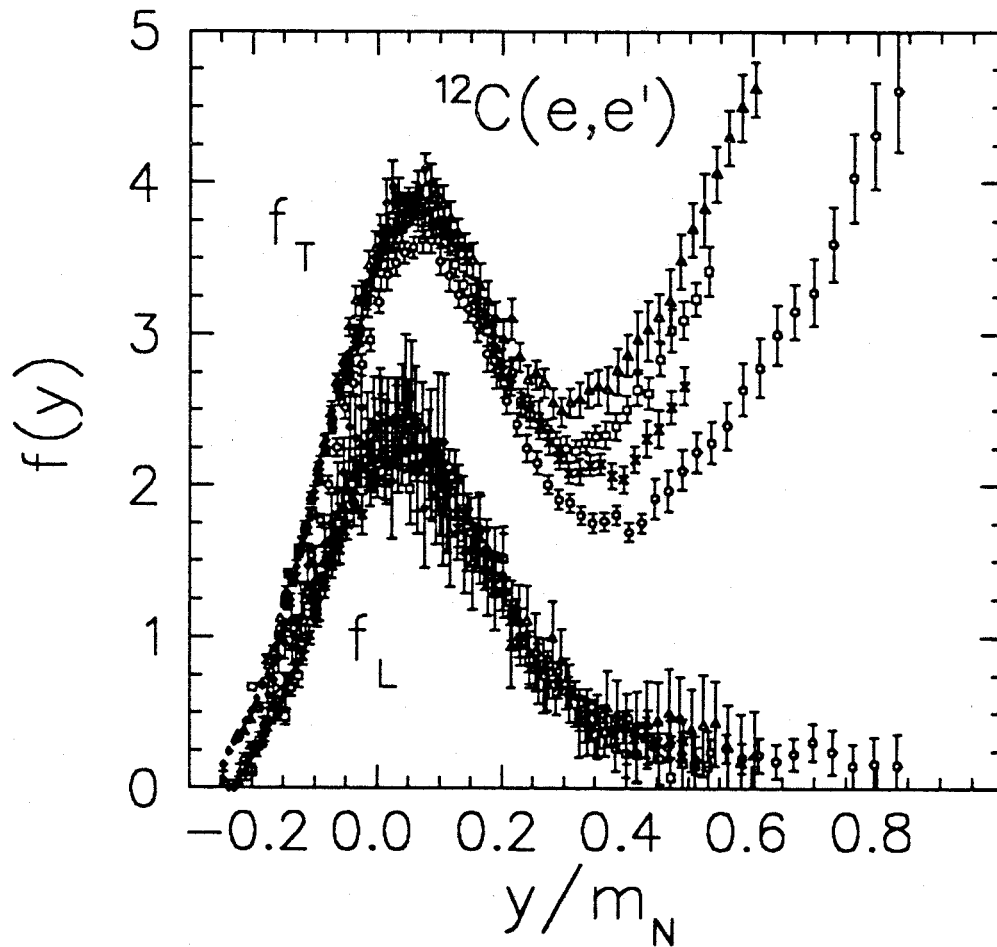
Electron Scattering at Fixed Q^2



Quasielastic Electron Scattering



R.R. Whitney et al., Phys. Rev. C **9**, 2230 (1974).



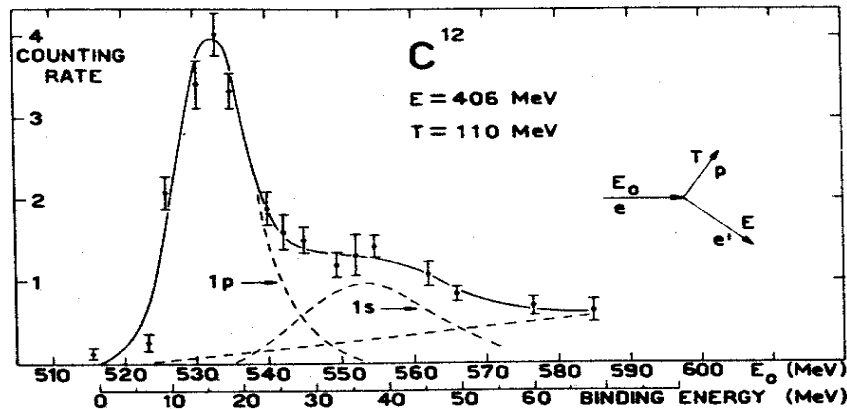
Data: P. Barreau *et al.*, Nucl. Phys. **A402**, 515 (1983).

y -scaling analysis: J.M. Finn, R.W. Lourie and B.H. Cottman,
Phys. Rev. C **29**, 2230 (1984).

Nuclear Structure

First, a bit of history: The first ($e, e'p$) measurement

$^{12}\text{C}(e, e'p)$



$^{27}\text{Al}(e, e'p)$

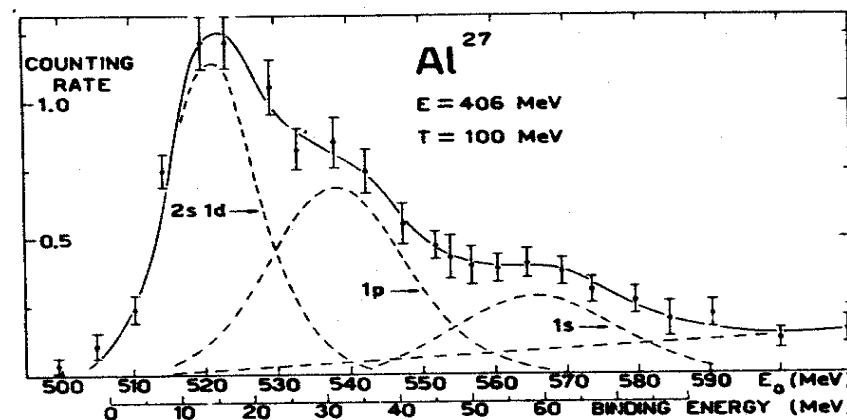


FIG. 2. Electron-proton coincidence counting rate per 10^{11} equivalent quanta at 550 MeV as a function of the incident energy. The dashed lines indicate the contributions of the various shells and the background as explained in the text.

Frascati
Synchrotron,
Italy

U. Amaldi, Jr. *et al.*,
Phys. Rev. Lett. 13,
341 (1964).

(e,e'p) advantages over (p,2p)

- Electron interaction relatively weak: OPEA is reasonably accurate.
- Nucleus is very transparent to electrons: Can probe deeply bound orbits.

However: ejected proton is strongly interacting. The “cleanness” of the electron probe is somewhat sacrificed.

FSI must be taken into account.

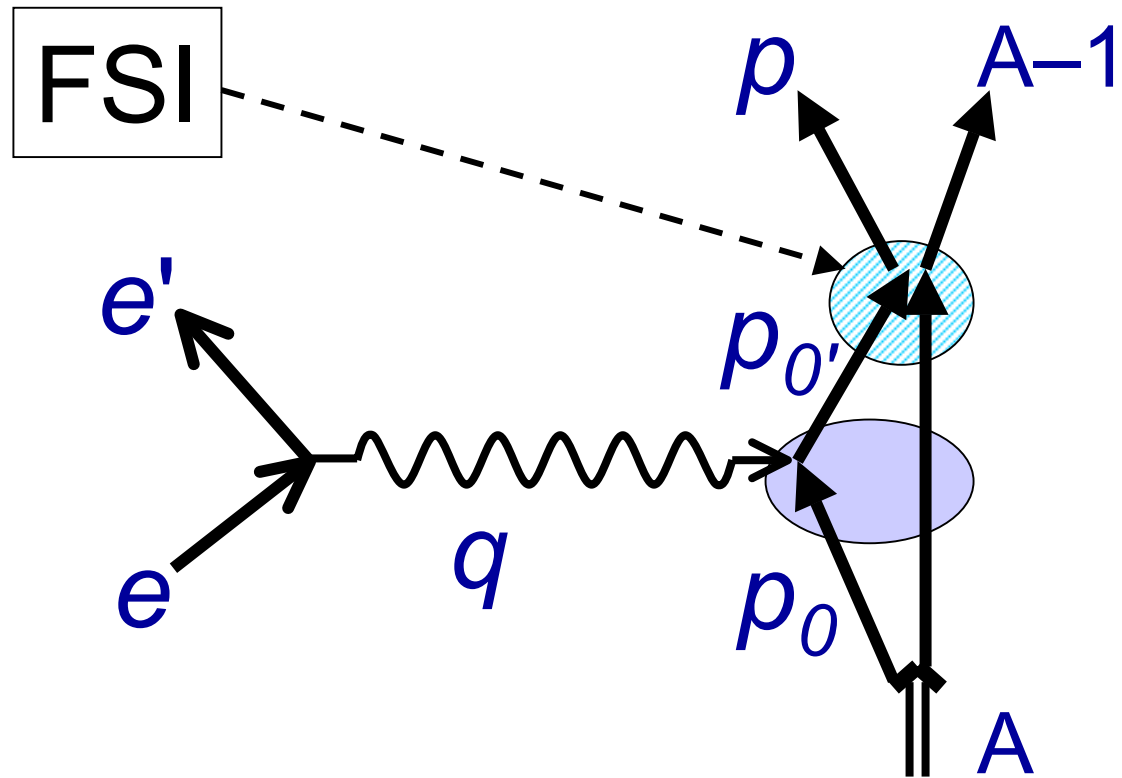
Recall, in nonrelativistic PWIA:

$$\frac{d^6\sigma}{d\omega d\Omega_e dp d\Omega_p} = K \sigma_{ep} S(p_m, \epsilon_m)$$

where $\mathbf{q} - \mathbf{p} = \mathbf{p}_m = -\mathbf{p}_o$

FSI destroys simple connection
between the measured \mathbf{p}_m and the
proton initial momentum (not an
observable).

Final State Interactions (FSI)



$$\vec{q} - \vec{p} = \vec{p}_{A-1} \neq \vec{p}_0$$

Distorted Wave Impulse Approximation (DWIA)

Treat outgoing proton distorted waves in presence of potential produced by residual nucleus (*optical potential*).

$$\frac{d^6\sigma}{d\omega d\Omega_e dp d\Omega_p} = K \sigma_{ep} [S^D(p_m, \varepsilon_m, p)]$$

“Distorted” spectral function



Optical potential is constrained by proton elastic scattering data.

Problems with this approach:

- Residual nucleus contains hole state, unlike the target in p+A scattering.
- Proton scattering data is surface dominated, whereas ejected protons in (e,e'p) are produced within entire nuclear volume.

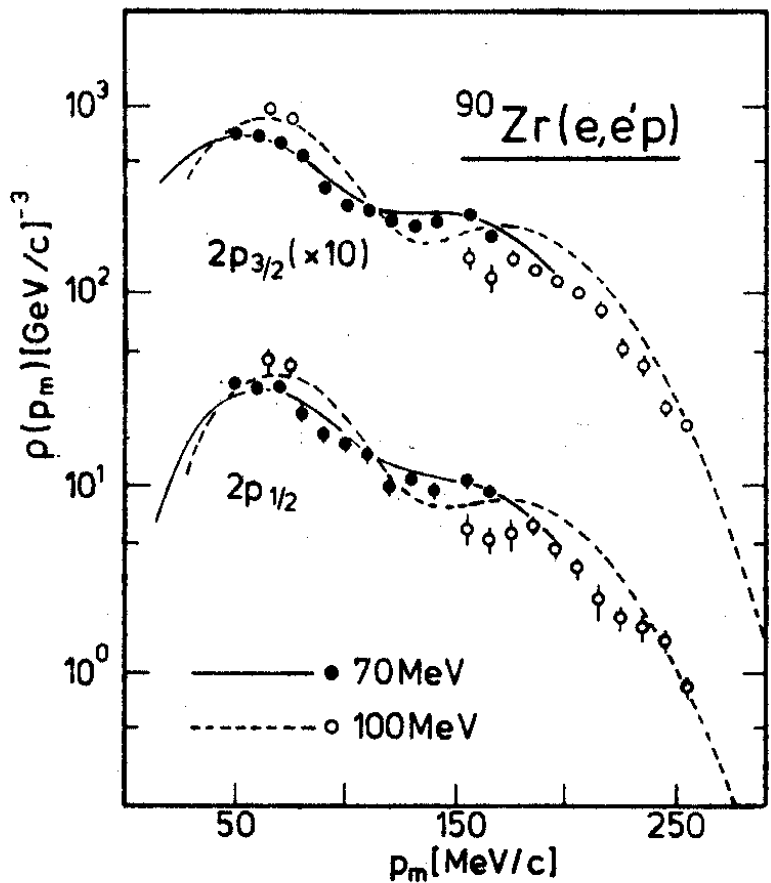


Fig. 1. Experimental momentum distributions for the $2p_{3/2}$ and $2p_{1/2}$ transitions in the $^{90}\text{Zr}(e,e'p)^{89}\text{Y}$ reaction. The curves correspond to DWIA calculations for the two proton energies (set I in table 1).

100 MeV data
is significantly
overestimated
by DWIA near
2nd maximum.

NIKHEF-K
Amsterdam

J.W.A. den Herder, et al., Phys. Lett. B 184, 11 (1987).

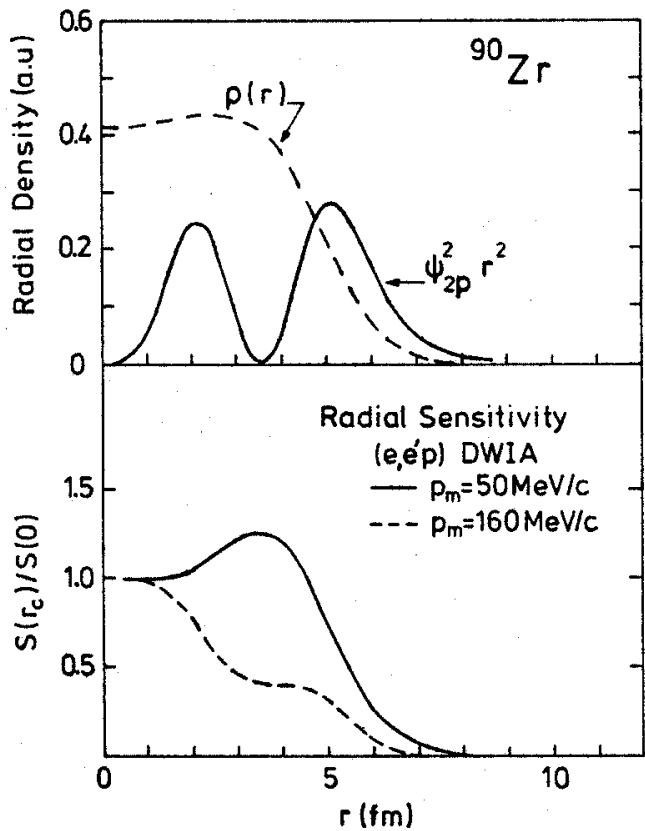
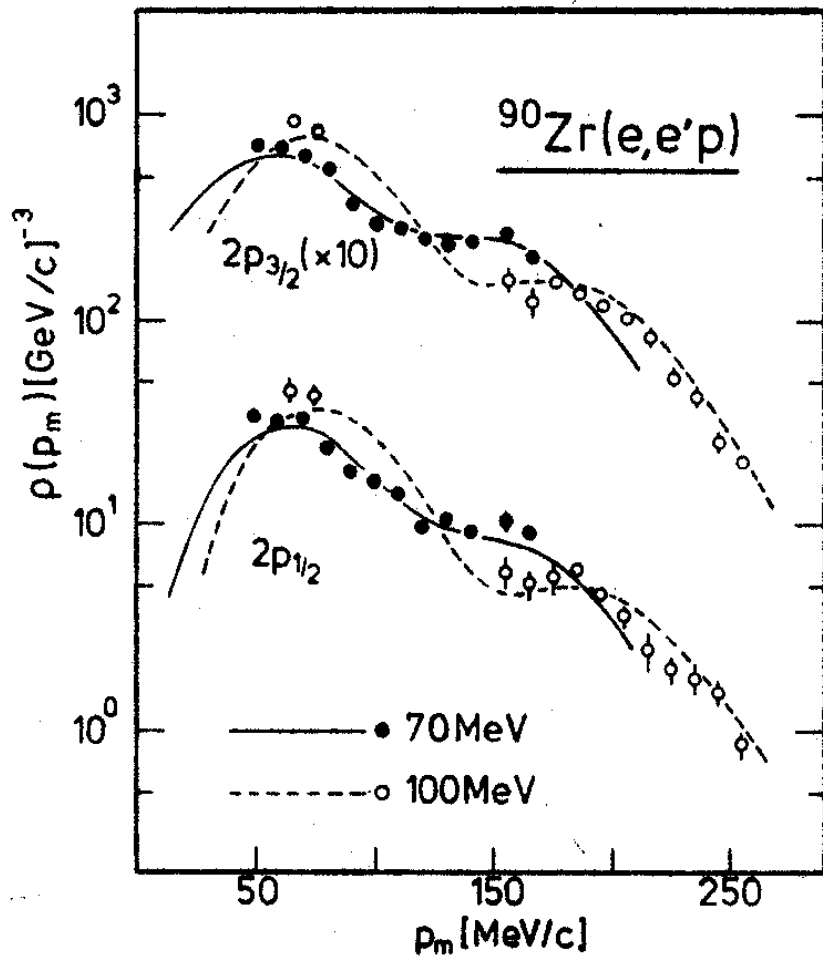


Fig. 2. Radial sensitivity, $S(r_c)$, as a function of the lower integration limit r_c (see text). For reference the radial dependence of the charge density (ρ) and of the 2p wave functions (ψ_{2p}) are indicated as well (not to scale).

$$\rho_a^{\text{th}}(p_m, \vec{p}) = S_a \left| \int_{r_c=0}^{\infty} \chi^{(-)*}(\vec{r}_p, \vec{p}) \times \exp(i\vec{q} \cdot \vec{r}_p) \psi_a(\vec{r}_p) d\vec{r}_p \right|^2$$

At $p_m \approx 160$ MeV/c,
wf is probed in
nuclear interior.

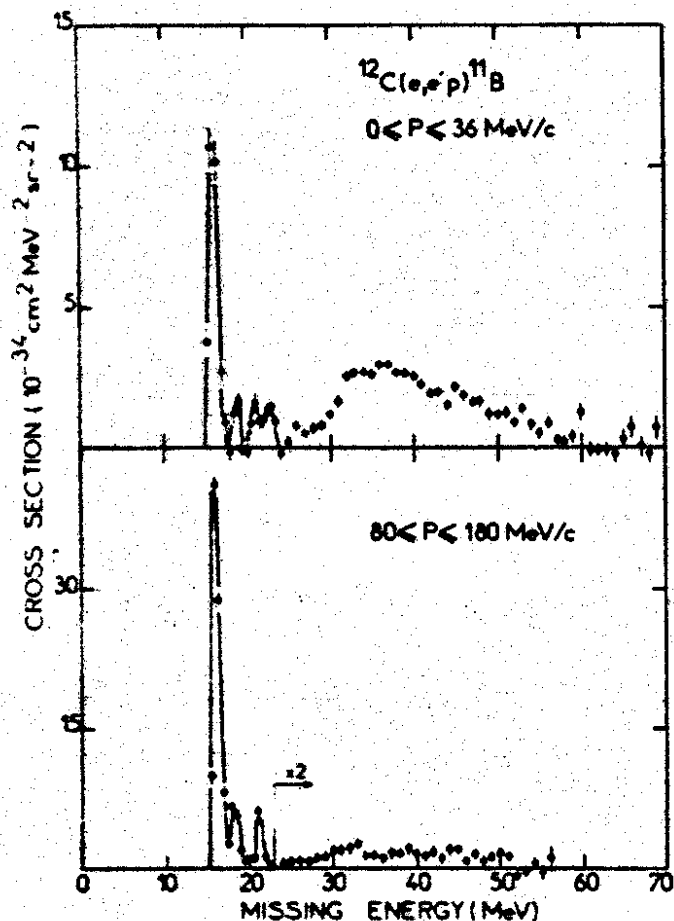


Adjusting optical potential renders good agreement while maintaining agreement with p+A elastic.

Fig. 3. Same as fig. 1, but for the modified optical potential (set II in table 1).

J.W.A. den Herder, et al., Phys. Lett. B 184, 11 (1987).

Saclay
Linac,
France



$^{12}\text{C}(\text{e}, \text{e}'\text{p})^{11}\text{B}$

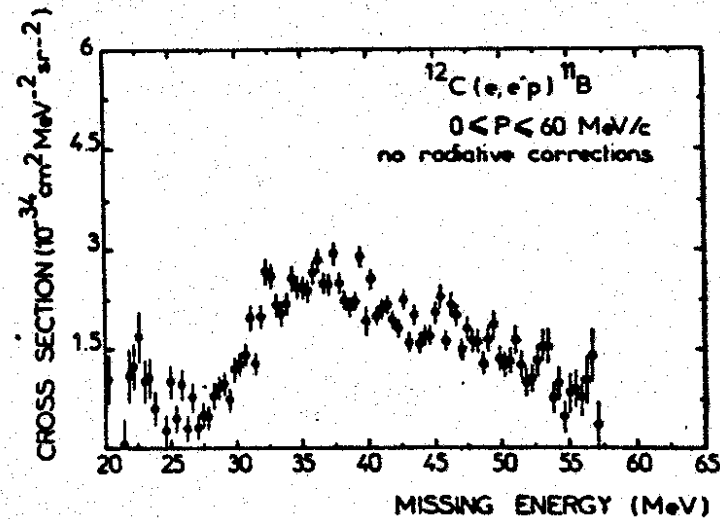
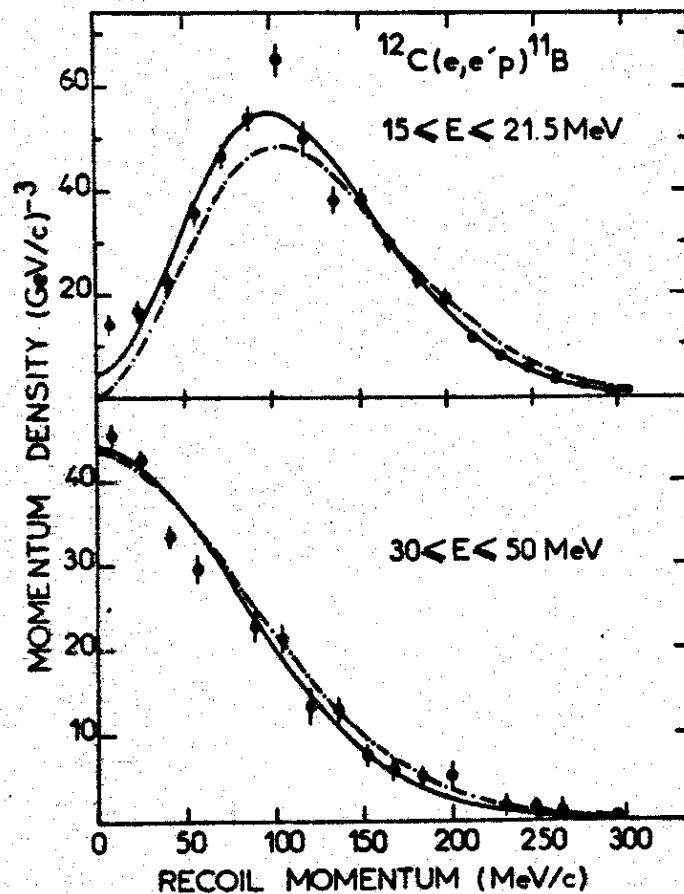


Fig. 9. Missing energy spectra from $^{12}\text{C}(\text{e}, \text{e}'\text{p})$, (a) $0 \leq P \leq 36 \text{ MeV}/c$, (b) $80 \leq P \leq 180 \text{ MeV}/c$ and (c) $0 \leq P \leq 60 \text{ MeV}/c$ for $20 \leq E \leq 60 \text{ MeV}$.

p-shell
 $l=1$

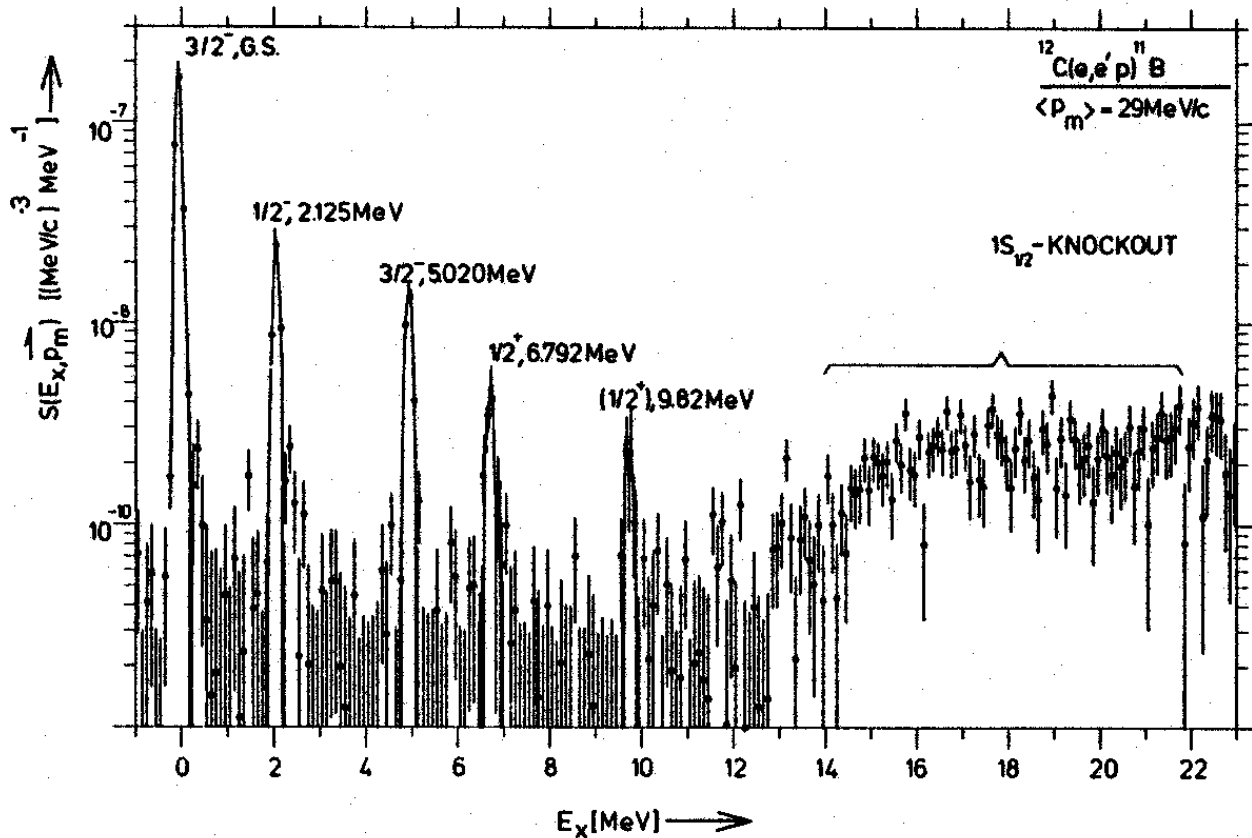
s-shell
 $l=0$



$^{12}\text{C}(\text{e}, \text{e}'\text{p})^{11}\text{B}$

Saclay
Linac,
France

Fig. 10. Momentum distribution from $^{12}\text{C}(\text{e}, \text{e}'\text{p})$; (a) $15 \leq E \leq 21.5 \text{ MeV}$ and (b) $30 \leq E \leq 50 \text{ MeV}$. The solid and dashed lines represent DWIA and PWIA calculations respectively, with normalization obtained by a fit to the data.

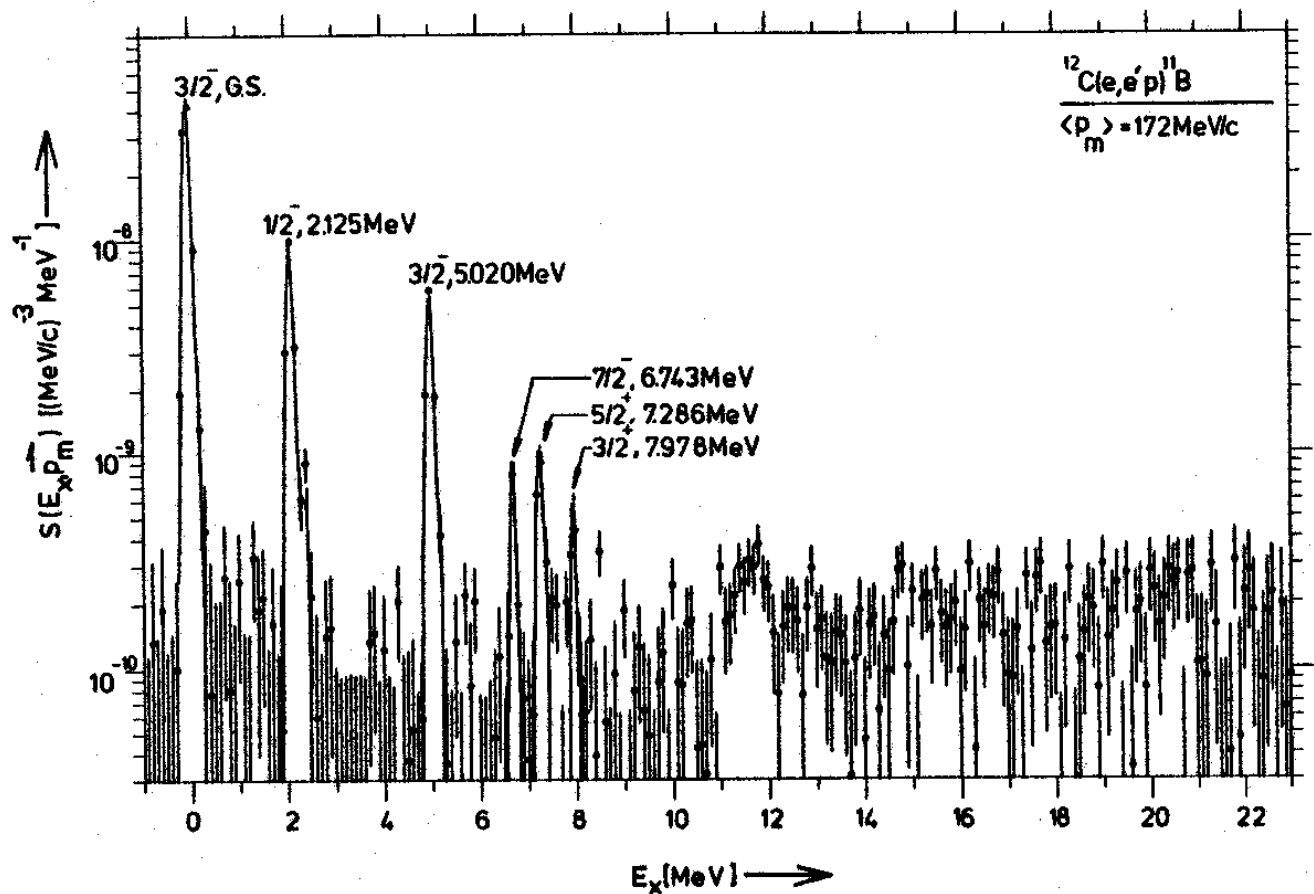


12C(e,e'p)¹¹B

NIKHEF-K
Amsterdam

Fig. 1. Excitation-energy spectrum of the reaction $^{12}\text{C}(\text{e},\text{e}'\text{p})^{11}\text{B}$ at a central value of the missing momentum $p_m = 29 \text{ MeV}/c$. The spectrum has been sorted in 100 keV bins.

G. van der Steenhoven *et al.*, Nucl. Phys. **A484**, 445 (1988).



$^{12}\text{C}(\text{e}, \text{e}'\text{p})^{11}\text{B}$

NIKHEF-K
Amsterdam

Fig. 2. Same as fig. 1 but for $p_m = 172 \text{ MeV}/c$.

G. van der Steenhoven *et al.*, Nucl. Phys. **A484**, 445 (1988).

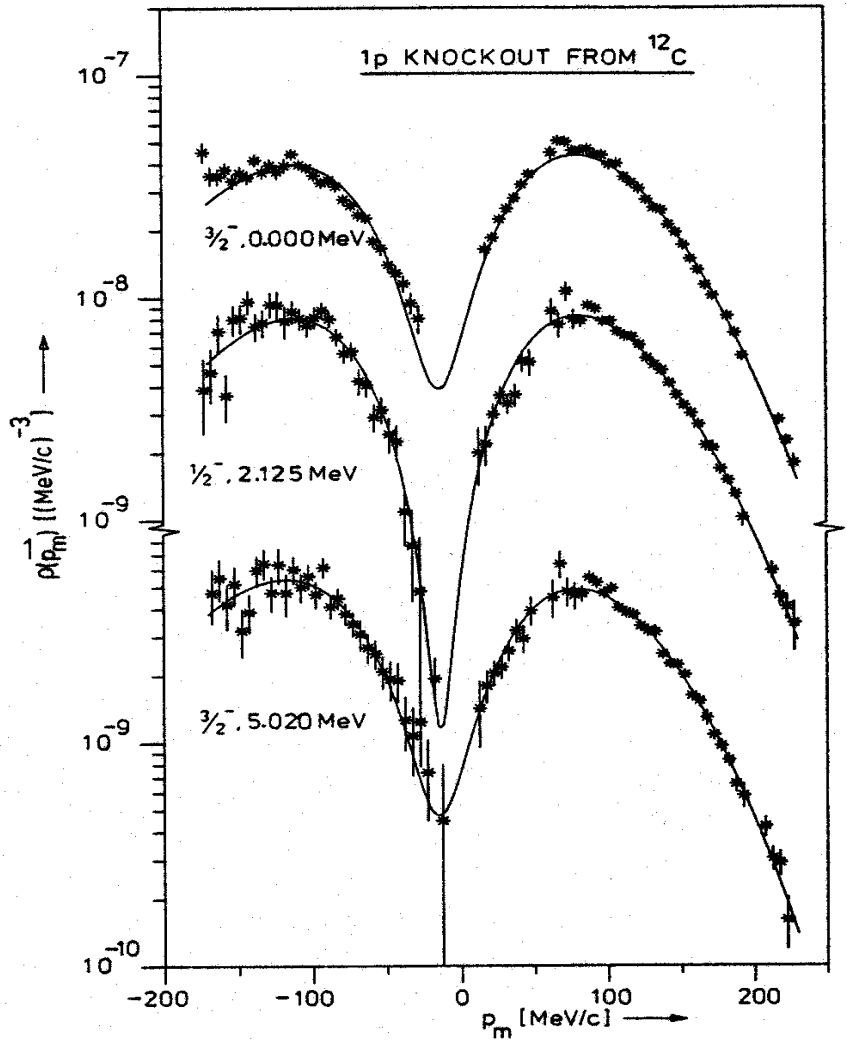


Fig. 11. Momentum distributions for 1p knockout from ^{12}C leading to the $\frac{3}{2}^-$ ground state, the $\frac{1}{2}^-$ state at 2.125 MeV and the $\frac{3}{2}^-$ state at 5.020 MeV in ^{11}B . The curves represent DWIA calculations employing the MCO potential. The fitted parameters are listed in table 6 (after a correction for the omitted couplings using table 5).

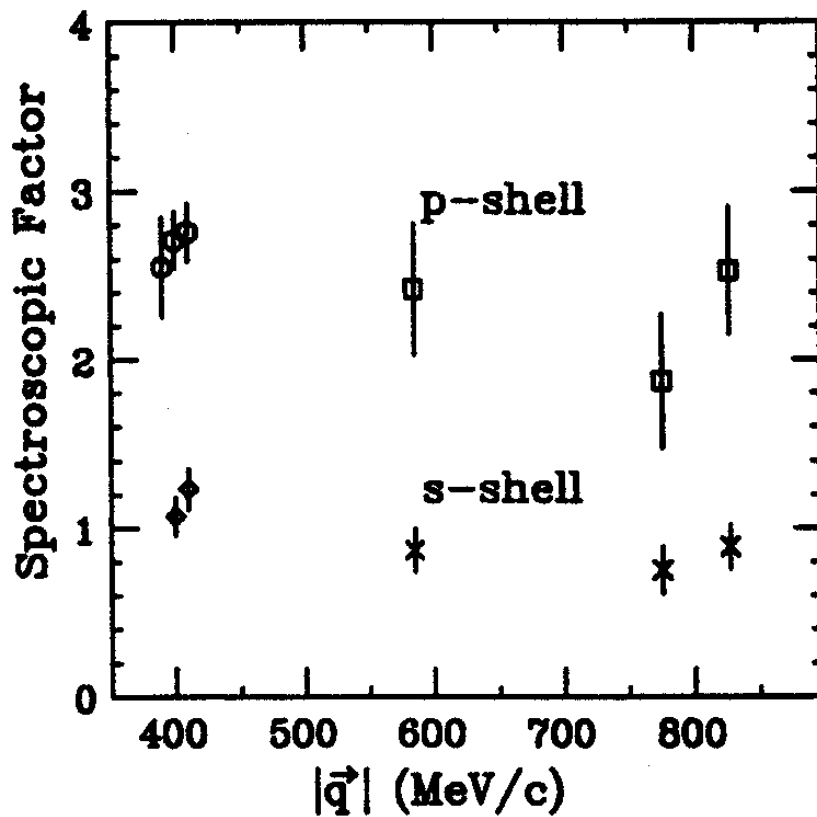
$^{12}\text{C}(\text{e},\text{e}'\text{p})^{11}\text{B}$

NIKHEF-K
Amsterdam

DWIA
calculations fit
data reasonably
well.

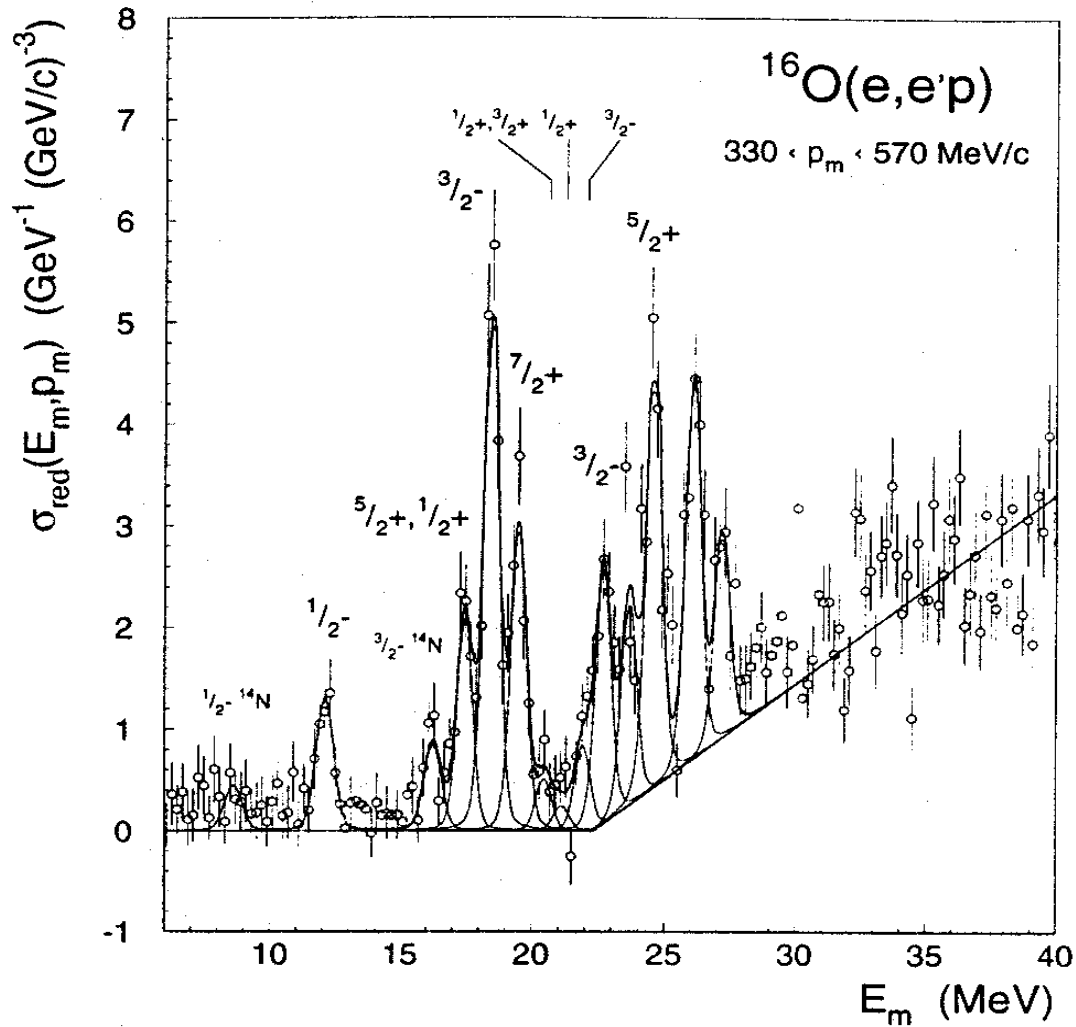
Missing strength
observed
however.

$^{12}\text{C}(\text{e},\text{e}'\text{p})$



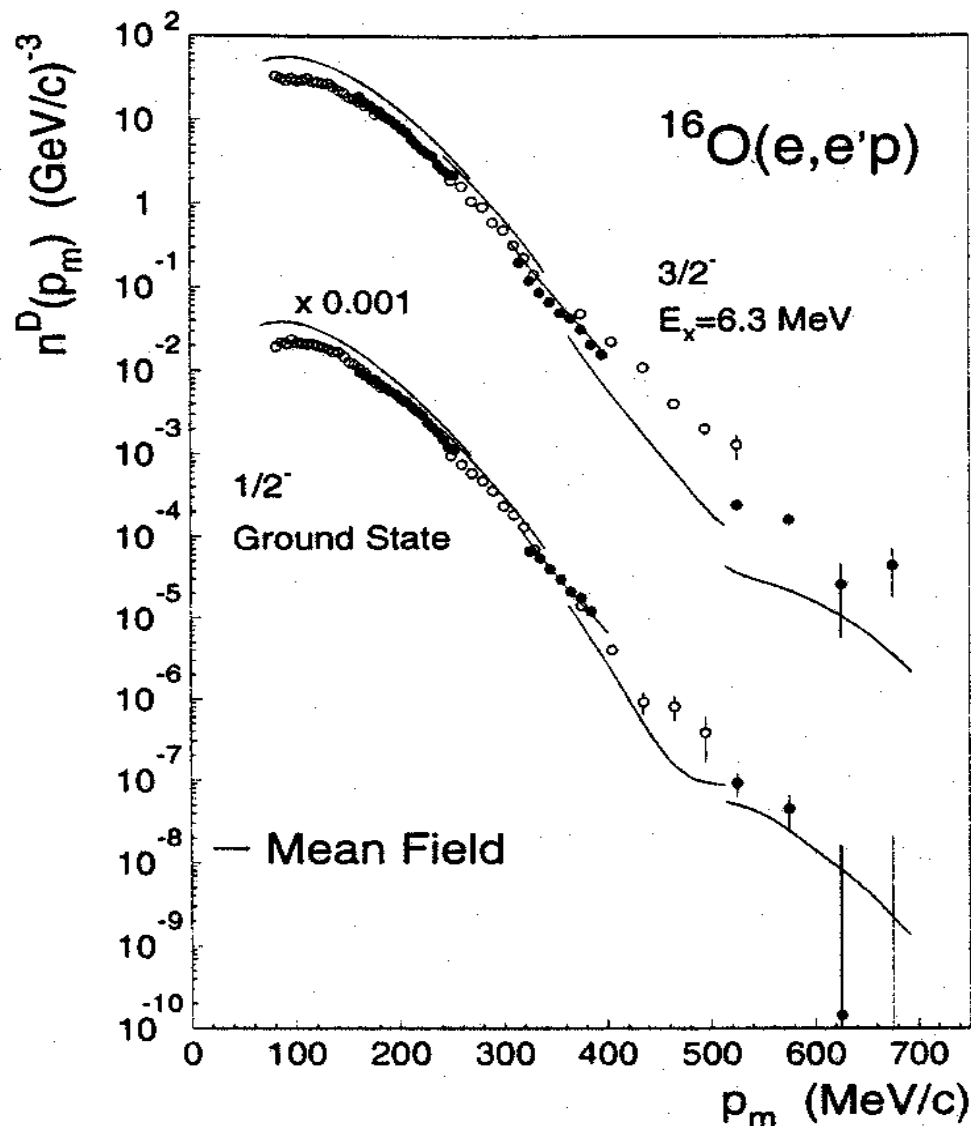
Bates
Linear
Accelerator

L.B. Weinstein *et al.*, Phys. Rev. Lett. **64**, 1646 (1990).



MAMI
 Mainz,
 Germany

K.I. Blomqvist *et al.*, Phys. Lett. B 344, 85 (1995).

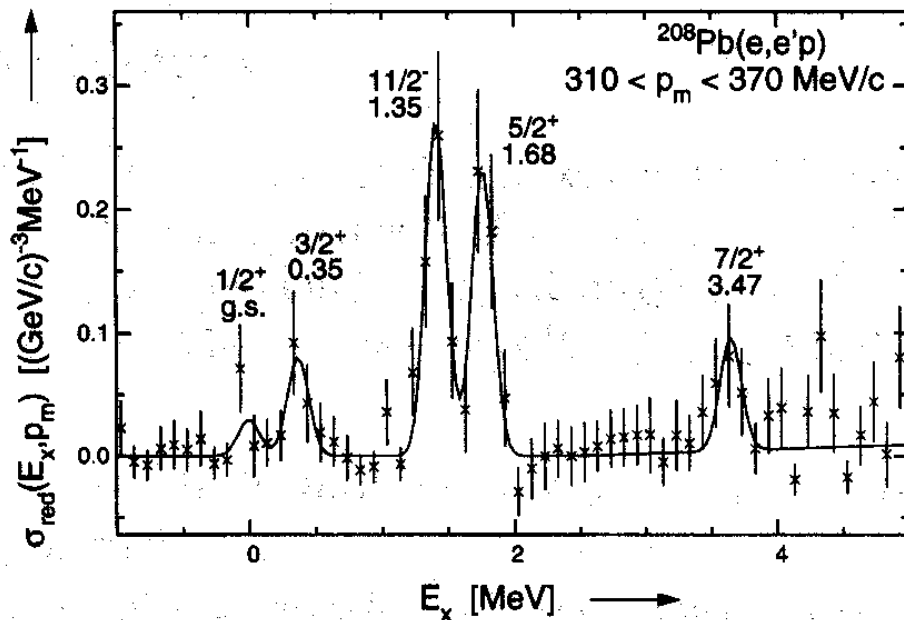


MAMI
Mainz,
Germany

Factorization violated.

DWIA calculations
underpredict at high p_m .

Neglected MEC's &
relativistic effects.
Offshell effects
uncertain at high p_m .



208Pb(e,e'p)

AmPS NIKHEF-K
Amsterdam

FIG. 1. The reduced cross section of the reaction $^{208}\text{Pb}(e, e'p)$ at an average missing momentum of 340 MeV/c, showing the knock out of valence protons to discrete states in ^{207}Tl , labeled by their spin, parity, and excitation energy. The solid curve is the result of a fit to the spectrum.

I. Bobeldijk *et al.*, Phys. Rev. Lett. **73**, 2684 (1994).

$^{208}\text{Pb}(e, e'p)$

AmPS NIKHEF-K Amsterdam

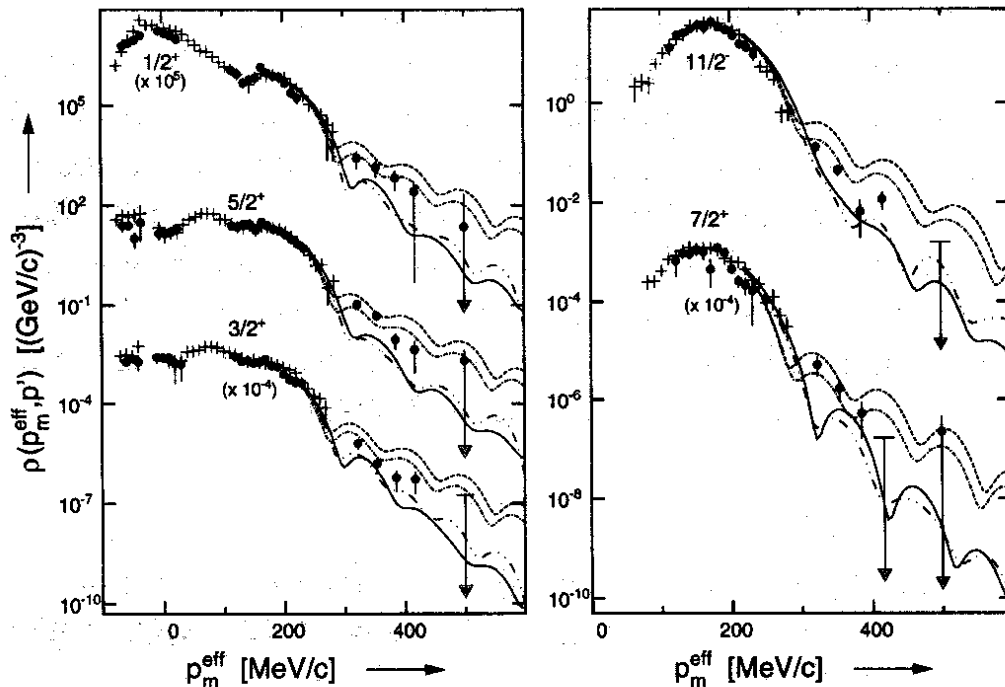


FIG. 2. Missing-momentum distributions for the transitions to the $\frac{1}{2}^+$, $\frac{3}{2}^+$, $\frac{11}{2}^-$, $\frac{5}{2}^+$, and $\frac{7}{2}^+$ states in the reaction $^{208}\text{Pb}(e, e'p)$ at excitation energies of 0.00, 0.35, 1.35, 1.68, and 3.47 MeV, respectively. The present data are represented by solid circles, the plus marks have been measured by Quint [16]. The solid curves are knockout calculations in the distorted-wave impulse approximation. The calculations including correlations as proposed by Pandharipande [8], Ma and Wambach [10], and Mahaux and Sartor [12] are represented by dash-double-dotted, dashed, and dot-dashed curves, respectively.

Long-range correlations important.

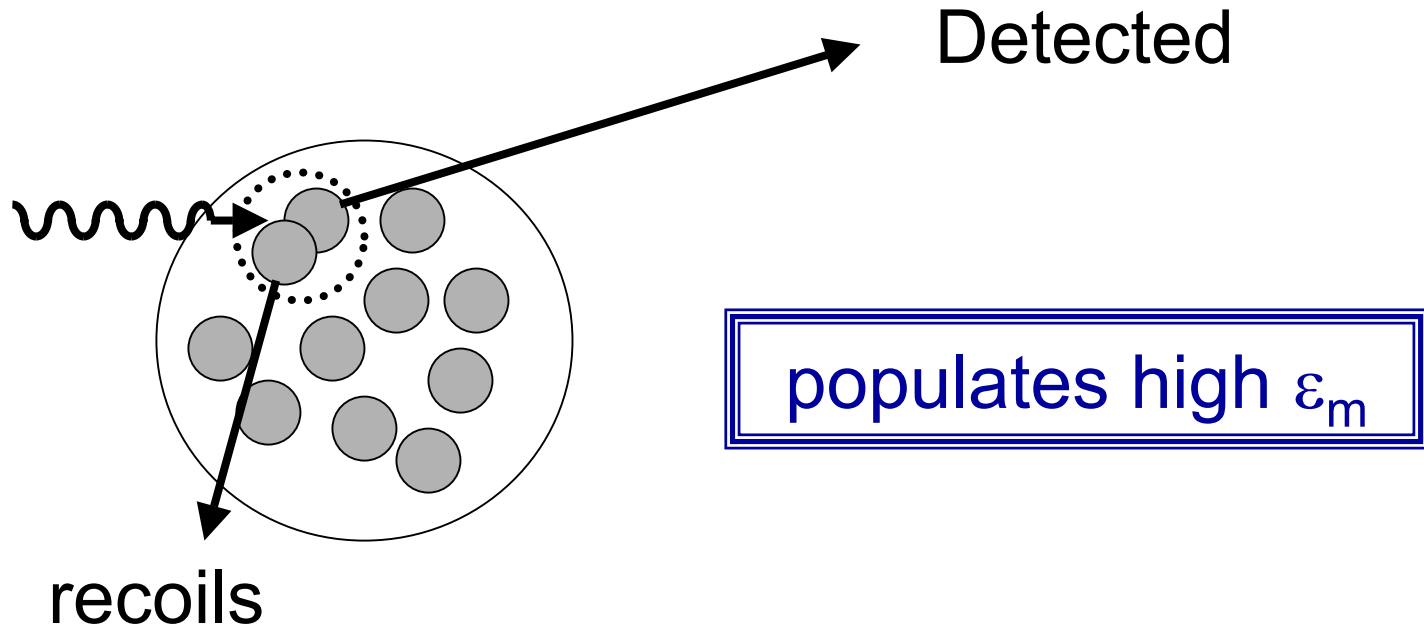
SRC and TC less so, but expected to grow with ε_m .

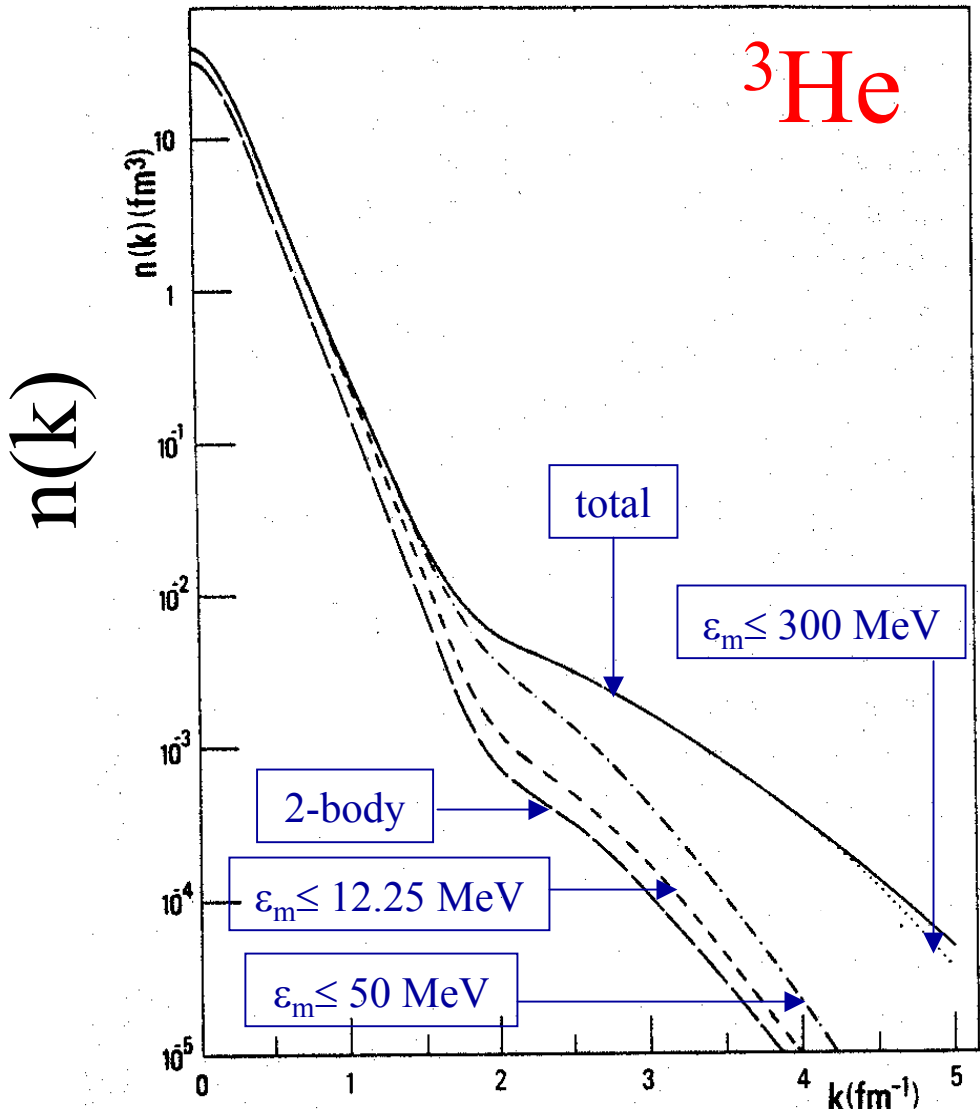
Some of the lessons learned:

- ($e, e'p$) sensitive probe of single-particle orbits.
- Proton distortions (FSI) must be accounted for to reproduce shape of spectral function. Energy dependence of FSI breaks factorization.
- Missing strength in valence orbits, even after accounting for FSI
- At high P_m significant discrepancies found relative to calculations.

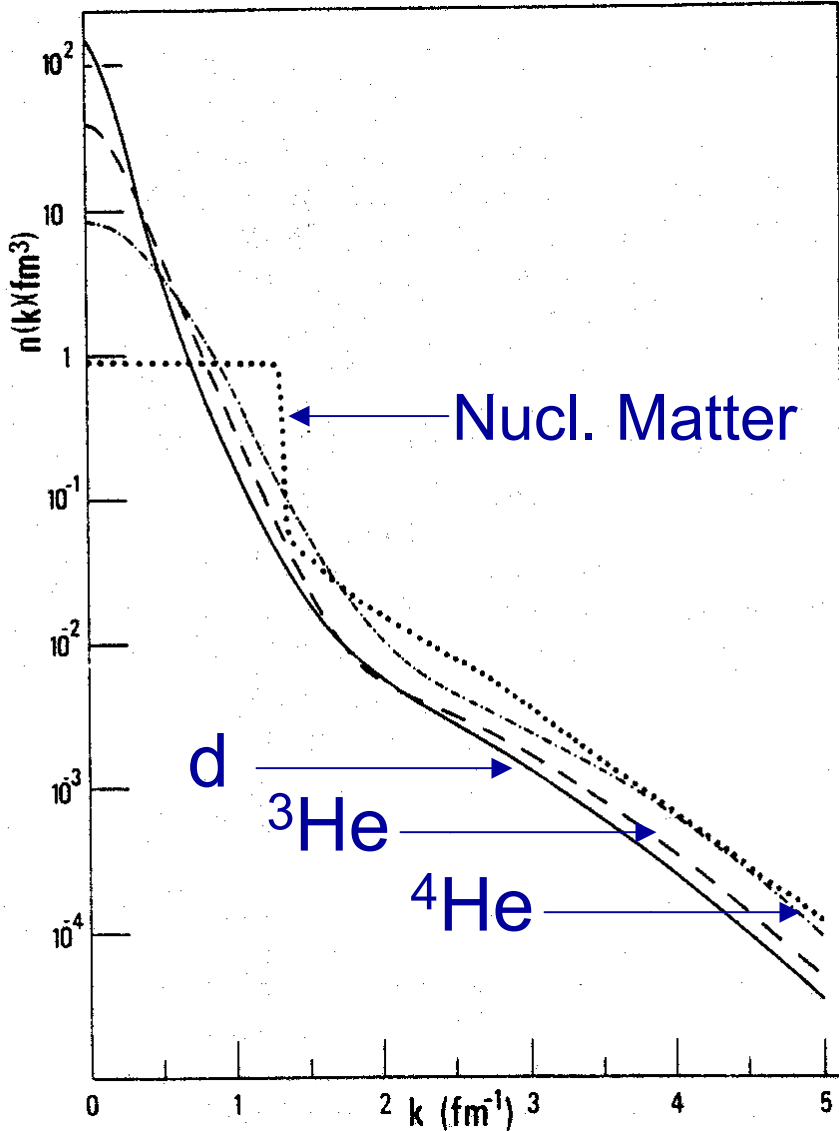
Where does the “missing” strength go?

One possibility:





SRC
dominate
high $k (=p_m)$
and are
related to
large values
of ε_m .



Similar shapes for
few-body nuclei
and nuclear matter
at high k ($=p_m$).

C. Ciofi degli Atti, E. Pace and G. Salmè,
Phys. Lett. **141B**, 14 (1984).

Medium-Modified Nucleons

Searching for Medium Effects on the Nucleon ...

In parallel kinematics:

$$\frac{d^6\sigma}{d\Omega_e d\Omega_p dp d\omega} = \frac{pE}{(2\pi)^3} \sigma_M [v_L R_L + v_T R_T]$$

Can write ep elastic cross section as:

$$\frac{d\sigma}{d\Omega} = f_{rec} \sigma_M [v_L k_L G_E^2 + v_T k_T G_M^2]$$

with $k_L = \frac{|\vec{q}|^2}{Q^2}$ and $k_T = \frac{Q^2}{2m^2}$

Relate R_T/R_L to in-medium proton FF's

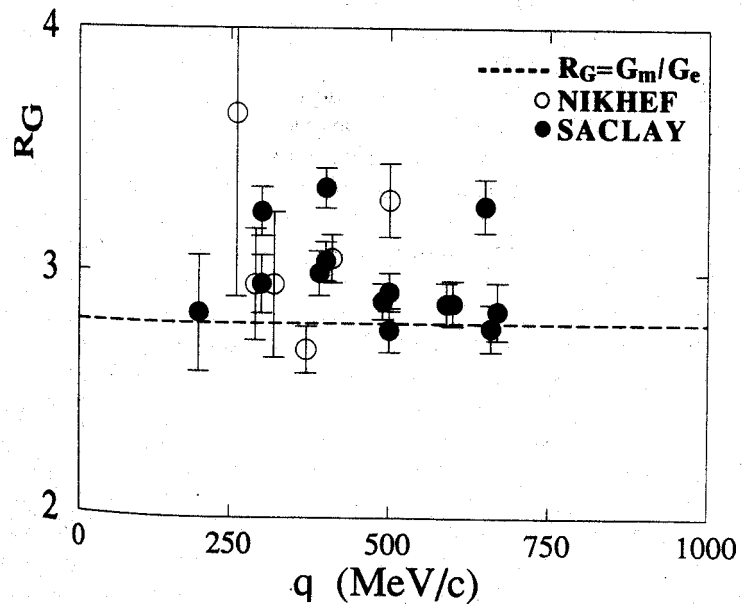
$$R_G \equiv \frac{m|\vec{q}|}{Q^2} \sqrt{\frac{2R_T}{R_L}} \rightarrow \frac{\tilde{G}_M}{\tilde{G}_E}$$

↑
PWIA

This relies on (unrealistic) model assumptions!

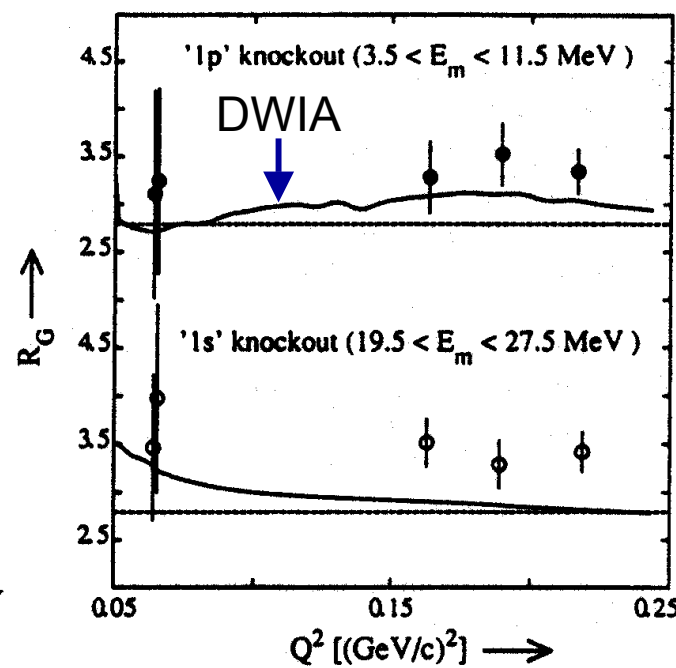
Nonetheless ...

$^2\text{H}(\text{e},\text{e}'\text{p})\text{n}$



J.E. Ducret *et al.*,
Phys. Rev. C **49**, 1783 (1994).

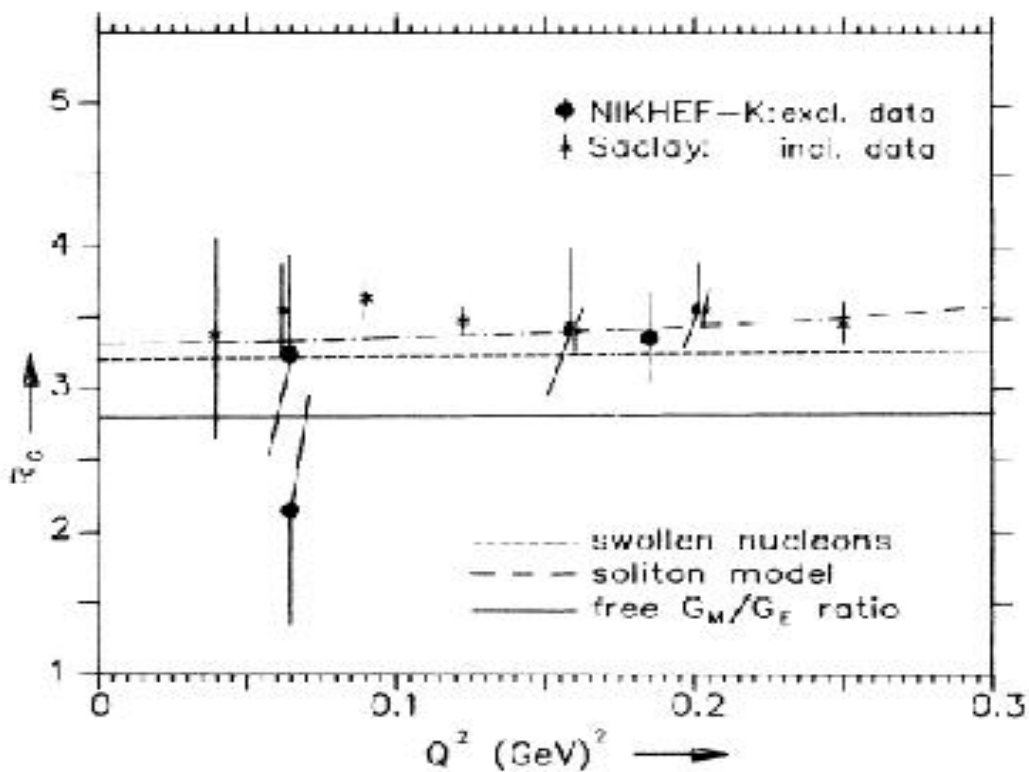
$^6\text{Li}(\text{e},\text{e}'\text{p})$



J.B.J.M. Lanen *et al.*,
Phys. Rev. Lett. **64**, 2250 (1990).

NIKHEF-K
Amsterdam

$^{12}\text{C}(\text{e},\text{e}'\text{p})$ and $^{12}\text{C}(\text{e},\text{e}')$



G. Van der Steenhoven *et al.*,
Phys. Rev. Lett. 57, 182 (1986)

JLab
Hall C

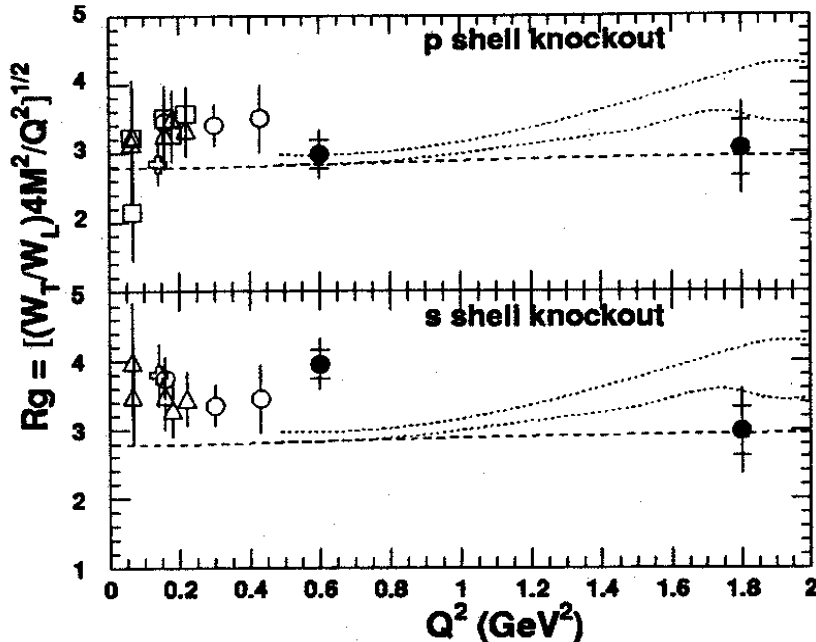
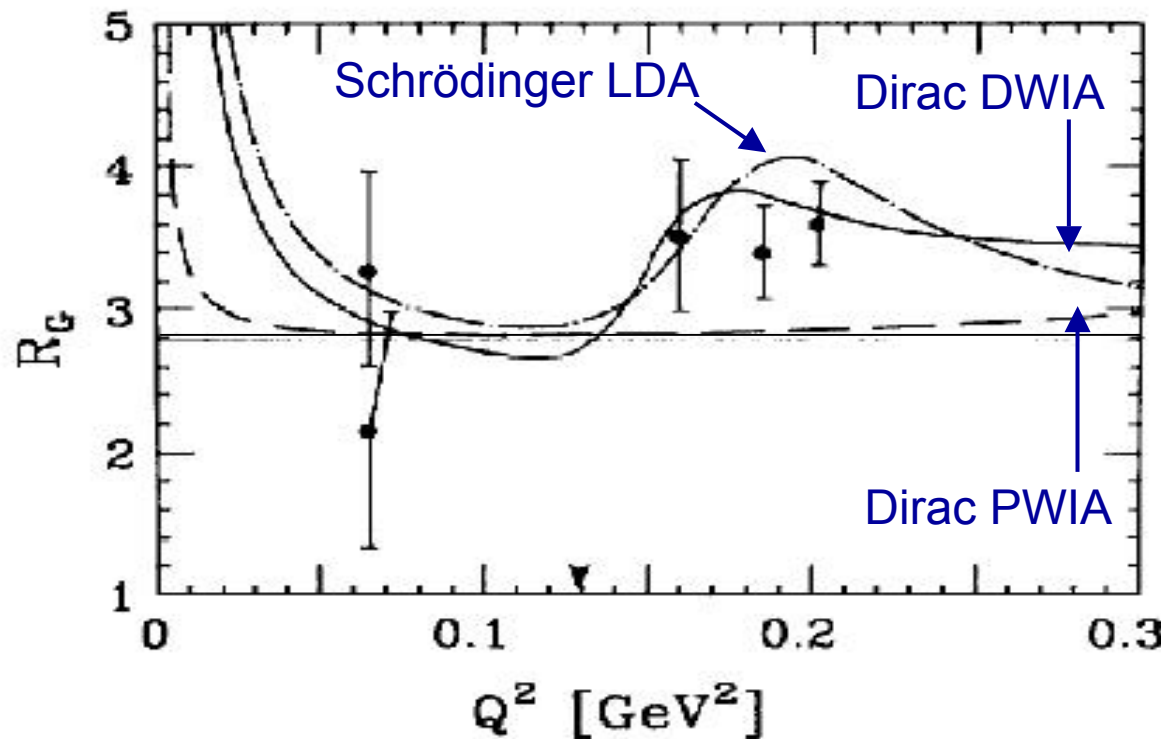


FIG. 3. $R_G = \sqrt{W_T 4M_p^2 / W_L Q^2}$ for ^{12}C (solid) from the measurements of this experiment with ^6Li (p shell: open squares [3], open circles [25], and s shell: open triangles [3], open circles [25]) and ^{12}C (p shell: open cross [1], open triangles [15], and s shell: open cross [1]). The top panel is for the p shell region and bottom panel is for the s shell region. The inner error bar represents that statistical error and the outer error bar includes the systematic error. The dashed line represents R_G for the free proton with the dipole electric and Ref. [18] magnetic form factor while the dotted lines represent the one sigma error band of the recent proton results of Ref. [27].

However, large FSI
effects can mimic this
behavior ...

FSI calculations for ^{16}O $1\text{p}_{3/2}$

Data for ^{12}C $1\text{p}_{3/2}$



T.D. Cohen, J.W. Van Orden, A. Picklesimer,
Phys. Rev. Lett. **59**, 1267 (1987)

Another, less model-dependent,
method ...

Polarization Transfer

Proton Polarization and Form Factors

Free $\vec{e} p$ scattering

$$I_0 P'_x = -2 \sqrt{\tau(1 + \tau)} G_E G_M \tan\left(\frac{\theta_e}{2}\right)$$

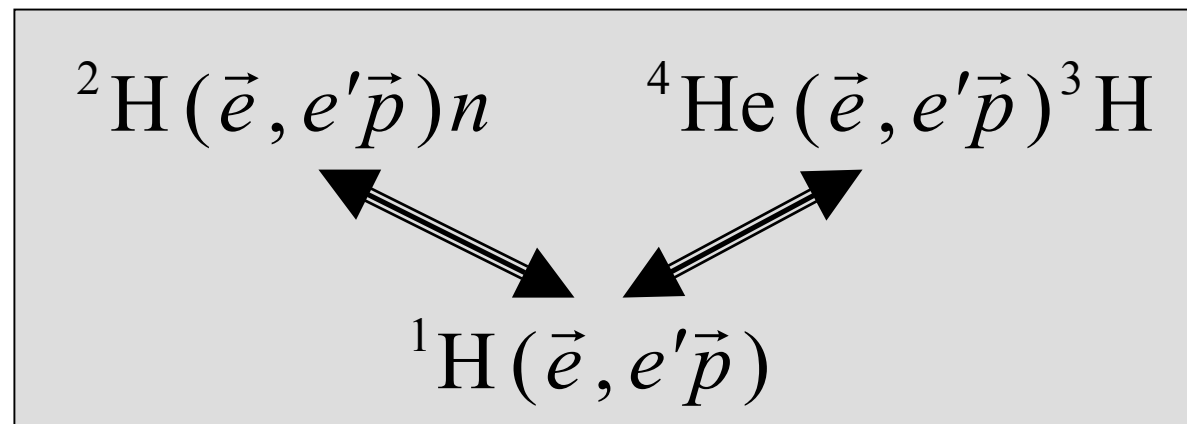
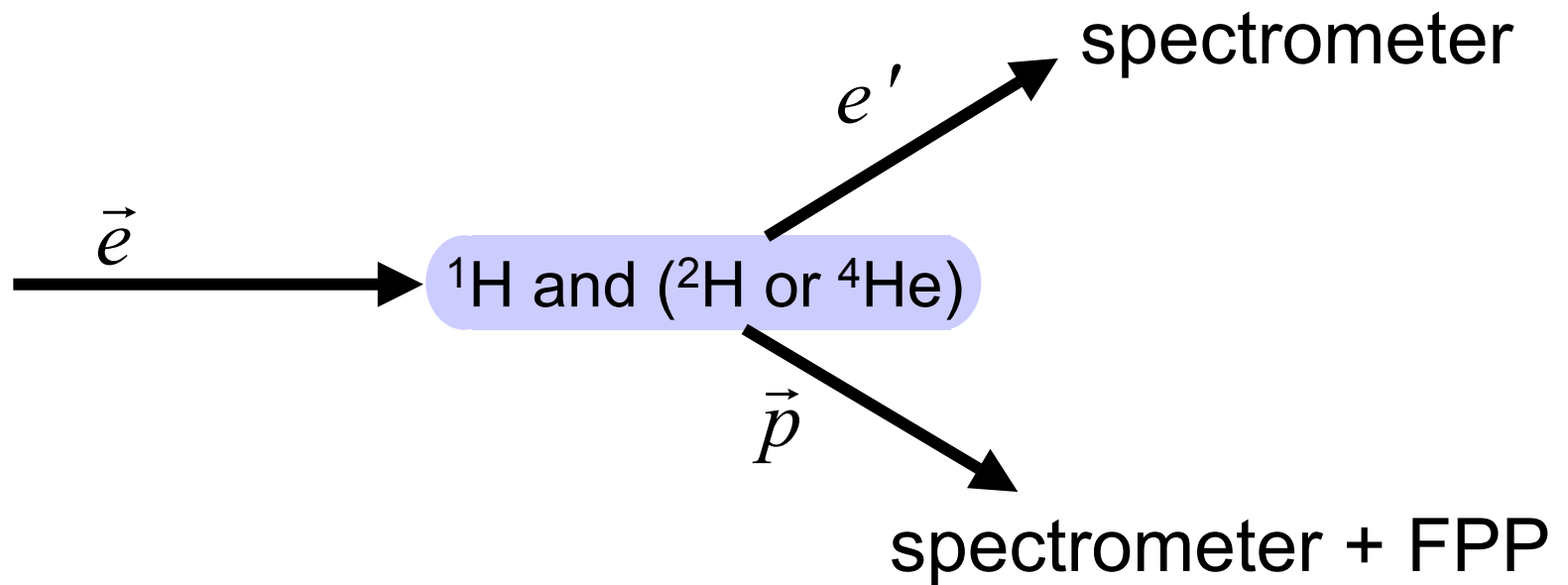
$$I_0 P'_z = \frac{e + e'}{m} \sqrt{\tau(1 + \tau)} G_M^2 \tan^2\left(\frac{\theta_e}{2}\right)$$

$$I_0 = G_E^2 + \tau G_M^2 \left[1 + 2(1 + \tau) \tan^2\left(\frac{\theta_e}{2}\right) \right]$$

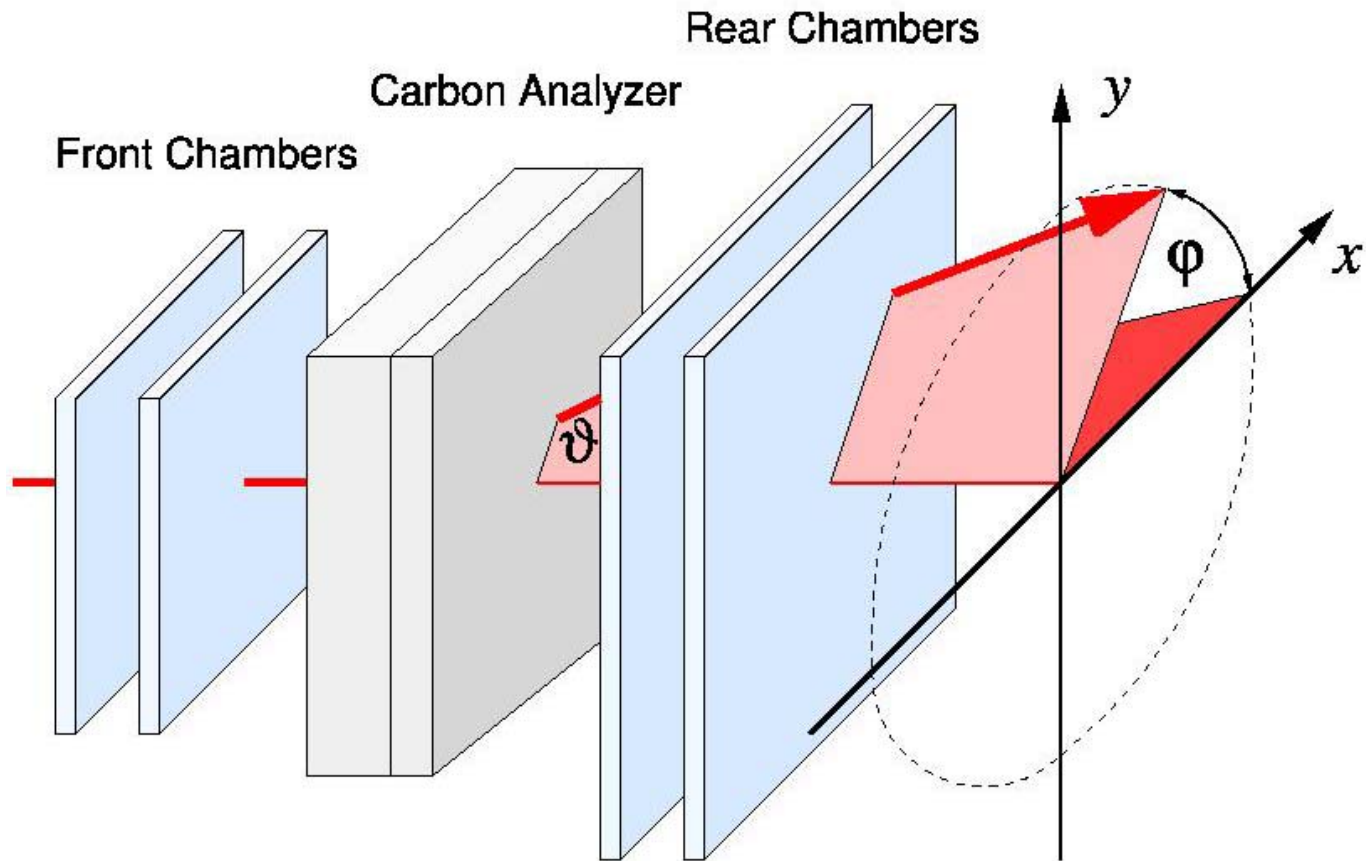
$$\frac{G_E}{G_M} = -\frac{P'_x}{P'_z} \cdot \frac{e + e'}{2m} \tan\left(\frac{\theta_e}{2}\right)$$

R. Arnold, C. Carlson and F. Gross, Phys. Rev. C **23**, 363 (1981)

Polarization Transfer in Hall A



Measuring the Proton Polarization: FPP



Density Dependent Form Factors

Quark-Meson Coupling Model (QMC):

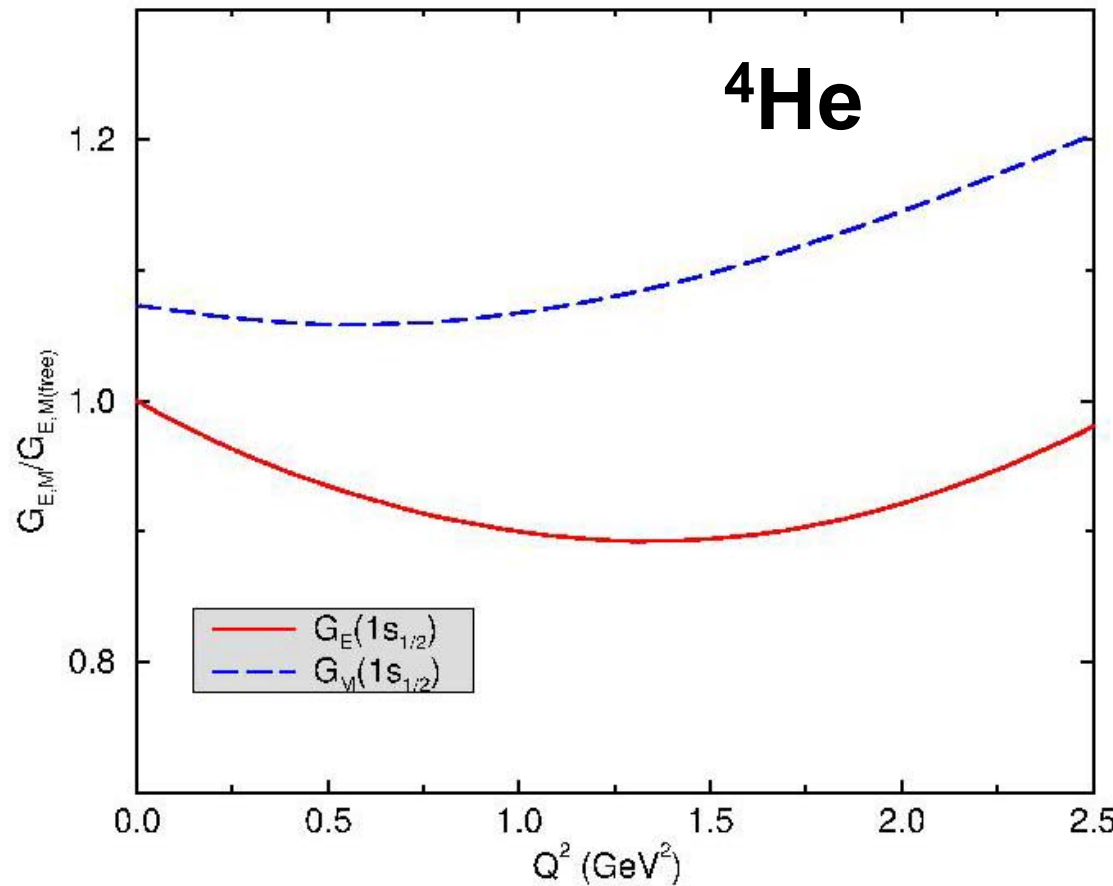
$$\overline{G}_\alpha(Q^2) = \frac{\int d^3r w_\alpha(r) G(Q^2, \rho_B(r))}{\int d^3r w_\alpha(r)}$$

For (e,e'p)

$$w_\alpha = \exp(i\vec{q} \cdot \vec{r}) \chi^{(-)}(\vec{p}', \vec{r})^* \phi_\alpha(r)$$

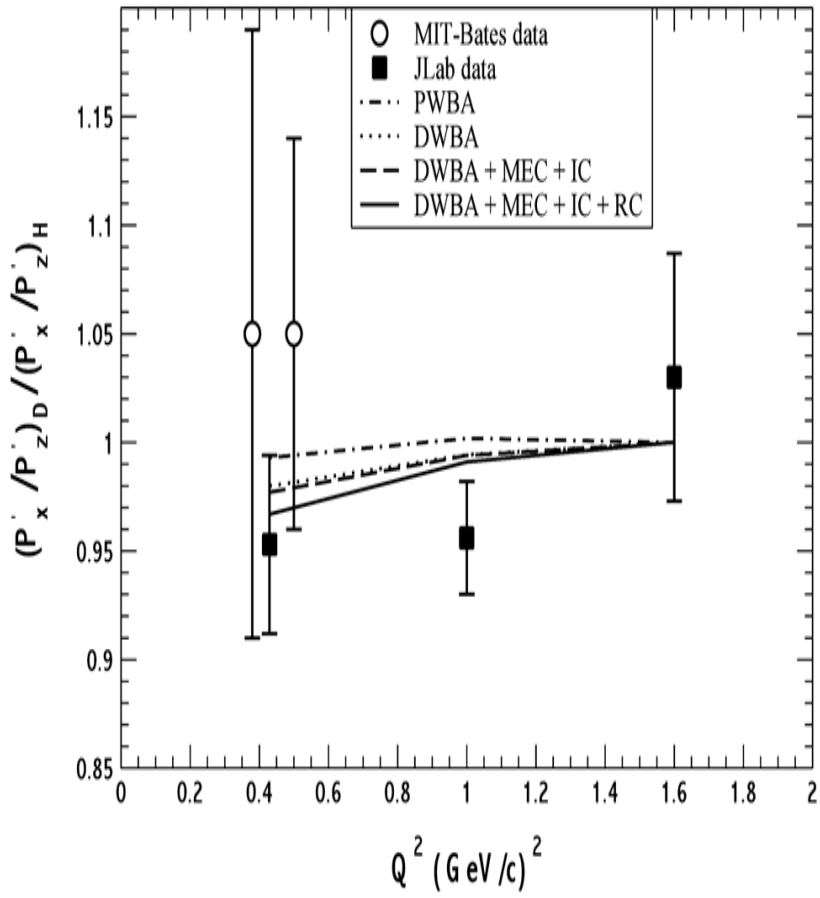
D.H. Lu, , A.W. Thomas, K. Tsushima, A.G. Williams, K. Saito, Phys. Lett. **B** 417, 217 (1998).

Quark-Meson Coupling Model



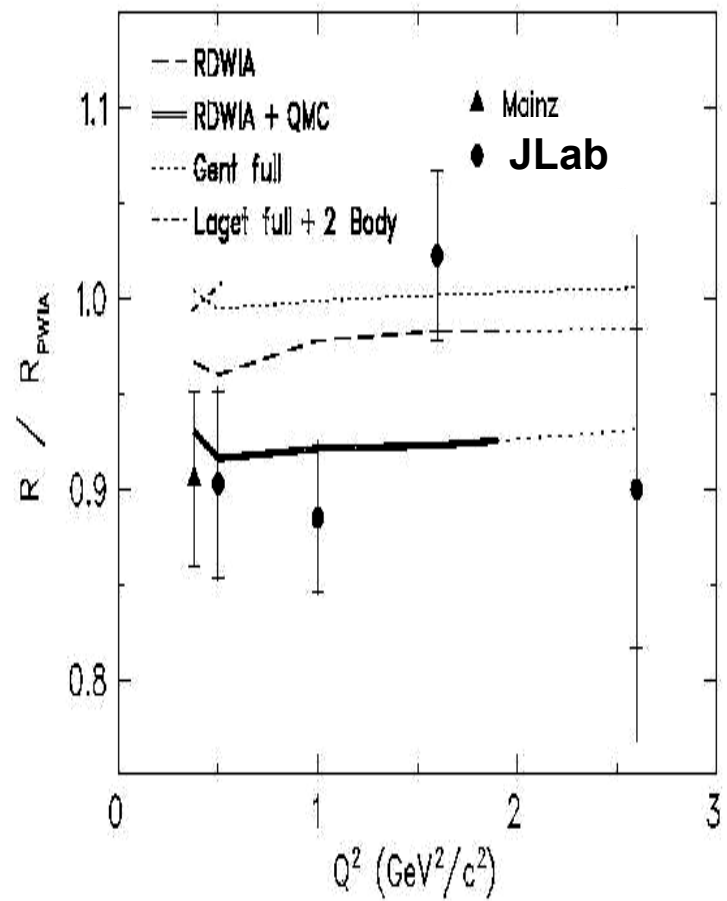
D.H. Lu, K. Tsushima, A.W. Thomas, A.G. Williams and K. Saito,
Phys. Lett. **B417**, 217 (1998) and Phys. Rev. C **60**, 068201 (1999).

$^2\text{H}(\vec{e}, e' \vec{p})n$



Calculations by Arenhövel

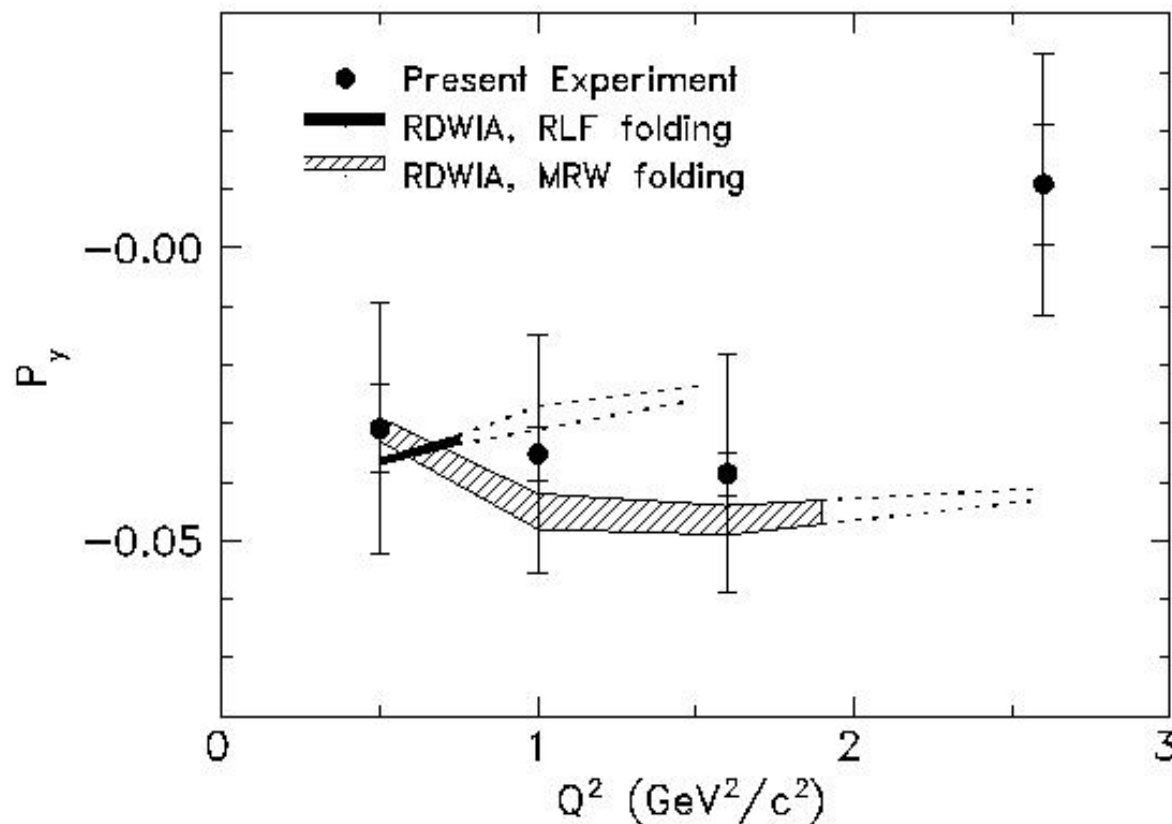
$^4\text{He}(\vec{e}, e' \vec{p})^3\text{H}$



RDWIA calculations by Udias *et al.*

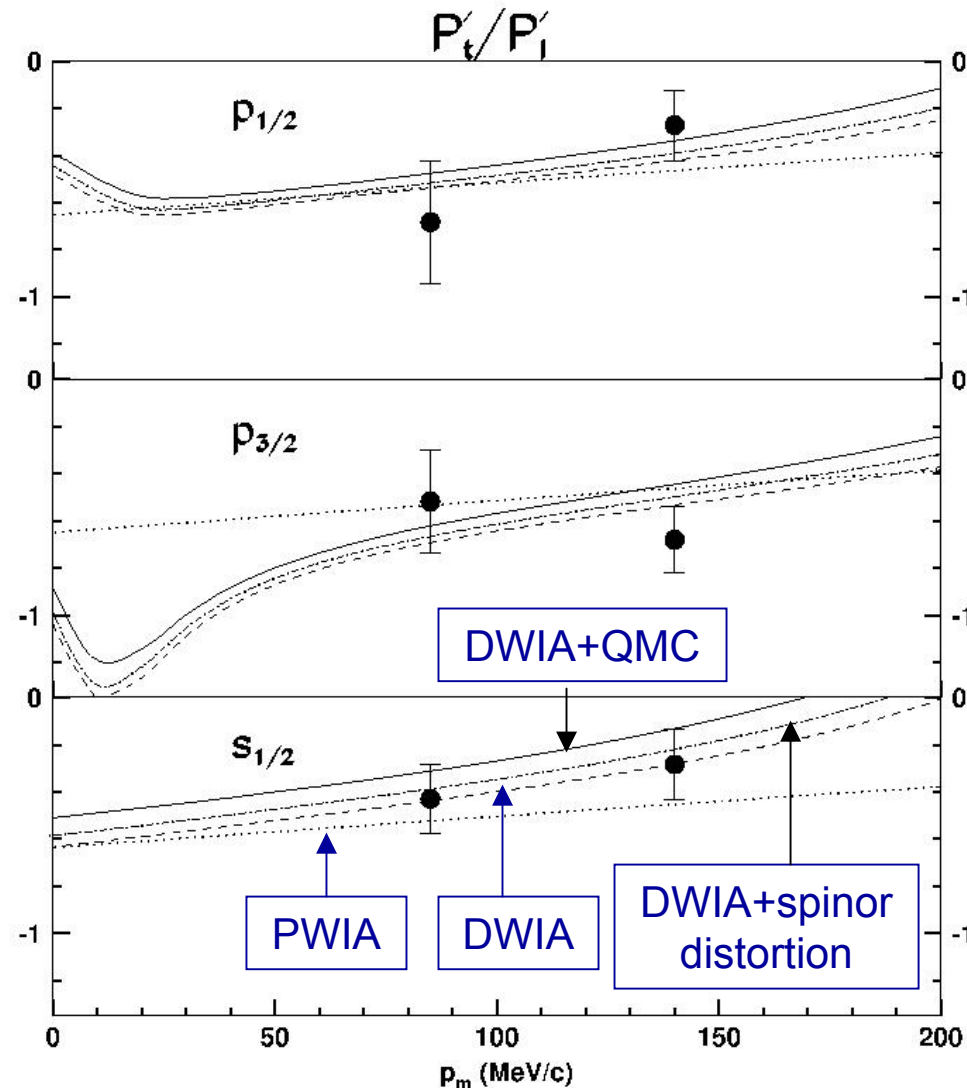
Induced Polarization – ${}^4\text{He}$

JLab E93-049



$P_y=0$ in PWIA: test of FSI

$^{16}\text{O}(\vec{e}, e' \vec{p})^{15}\text{N}$ at $Q^2 = 0.8 (\text{GeV}/c)^2$

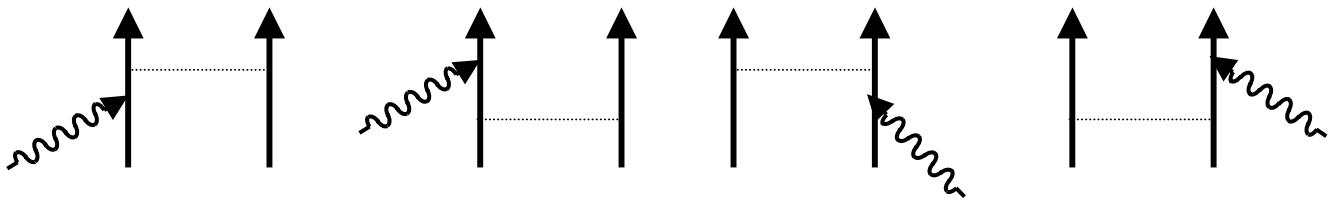


S. Malov *et al.*, Phys. Rev. C **62**, 057302 (2000).

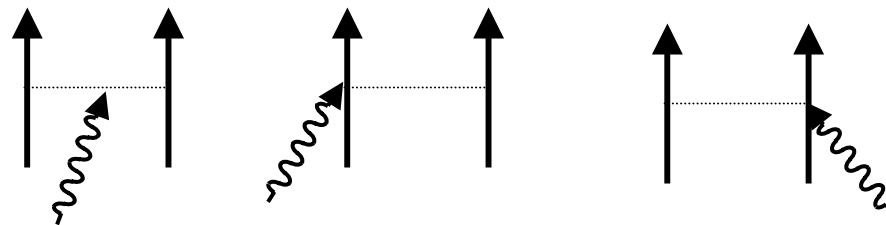
Studies of the Reaction Mechanism

Correlations and Interaction Currents

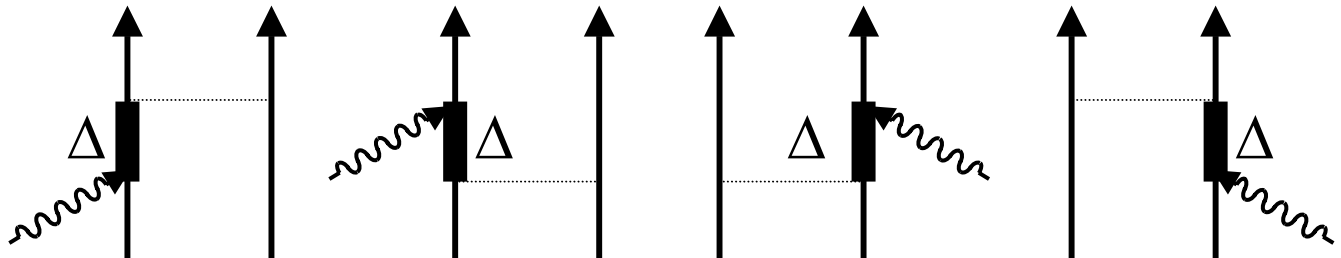
Correlations



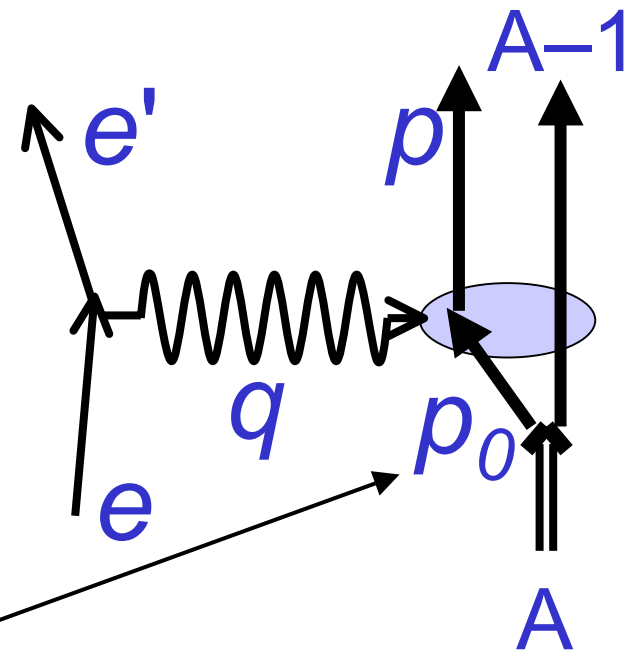
MEC's



IC's



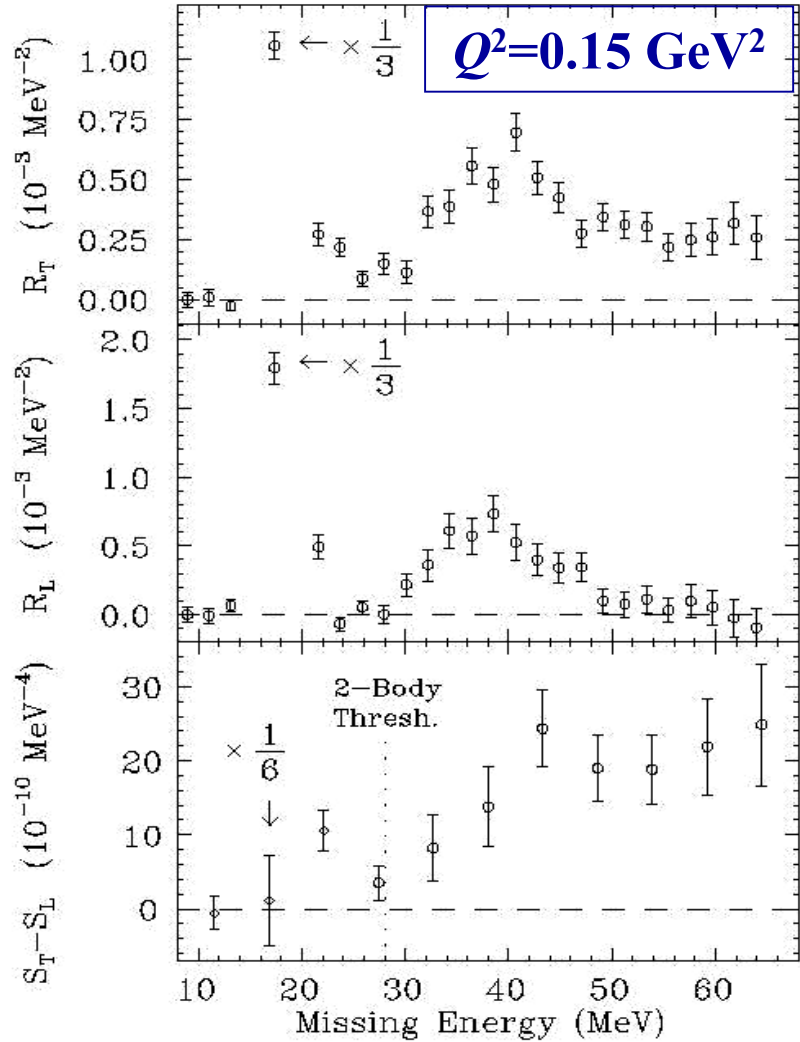
Off-shell Effects



initial proton is bound

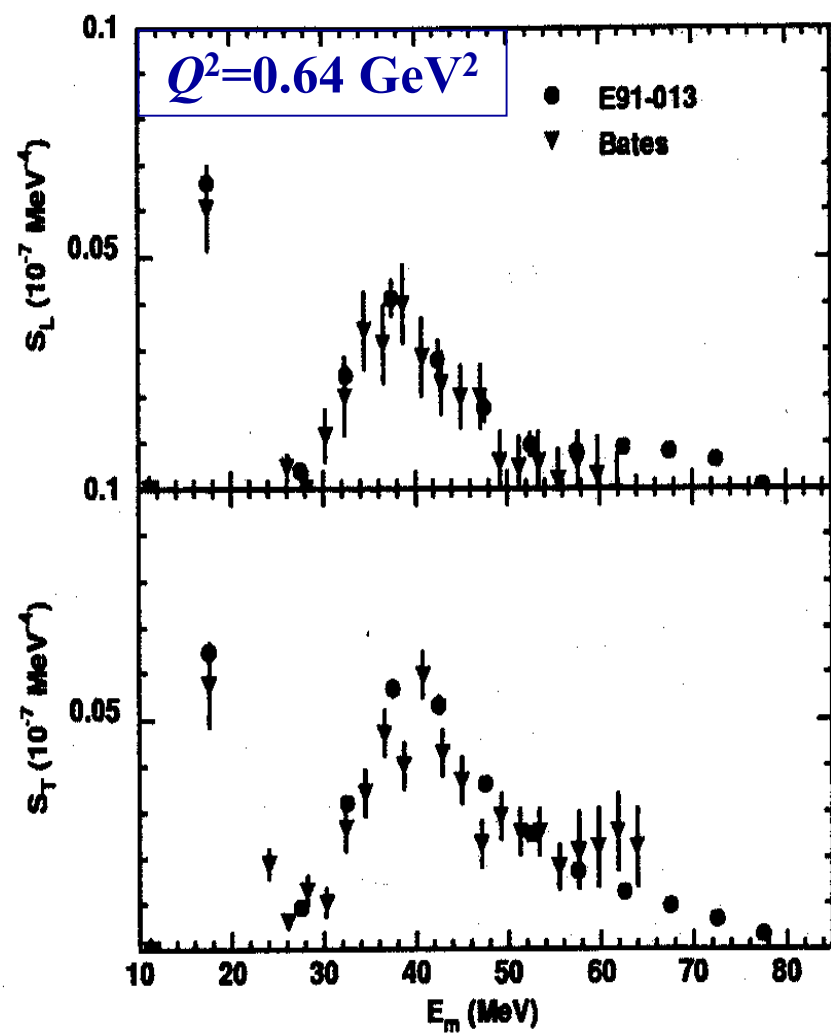
Vertex function is not well defined. The “Gordon identity” leads to alternative forms, equivalent only when proton is on-shell.

$^{12}\text{C}(\text{e},\text{e}'\text{p})$ L/T Separations



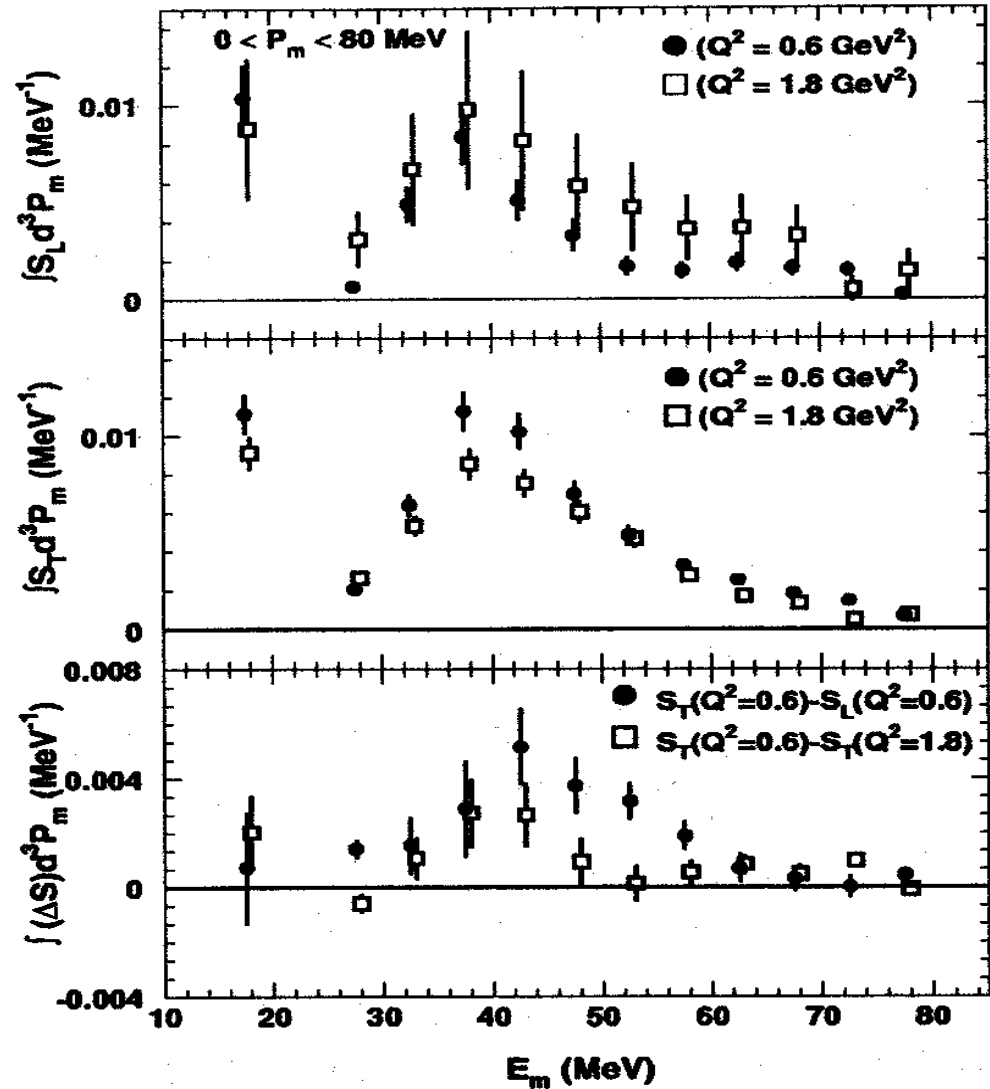
P.E. Ulmer *et al.*, Phys. Rev. Lett. **59**, 2259 (1987).

Bates Linear Accelerator



D. Dutta *et al.*, Phys. Rev. C **61**, 061602 (2000).

JLab Hall C

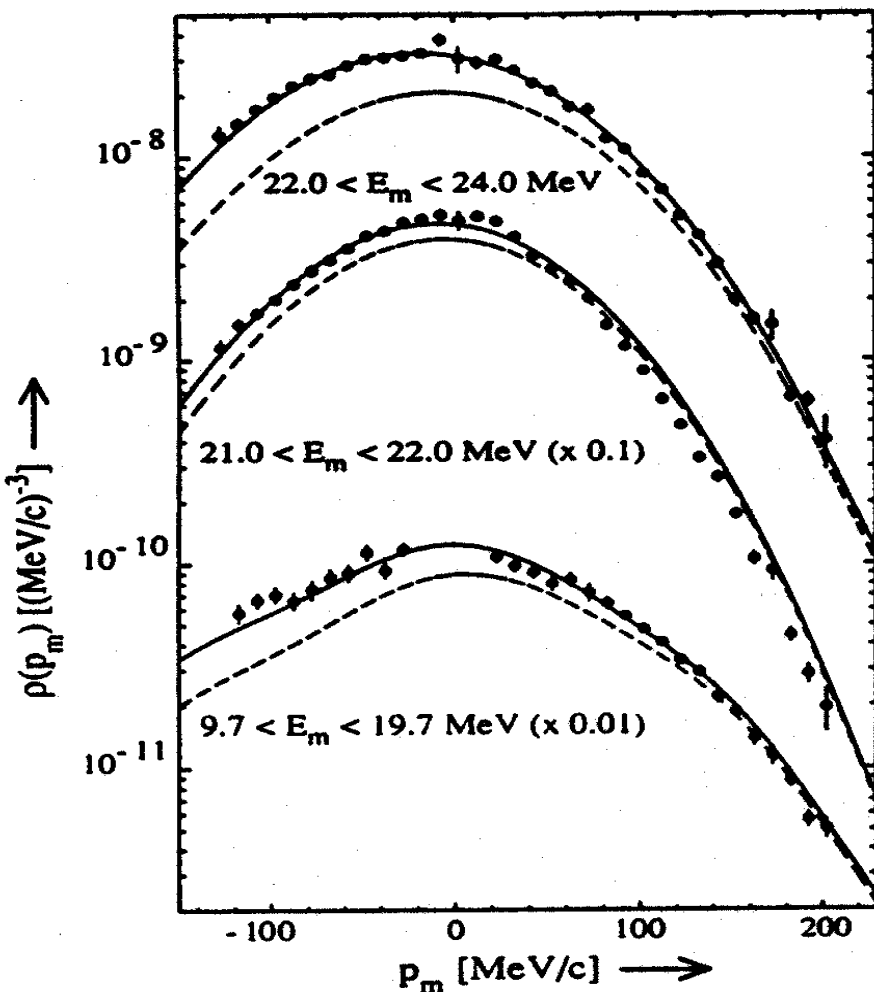


Excess transverse strength at high ε_m .
Persists, though perhaps declines, at higher Q^2 .

JLab Hall C

D. Dutta *et al.*, Phys. Rev. C 61, 061602 (2000).

${}^6\text{Li}(\text{e},\text{e}'\text{p})$ T/L Ratio



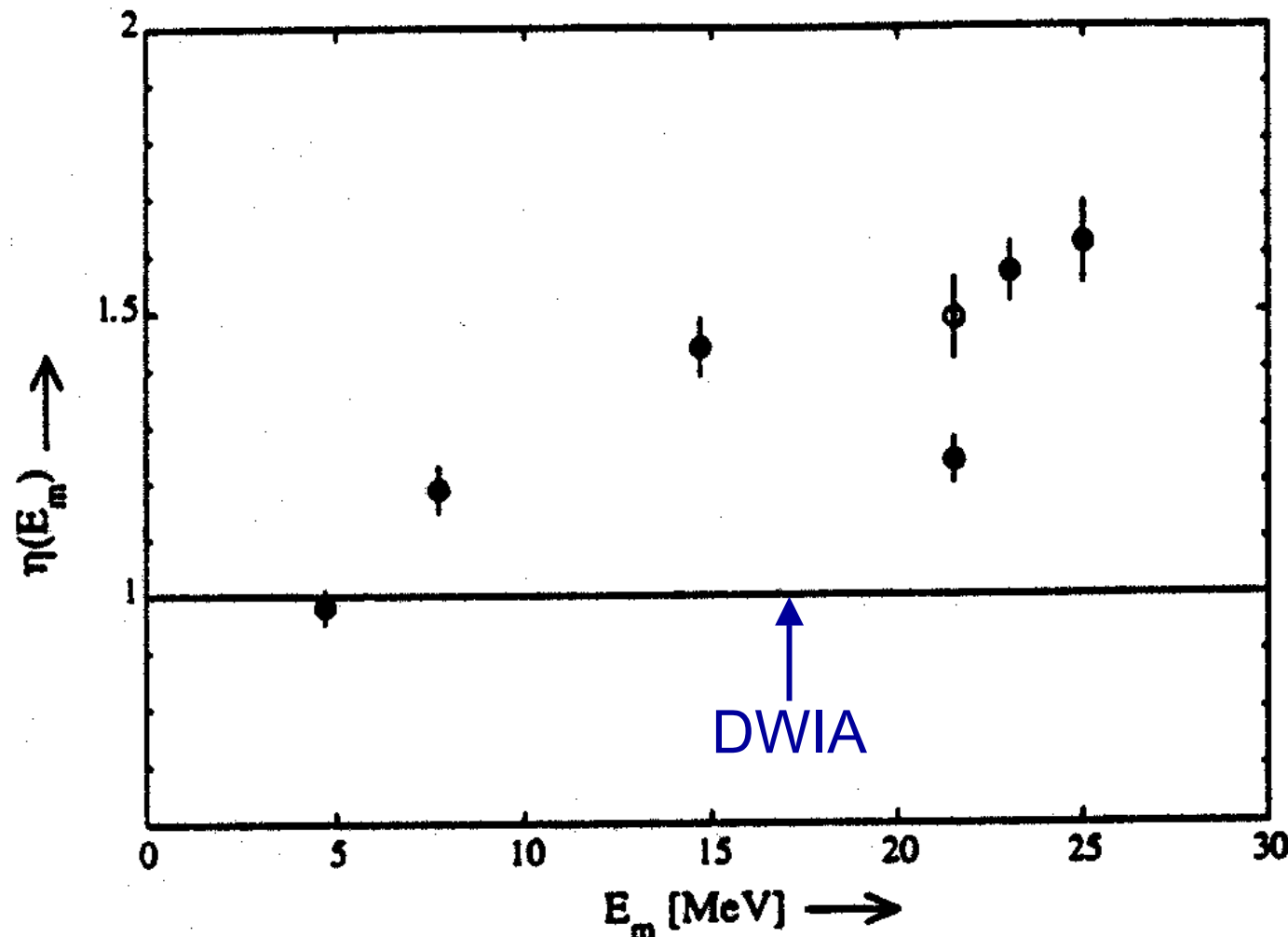
DWIA (dashed) fails to describe overall strength.

Scaling transverse amplitude in DWIA (solid) gives good agreement → deduce scale factor, η .

NIKHEF-K
Amsterdam

J.B.J.M. Lanen *et al.*, Phys. Rev. Lett. **64**, 2250 (1990).

${}^6\text{Li}(\text{e},\text{e}'\text{p})$ T/L Ratio



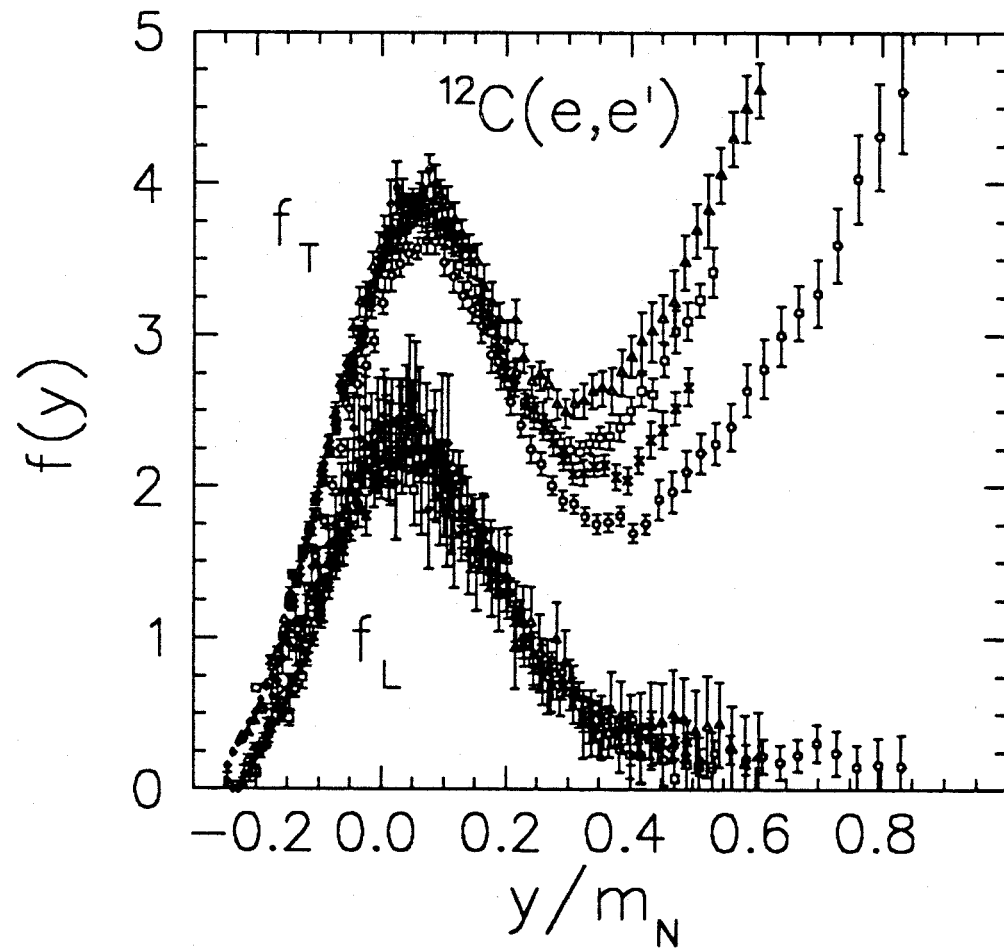
J.B.J.M. Lanen *et al.*, Phys. Rev. Lett. **64**, 2250 (1990).

The L/T separations suggest

- Additional transverse reaction mechanism above 2-nucleon emission threshold.
- MEC's primarily transverse in character. Suggestive of two-body current.

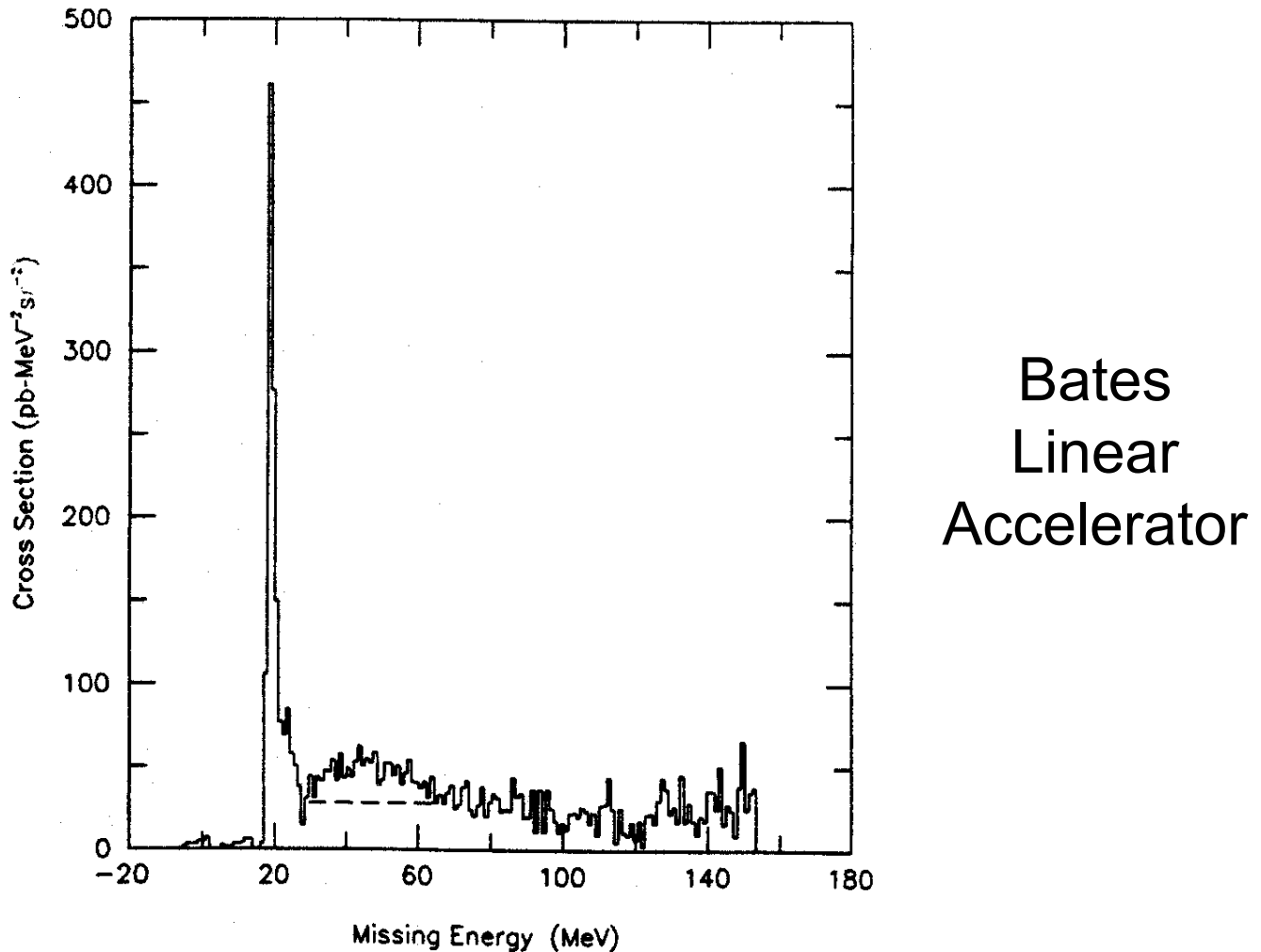
Reminiscent of ...

T/L anomaly
in inclusive
(e,e'):



J.M. Finn, R.W. Lourie and B.H. Cottman, Phys. Rev. C **29**, 2230 (1984).

$^{12}\text{C}(\text{e},\text{e}'\text{p})$ in “Dip Region”



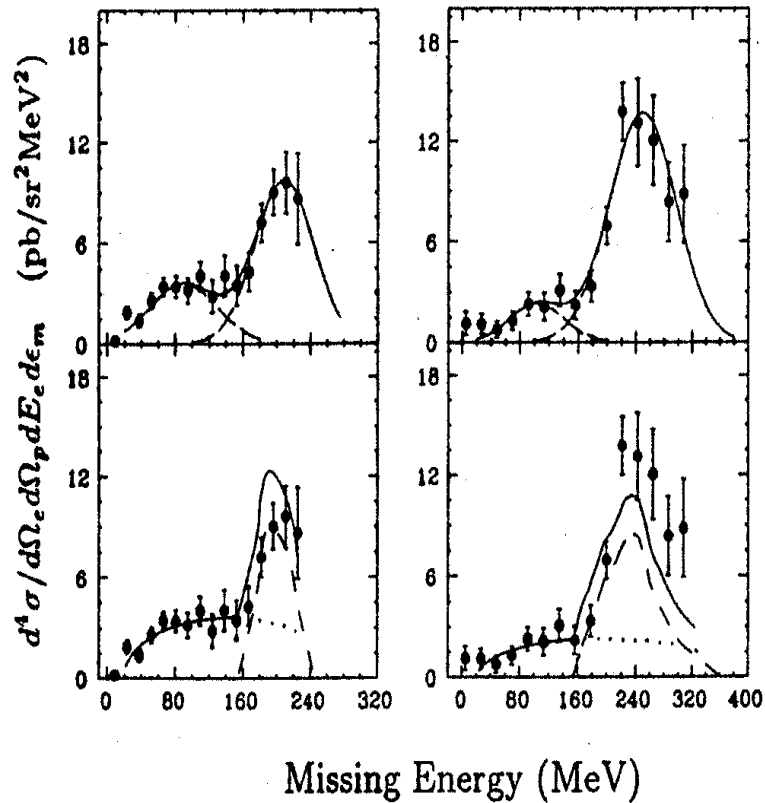
R.W. Lourie *et al.*, Phys. Rev. Lett. **56**, 2364 (1986).

Data from: Bates Linear Accelerator

$^{12}\text{C}(\text{e},\text{e}'\text{p})$

“Delta”

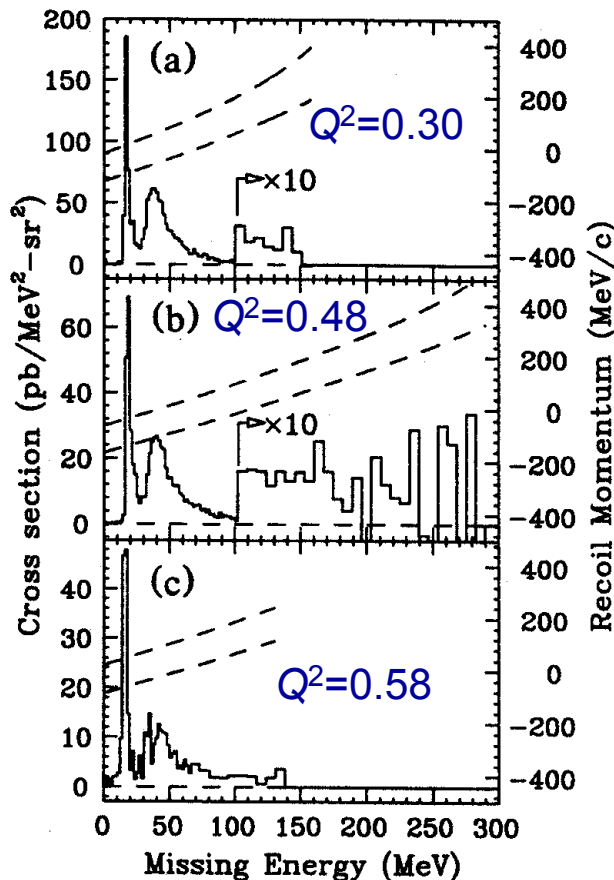
Between dip and Δ



H. Baghaei *et al.*,
 Phys. Rev. C **39**, 177 (1989).

Bates Linear Accelerator

Quasielastic



L.B. Weinstein *et al.*,
 Phys. Rev. Lett. **64**, 1646 (1990).

Bates Linear Accelerator

$^{12}\text{C}(\text{e},\text{e}'\text{p})$ $q=990 \text{ MeV}/c$, $\omega=475 \text{ MeV}$

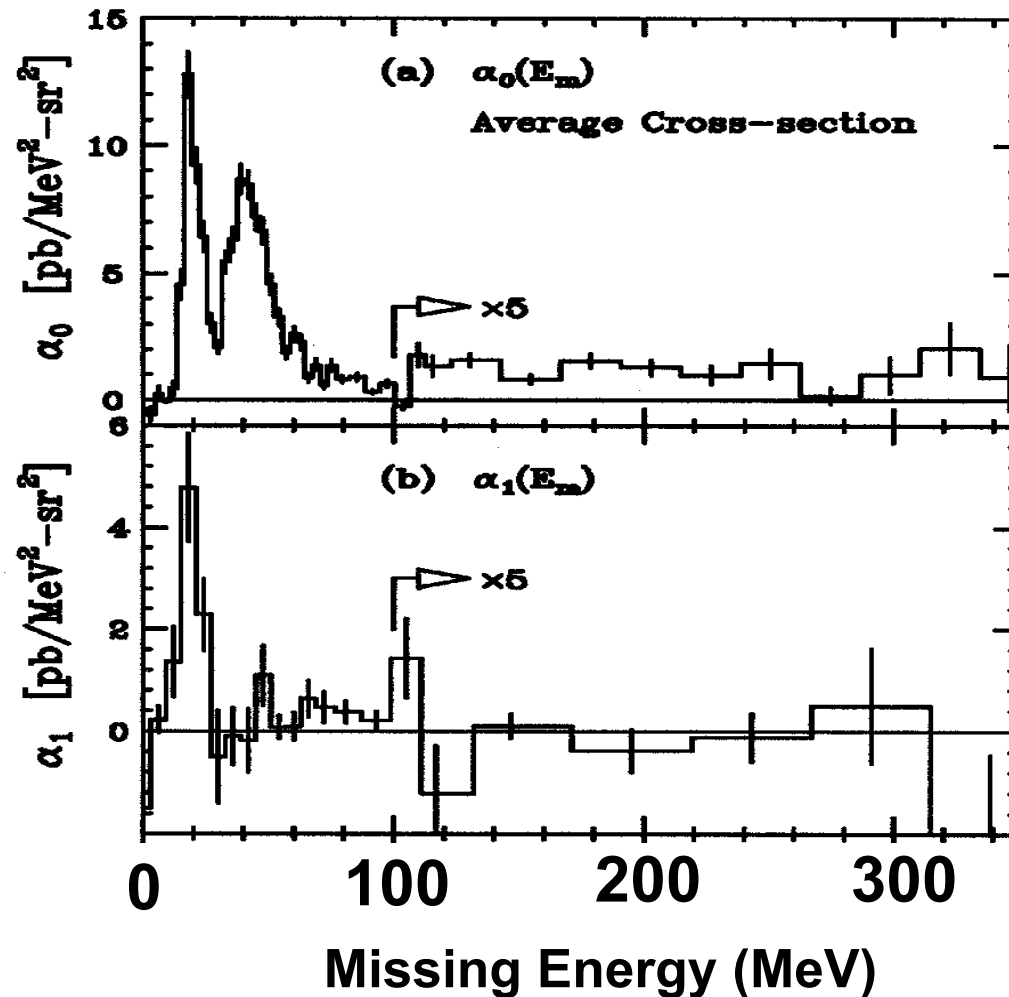


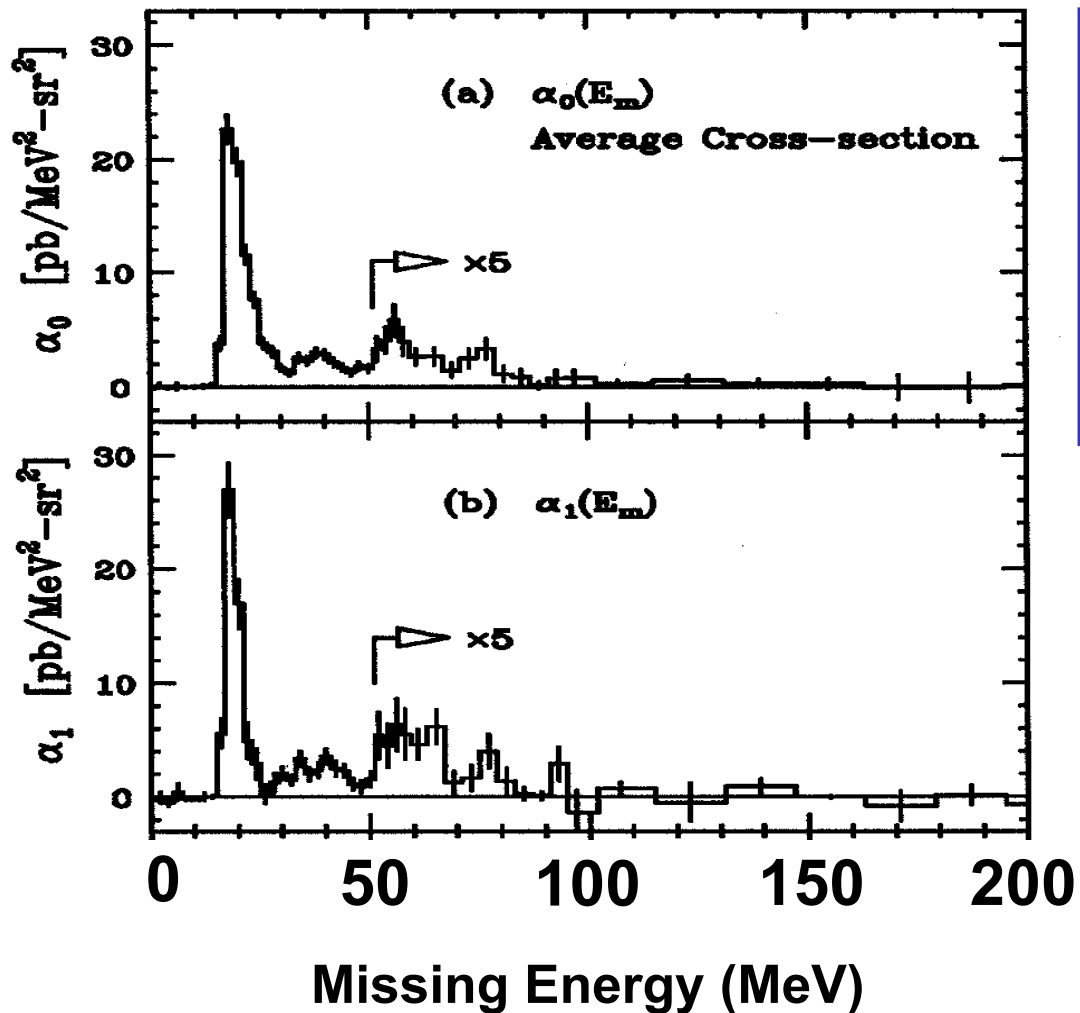
Figure adapted from J.H. Morrison *et al.*,
Phys. Rev. C **59**, 221 (1999).

$$\frac{d^6\sigma}{d\Omega_e d\Omega_p d\omega d\varepsilon_m} = \sum_{l=0}^{l_{\max}} \alpha_l(\varepsilon_m) P_l\left(\frac{\omega - \omega_0}{\Delta\omega/2}\right)$$

For $60 < \varepsilon_m < 100 \text{ MeV}$,
continuum cross section
increases strongly with ω .
Large continuum strength
continues up to 300 MeV.

Bates Linear
Accelerator

$^{12}\text{C}(\text{e},\text{e}'\text{p})$ $q=970 \text{ MeV}/c$, $\omega=330 \text{ MeV}$



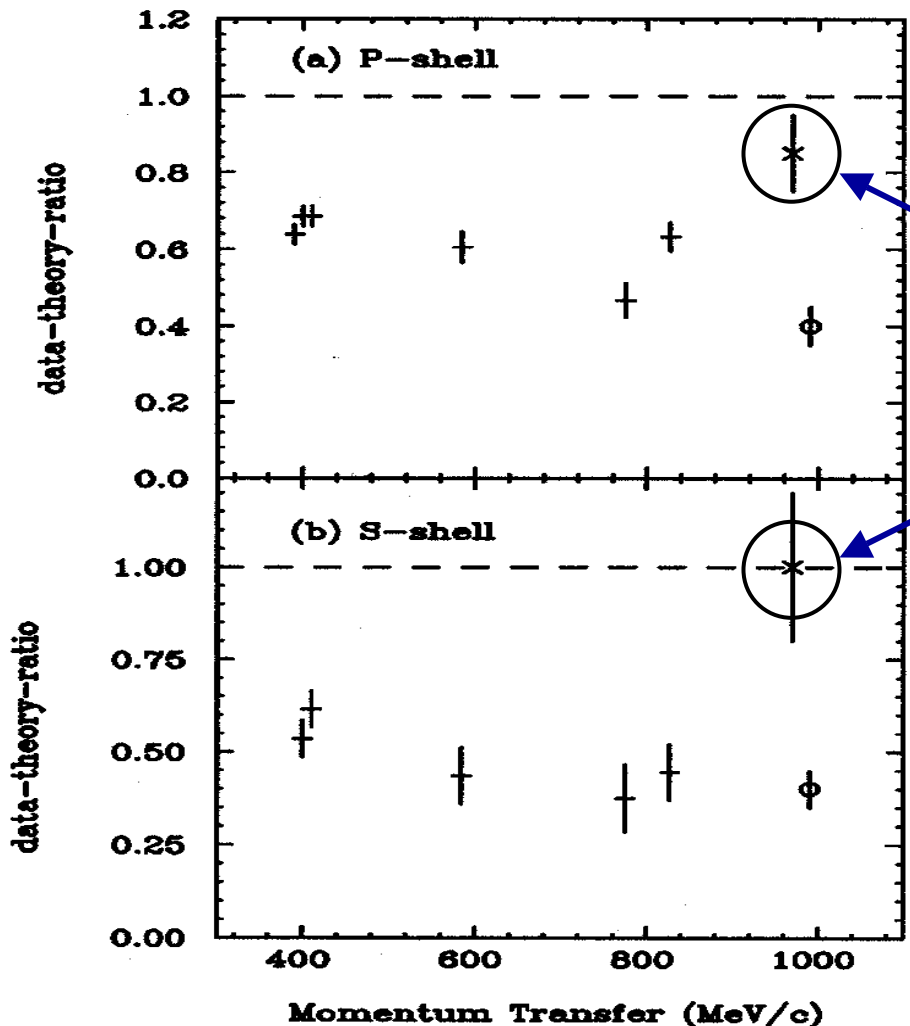
$$\frac{d^6\sigma}{d\Omega_e d\Omega_p d\omega d\varepsilon_m} = \sum_{l=0}^{l_{\max}} \alpha_l(\varepsilon_m) P_l\left(\frac{\omega - \omega_0}{\Delta\omega/2}\right)$$

Continuum strength increases strongly with ω .
Continuum cross section is smaller at high ε_m .

Figure adapted from J.H. Morrison *et al.*,
Phys. Rev. C **59**, 221 (1999).

Bates Linear Accelerator

$^{12}\text{C}(\text{e},\text{e}'\text{p})$

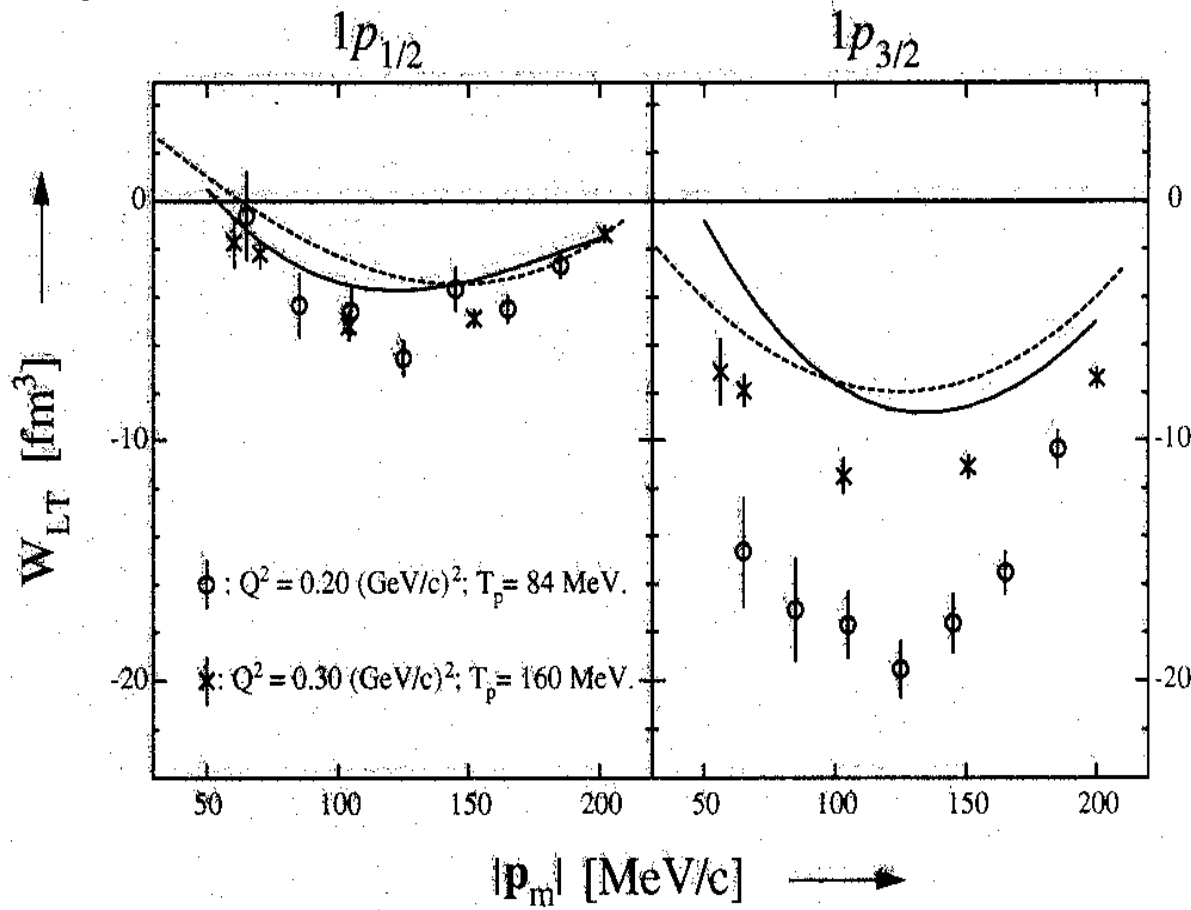


For $\omega < \omega_{QE}$,
spectroscopic
factors
consistent with
naïve
expectations.

Bates Linear
Accelerator

J.H. Morrison *et al.*, Phys. Rev. C 59, 221 (1999).

$^{16}\text{O}(\text{e},\text{e}'\text{p})$



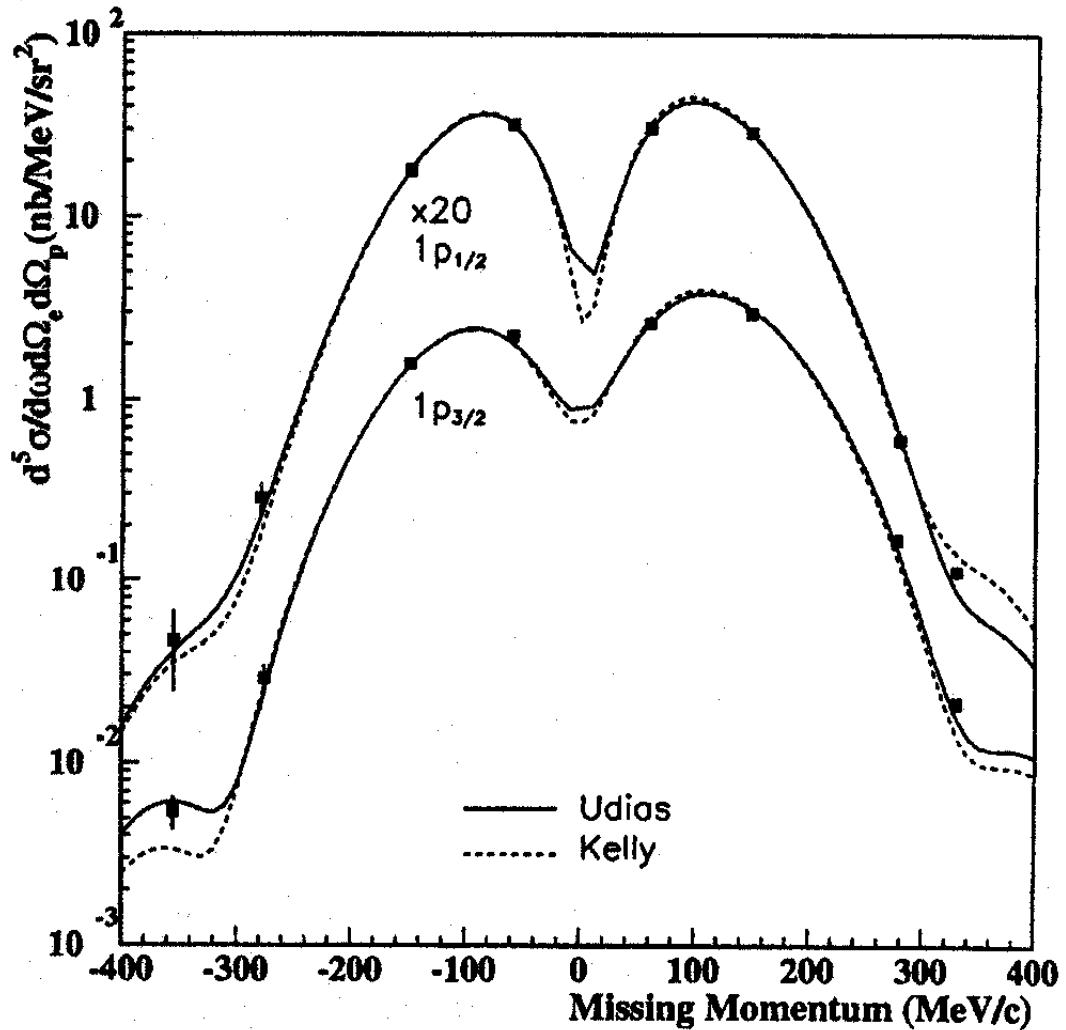
Large discrepancy for $1p_{3/2}$.
 Relativistic effects predicted to be small here.
 Two-body currents responsible??

C.M. Spaltro et al., Phys. Rev. C **48**, 2385 (1993).

Circles (solid) – NIKHEF-K

Crosses (dashed) - Saclay

$^{16}\text{O}(\text{e},\text{e}'\text{p})$ $Q^2=0.8 \text{ GeV}^2$ Quasielastic

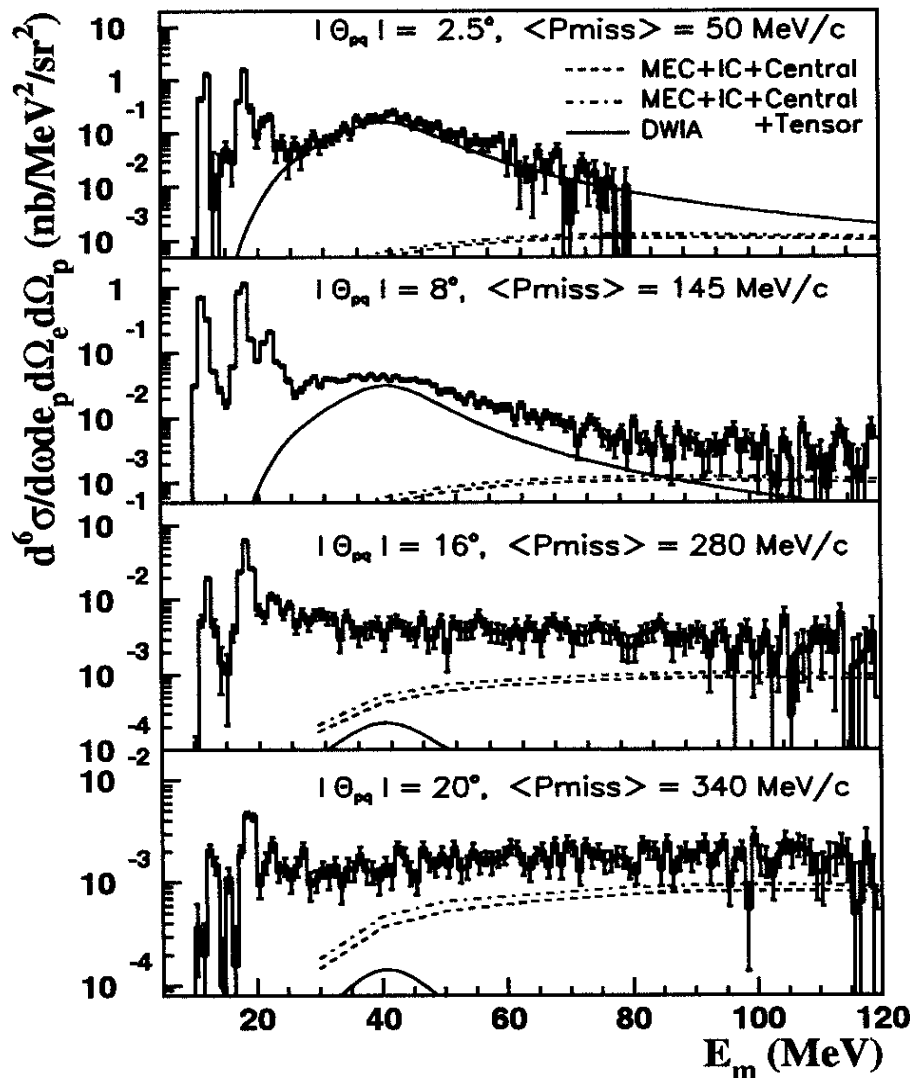


Relativistic
DWIA gives
good
agreement
with data.

JLab Hall A

J. Gao *et al.*, Phys. Rev. Lett. **84**, 3265 (2000).

$^{16}\text{O}(\text{e},\text{e}'\text{p})$ $Q^2=0.8 \text{ GeV}^2$ Quasielastic



Two-body calculations of Ryckebusch *et al.*, give flat distribution, as seen in the data, but underpredict by a factor of two.

JLab Hall A

N. Liyanage *et al.*, Phys. Rev. Lett. 86, 5670 (2001).

**At high energies, R_{LT}
interference response
function sensitive to
relativistic effects.**

**For example, spinor
distortion ...**

Spinor Distortions

$$\Psi = \begin{pmatrix} \Psi_+ \\ \Psi_- \end{pmatrix}$$

$$\Psi_- = \frac{\sigma \cdot p}{E + m + S - V} \Psi_+$$

N.R. reduction

$S + V \rightarrow$ Mean field

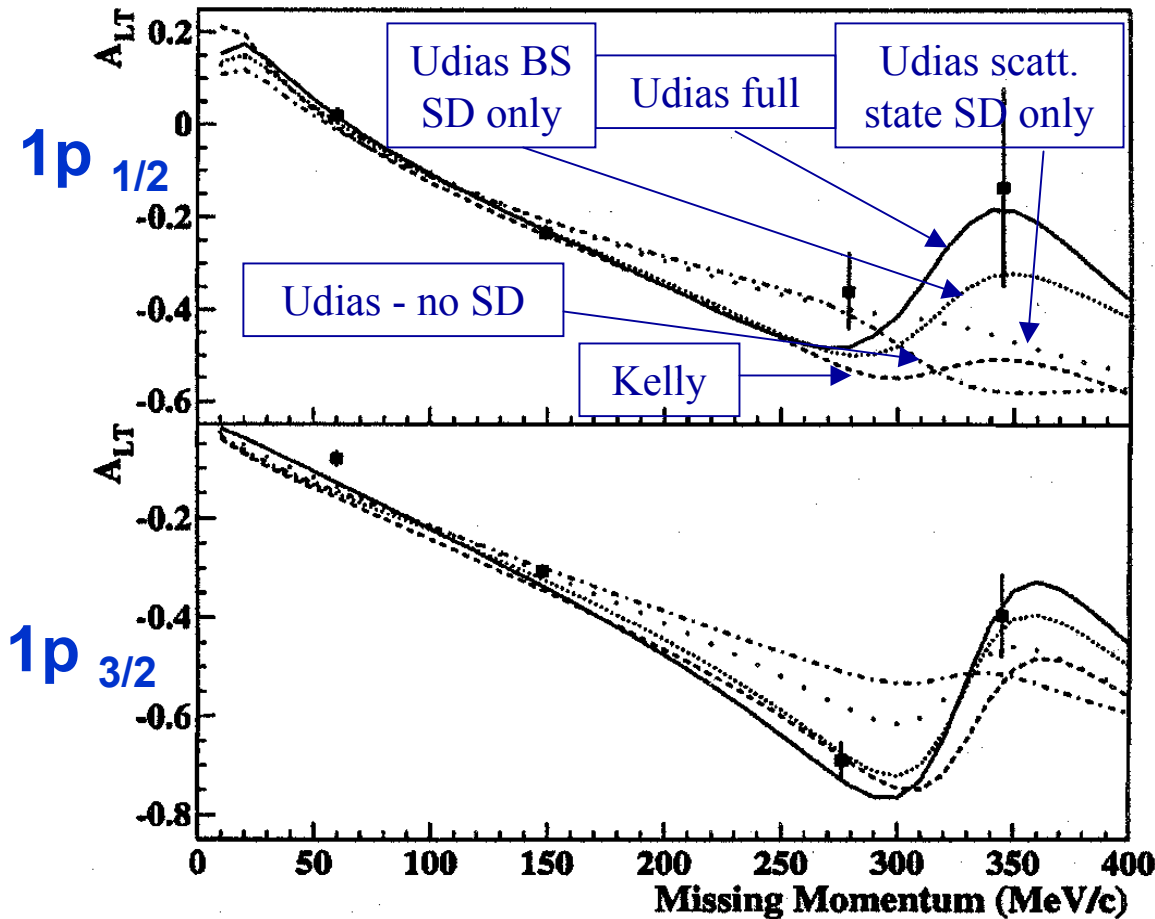
$S + V$ relatively small

Dirac spinor

$S - V$ affects lower components

$S - V$ large

$^{16}\text{O}(\text{e},\text{e}'\text{p}) Q^2=0.8 \text{ GeV}^2$ Quasielastic



Sensitive
to “spinor
distortions”

JLab Hall A

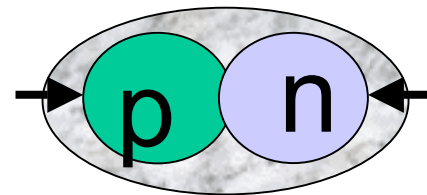
J. Gao *et al.*, Phys. Rev. Lett. **84**, 3265 (2000).

Few-body
Nuclei ...

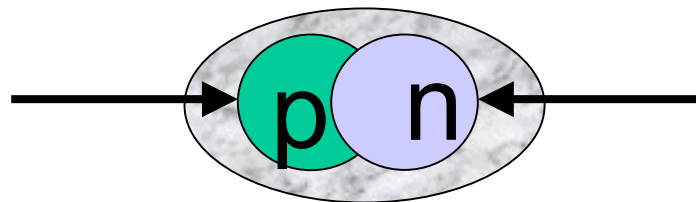
The Deuteron

Short-distance Structure

Low p_m

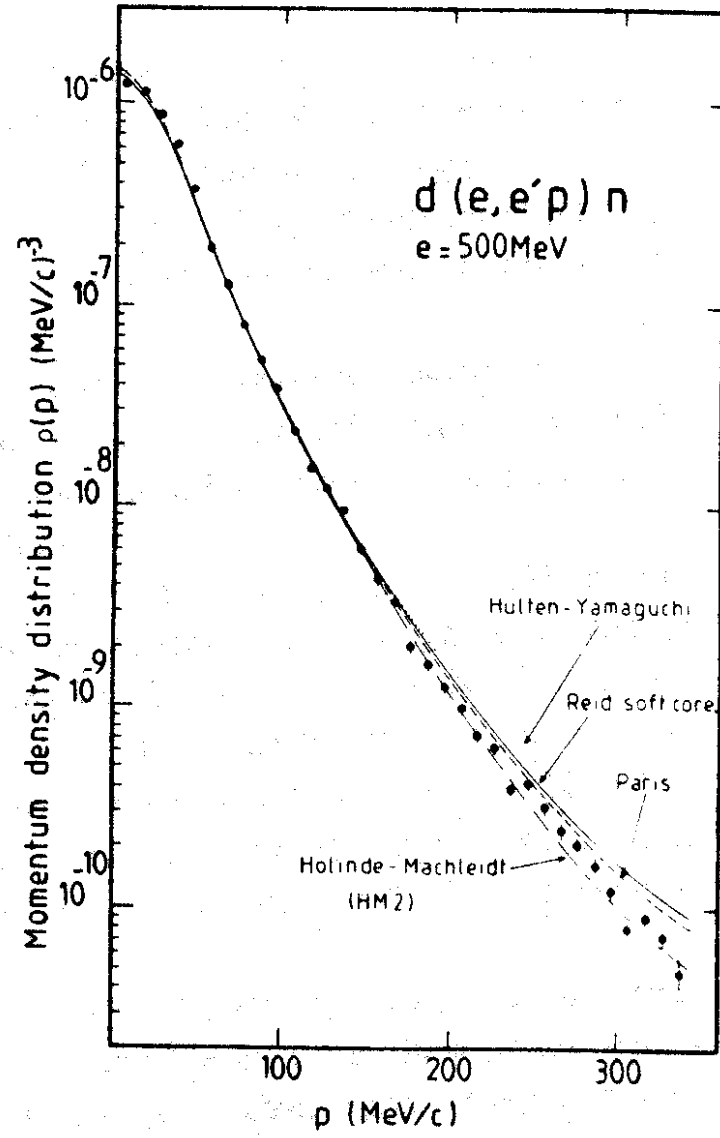


High p_m



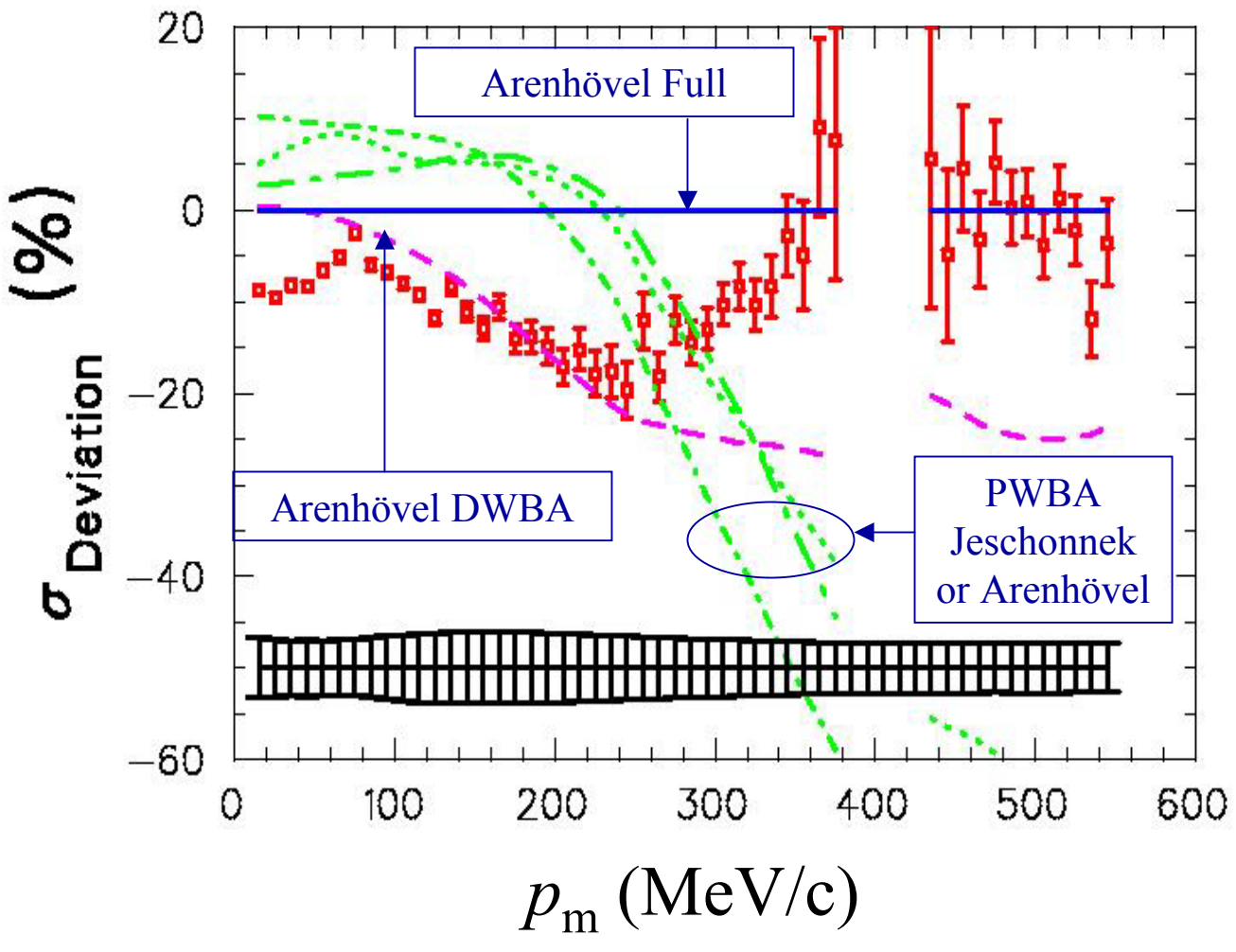
For large overlap, nucleons may lose individual identities:

Quark/gluon d.o.f.?



Saclay
Linac,
France

M. Bernheim *et al.*, Nucl. Phys. **A365**, 349 (1981).



Large FSI/non-nucleonic effects.
Problem at $p_m=0$.

P.E. Ulmer *et al.*, Phys. Rev. Lett. **89**, 062301 (2002).

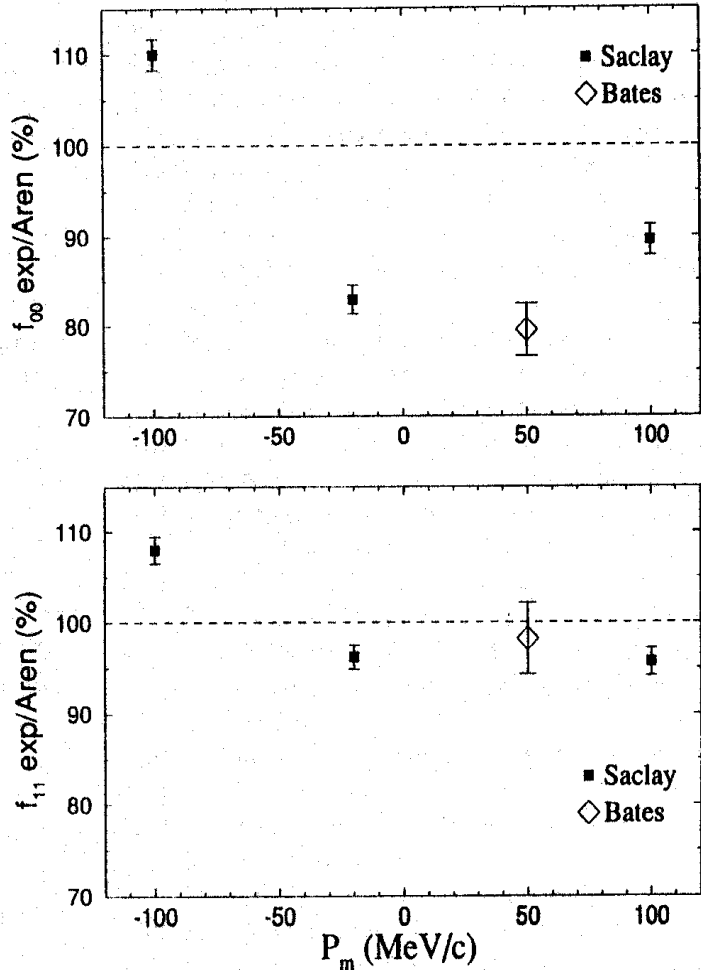


FIG. 1. Ratio of measured f_{00} and f_{11} structure functions to Arenhövel's calculation for this experiment and the Saclay experiment of Ducret *et al.* [6]. Only statistical errors are shown.

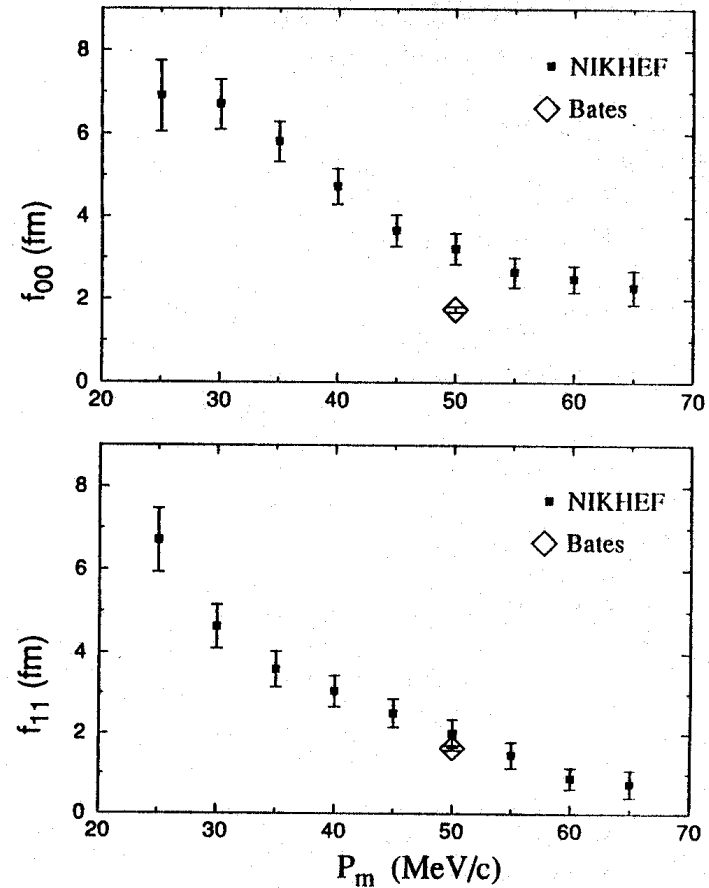
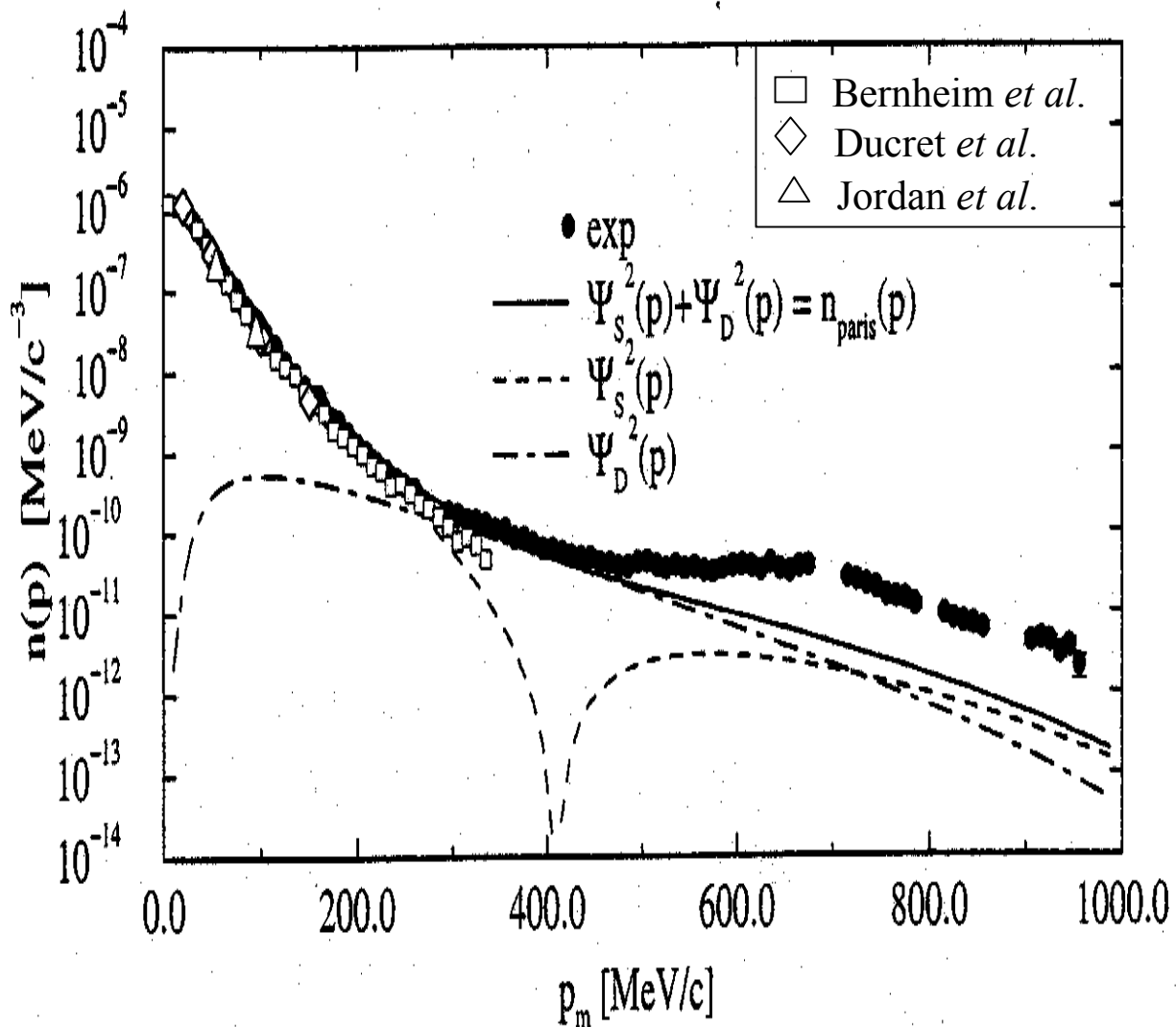


FIG. 2. Separated f_{00} and f_{11} structure functions for this experiment and the NIKHEF experiment of van der Schaer *et al.* [5]. The NIKHEF data ($q = 380$ MeV/c) are averaged over 5 MeV/c bins in p_m . The Bates data ($q = 400$ MeV/c) are averaged over the range of 30 to 70 MeV/c in p_m . Only statistical errors are shown.

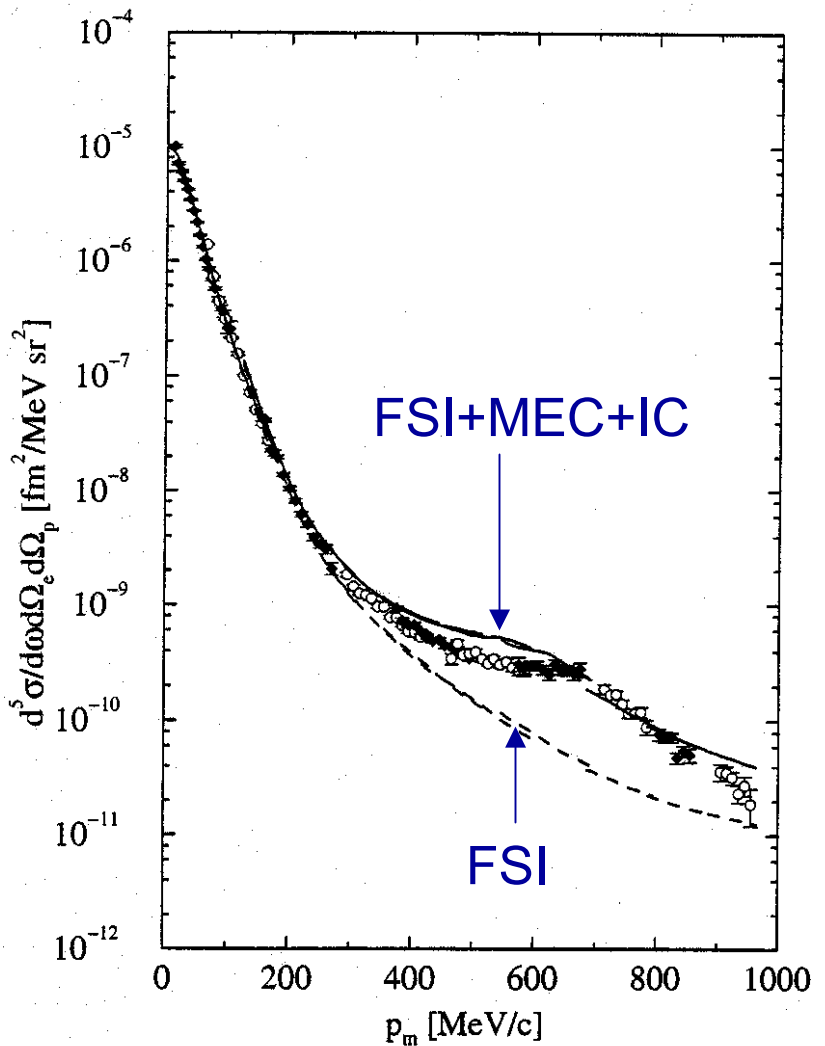
D. Jordan *et al.*, Phys. Rev. Lett. **76**, 1579 (1996).



Blomqvist *et al.*
data cover
kinematics
beyond Δ .
Also neutron
exchange
diagram
important.

MAMI
Mainz,
Germany

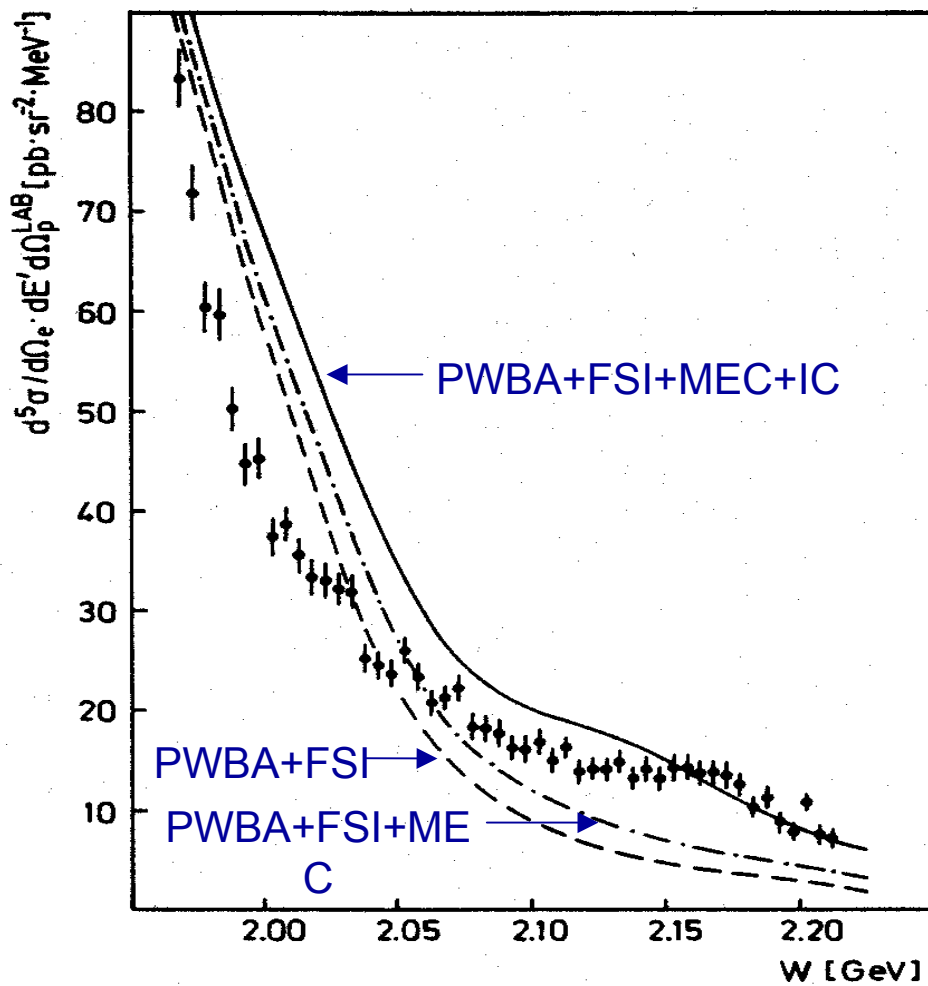
K.I. Blomqvist *et al.*, Phys. Lett. B 424, 33 (1998).



K.I. Blomqvist *et al.*, Phys. Lett. B **424**, 33 (1998).

Calculations: H. Arenhövel

$^2\text{H}(\text{e},\text{e}'\text{p})$ $Q^2=0.23 \text{ GeV}^2$ near Δ

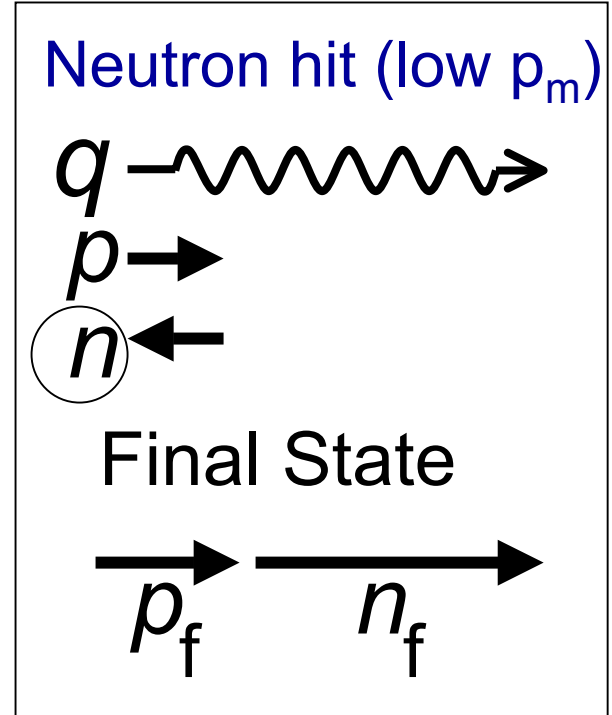
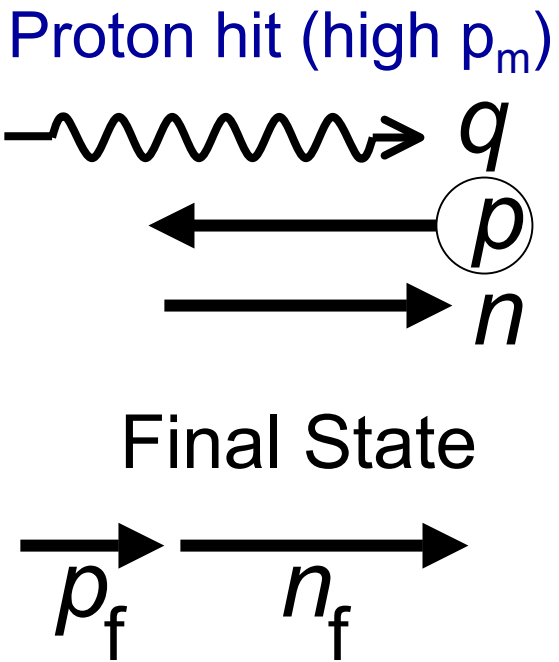
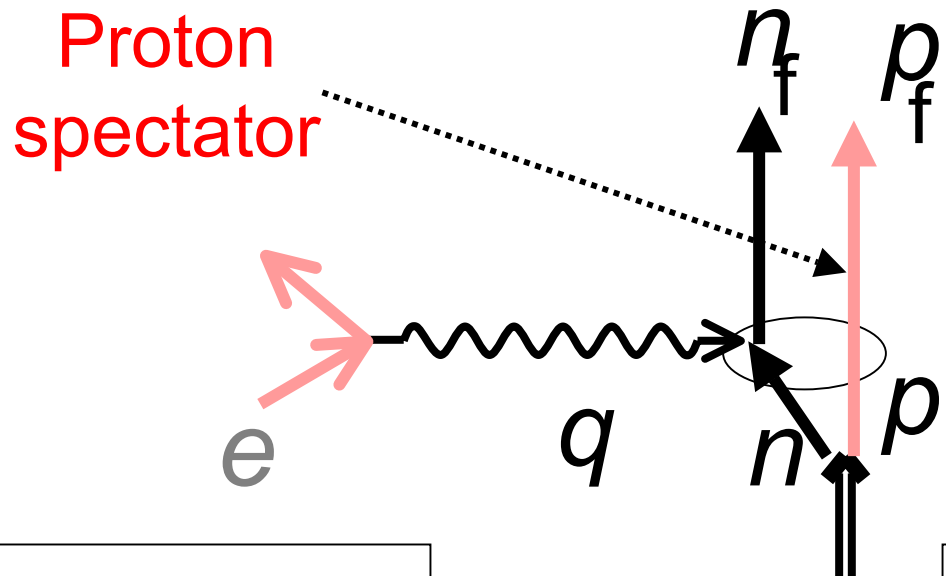


Δ clearly
important

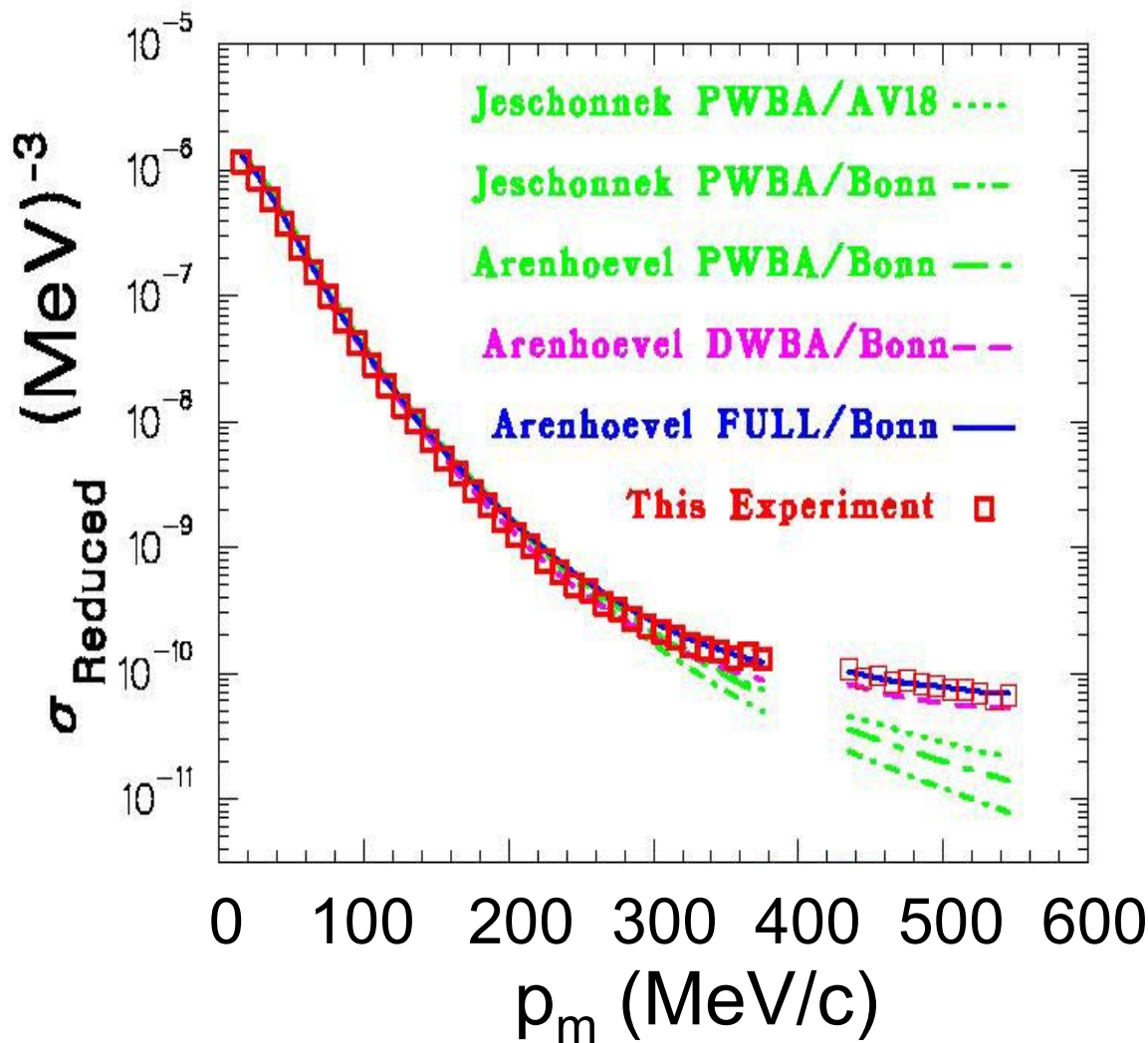
Bonn Electron
Synchrotron,
Germany

H. Breuker *et al.*, Nucl. Phys. **A455**, 641 (1986).

Calculations: Leidemann and Arenhövel



$Q^2=0.67 \text{ GeV}^2$ Quasielastic



Large FSI
effects.

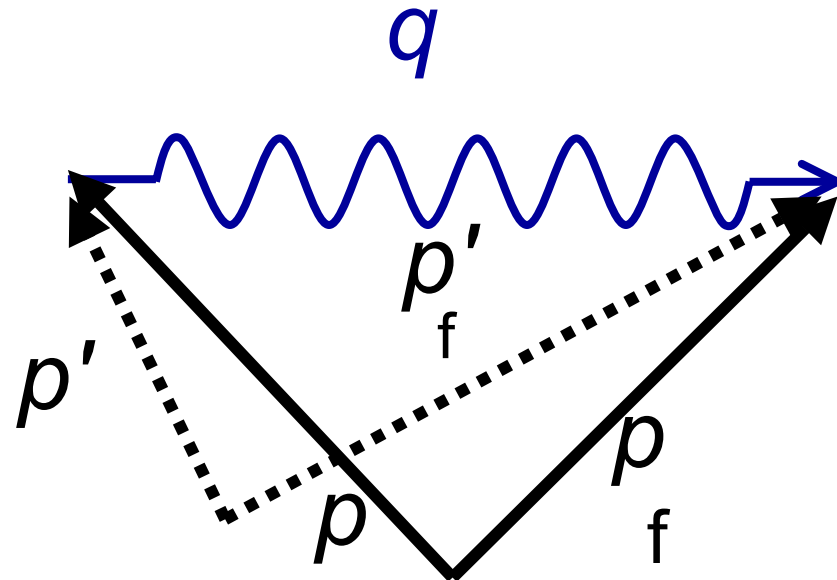
Also,
substantial
non-nucleonic
effects.

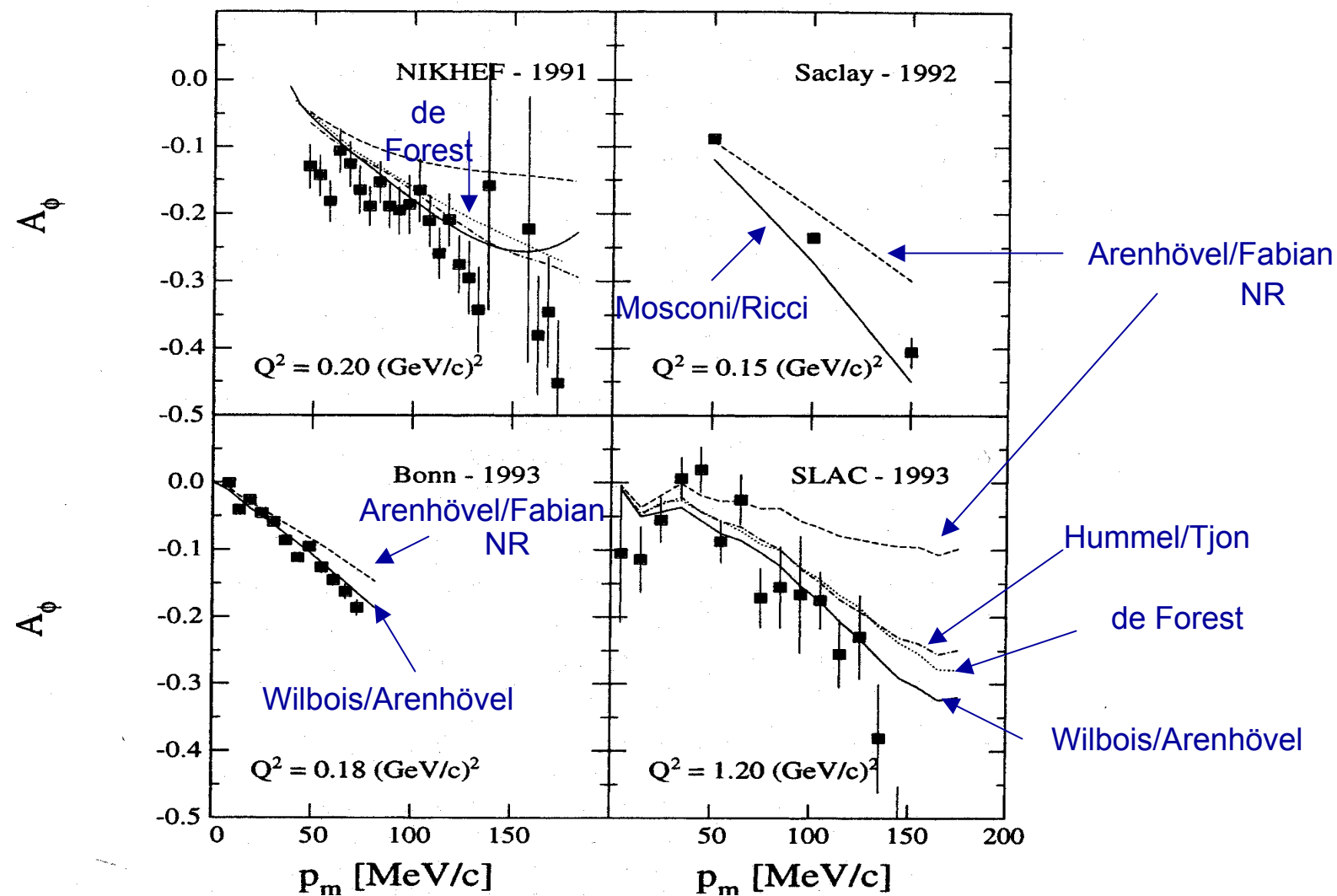
JLab
Hall A

P.E. Ulmer *et al.*, Phys. Rev. Lett. **89**, 062301 (2002).

Final State Interactions Can be LARGE

The diagram consists of two parts. At the top left, the word "actual" is written in a large, bold, black serif font. At the top right, the word "inferred" is also written in a large, bold, black serif font. Two thick black arrows point downwards from these words towards a yellow rectangular box. Inside this box, the mathematical inequality $p' < p$ is displayed in a large, black serif font.



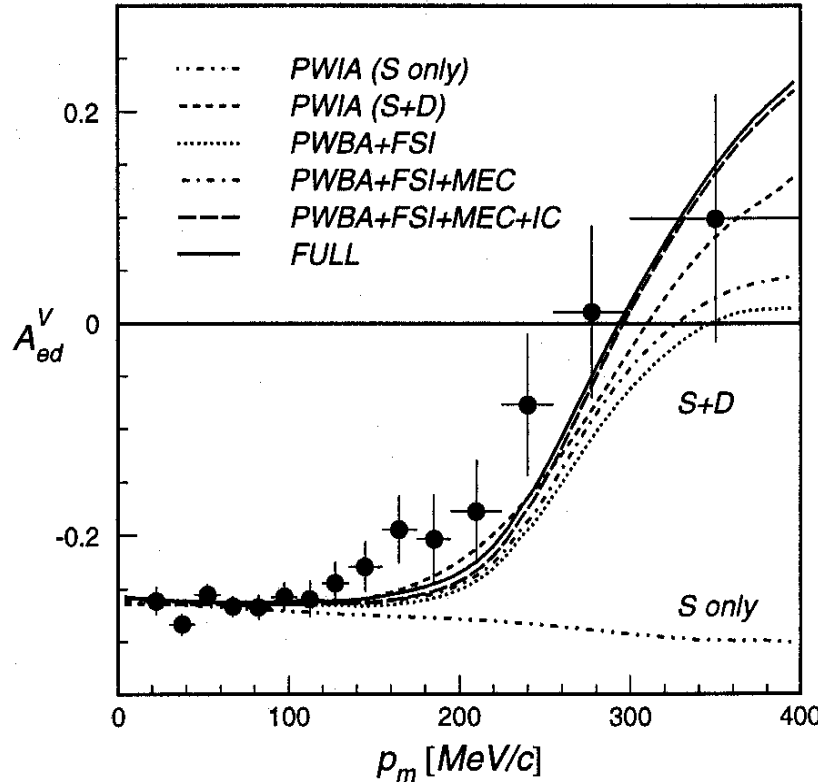


G. van der Steenhoven, Few-Body Syst. 17, 79 (1994).

What do all these data and curves suggest?

- Relativistic effects substantial in A_ϕ (and R_{LT}).
- de Forest “CC1” nucleon cross section gives same qualitative features as more complete calculations → here, relativity more related to nucleonic current, as opposed to deuteron structure.

$^2\vec{\text{H}}(\vec{e}, e' p)$



**D-state
important**

AmPS
NIKHEF-K
Amsterdam

I. Passchier *et al.*, Phys. Rev. Lett. **88**, 102302 (2002).

$$\sigma = \sigma_0 \left[1 + P_1^d A_d^V + P_2^d A_d^T + h \left(A_e + P_1^d \boxed{A_{ed}^V} + P_2^d A_{ed}^T \right) \right]$$

**Lots more $d(e,e'p)$
data on the way!**

$^2\text{H}(\text{e}, \text{e}'\text{p})\text{n}$ E01-020 Hall A

Perpendicular: R_{LT}

$Q^2 : 0.80, 2.10, 3.50 \text{ (GeV/c)}^2$

$x=1: p_m$ from 0 to $\pm 0.5 \text{ GeV/c}$

Parallel/Anti-parallel

$Q^2 : 2.10 \text{ (GeV/c)}^2$

vary $x: p_m$ from 0 to 0.5 GeV/c

Neutron angular distribution

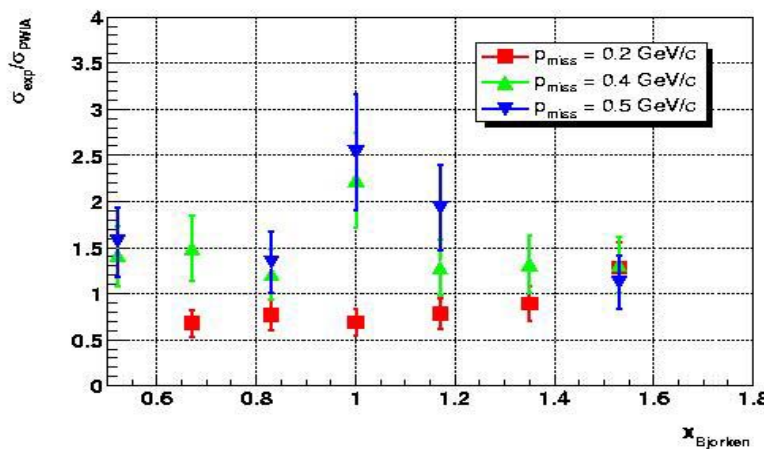
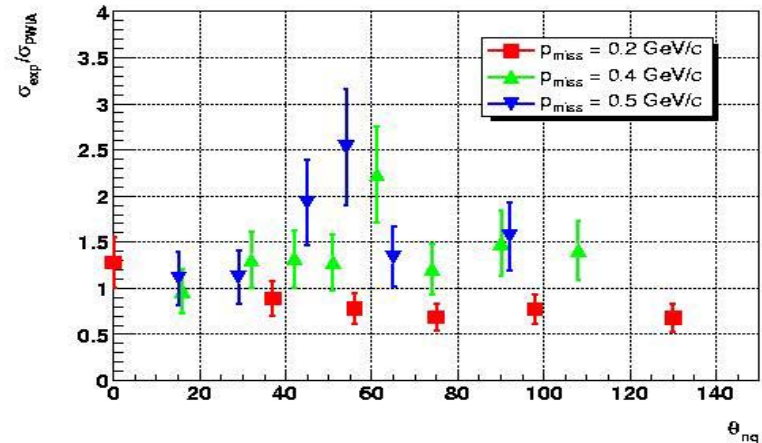
$Q^2 : 0.80, 2.10, 3.50 \text{ (GeV/c)}^2$

$$Q^2 = 0.8 \text{ (GeV/c)}^2$$

PRELIMINARY

20% error added to statistical error

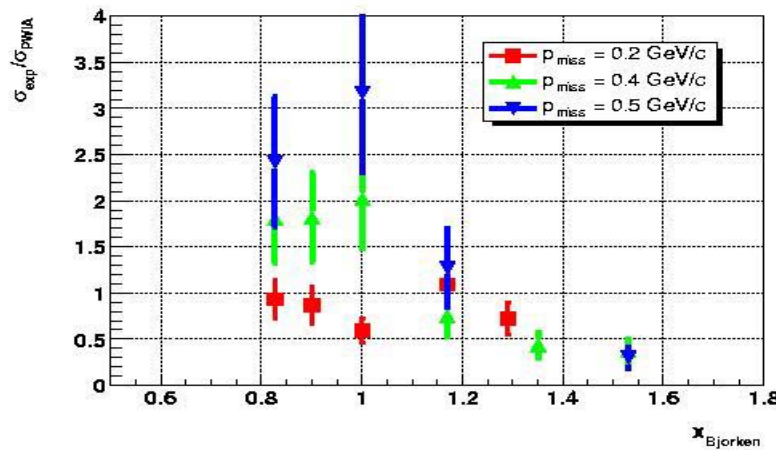
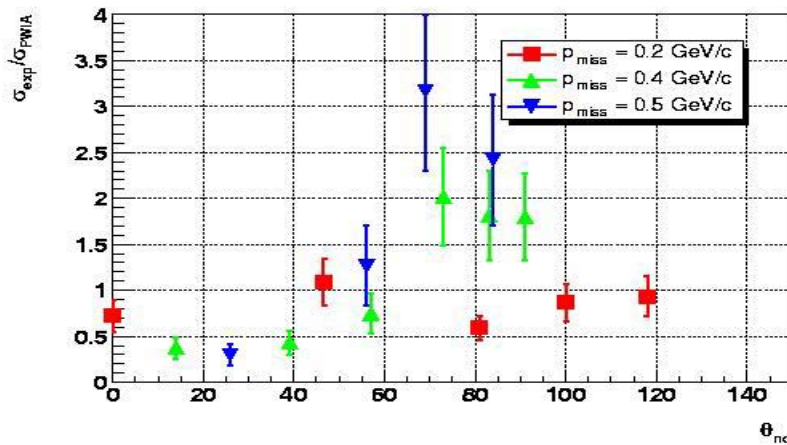
${}^2\text{H}(\text{e},\text{e}'\text{p})\text{n}$
E01-020 Hall A



$$Q^2 = 3.5 \text{ (GeV/c)}^2$$

PRELIMINARY

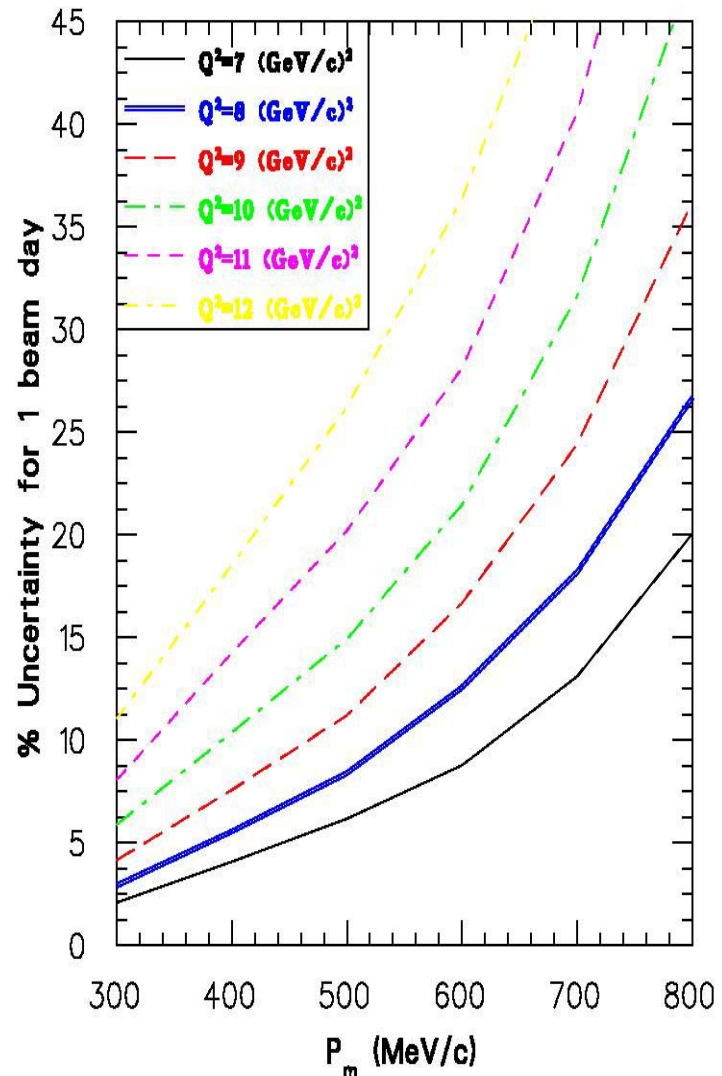
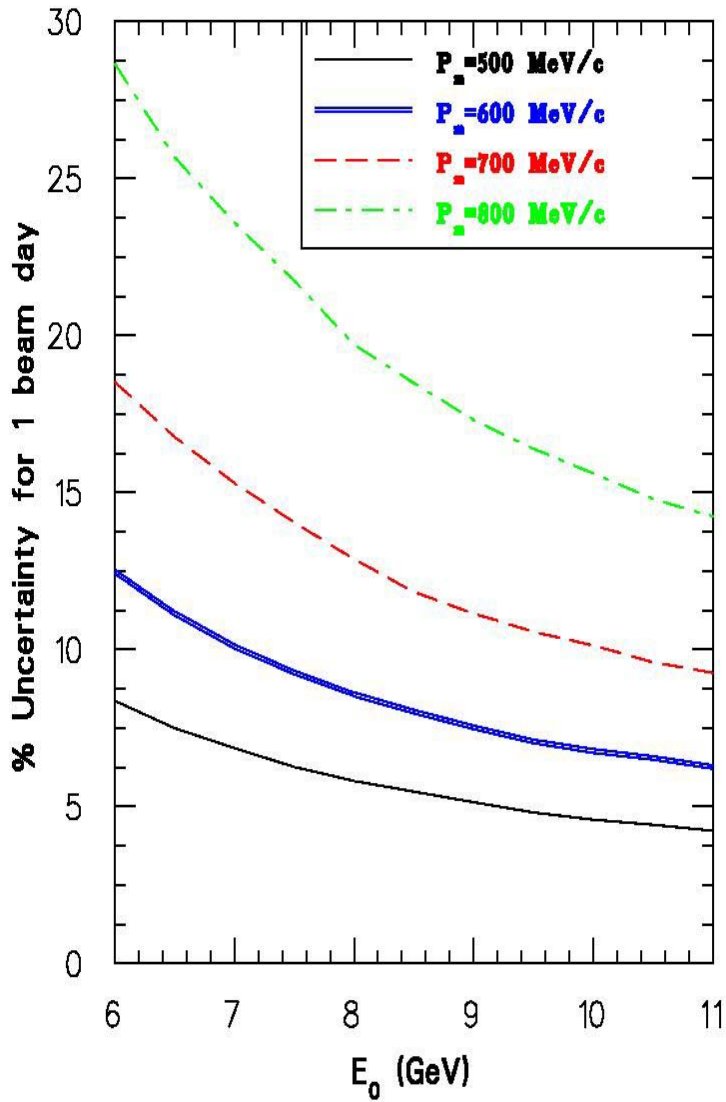
20% error added to statistical error



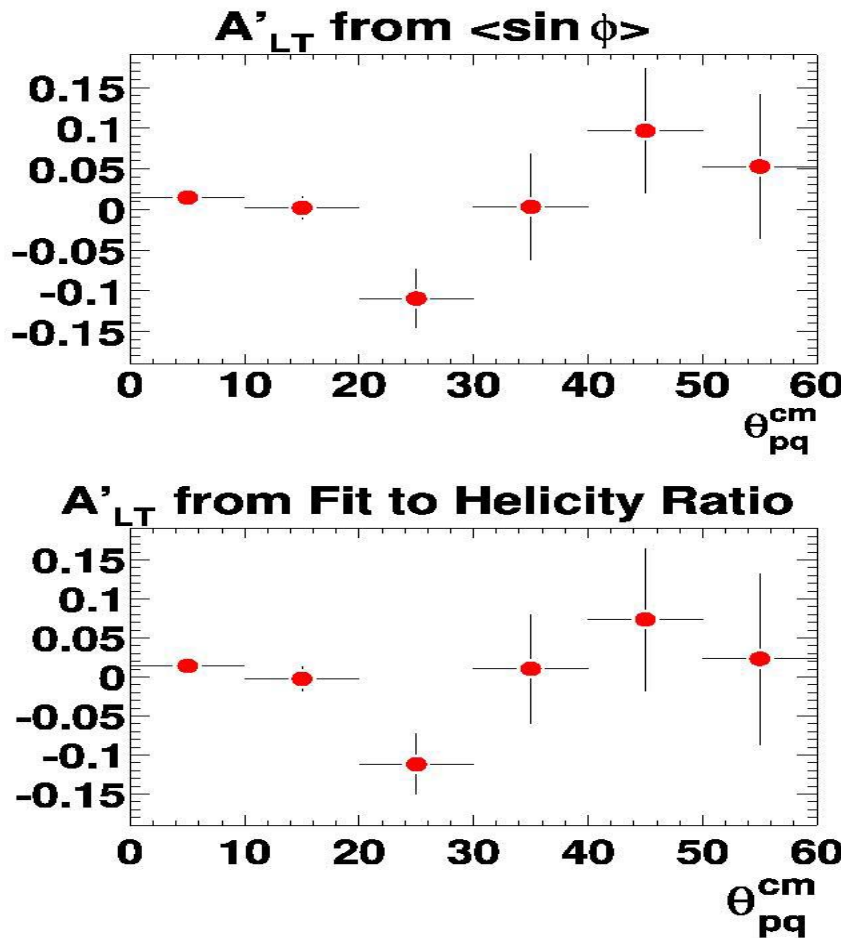
${}^2\text{H}(\text{e},\text{e}'\text{p})\text{n}$

E01-020 Hall A

$^2\text{H}(\text{e},\text{e}'\text{p})\text{n}$ with JLab 12 GeV upgrade



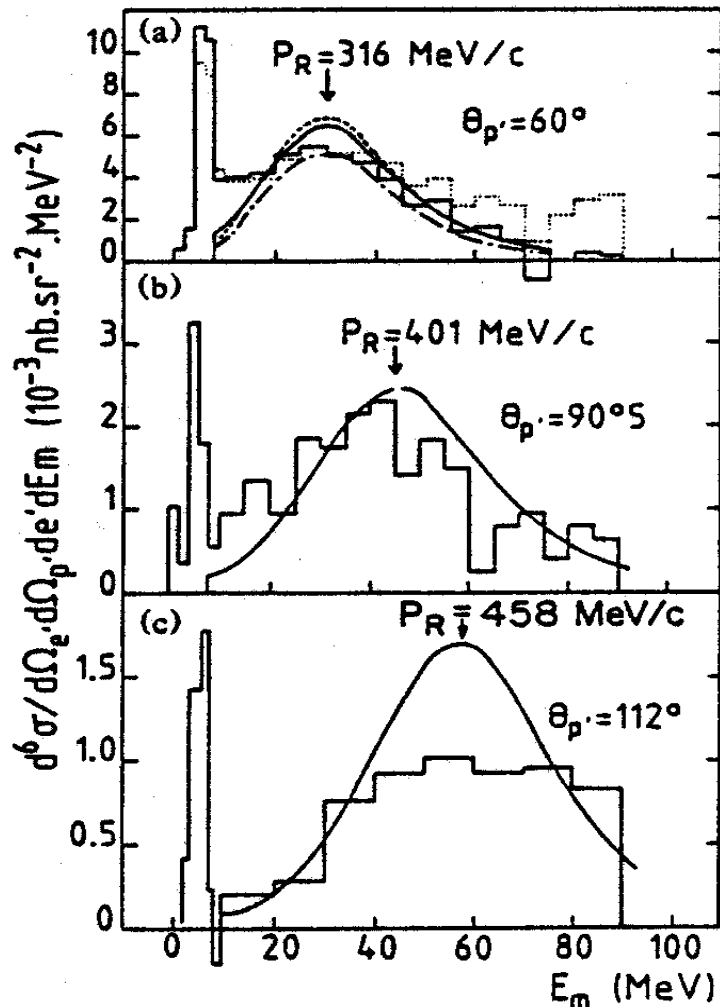
Preliminary Hall B E5 Data – ${}^2\text{H}(\text{e},\text{e}'\text{p})$



Hall B data covers large range of Q^2 and excitation as well as ϕ coverage to separate R_{LT} , R_{LT}' and R_{TT} .

$^{3,4}\text{He}$

$^3\text{He}(e, e'p)$



C. Marchand *et al.*,
Phys. Rev. Lett. **60**, 1703 (1988).

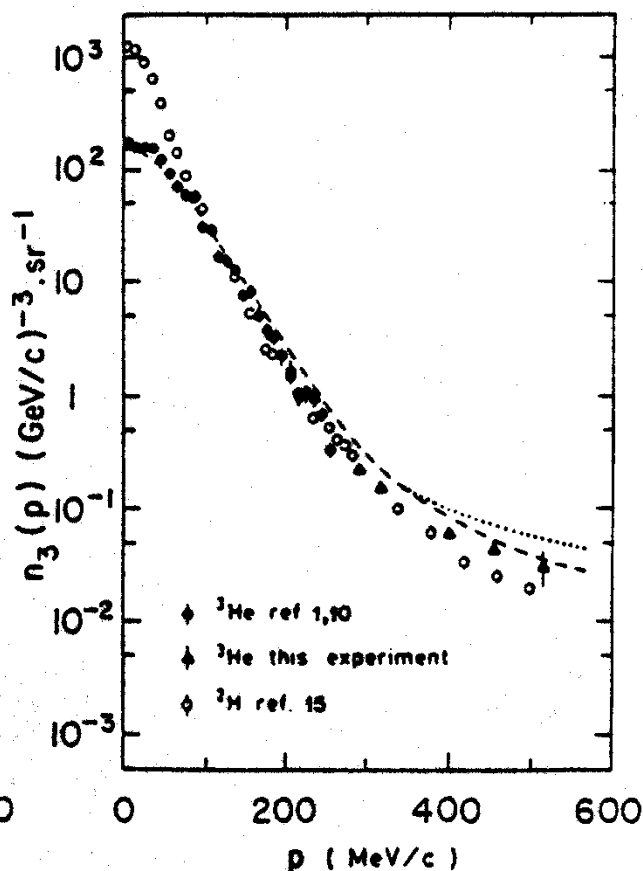
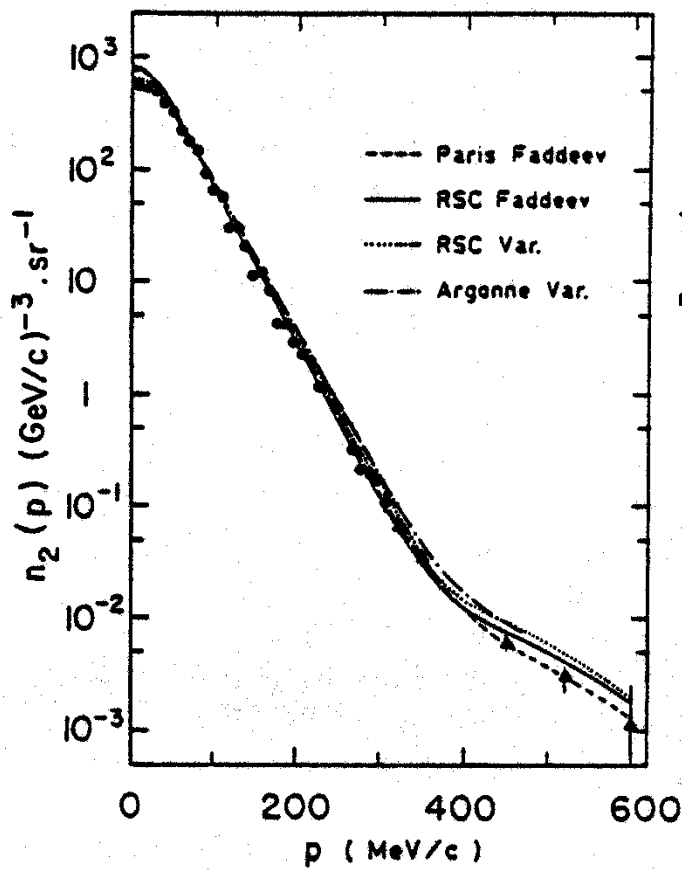
Calculations by Laget:
dashed=PWIA
dot-dashed=DWIA
solid=DWIA+MEC

Arrows indicate expected position for correlated pair.

Saclay
Linear
Accelerator

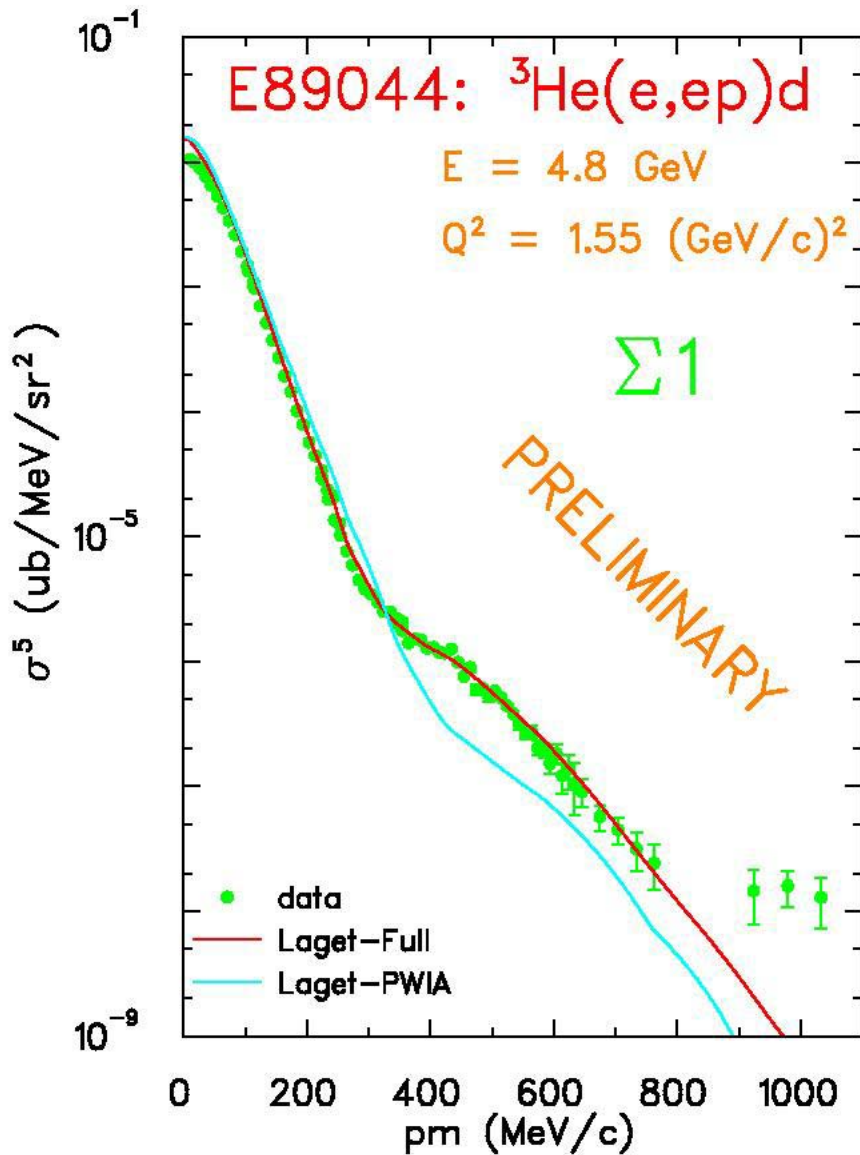
$^3\text{He}(e,e'p)d$

$^3\text{He}(e,e'p)np$



3BBU
similar
to
 $d \rightarrow np$

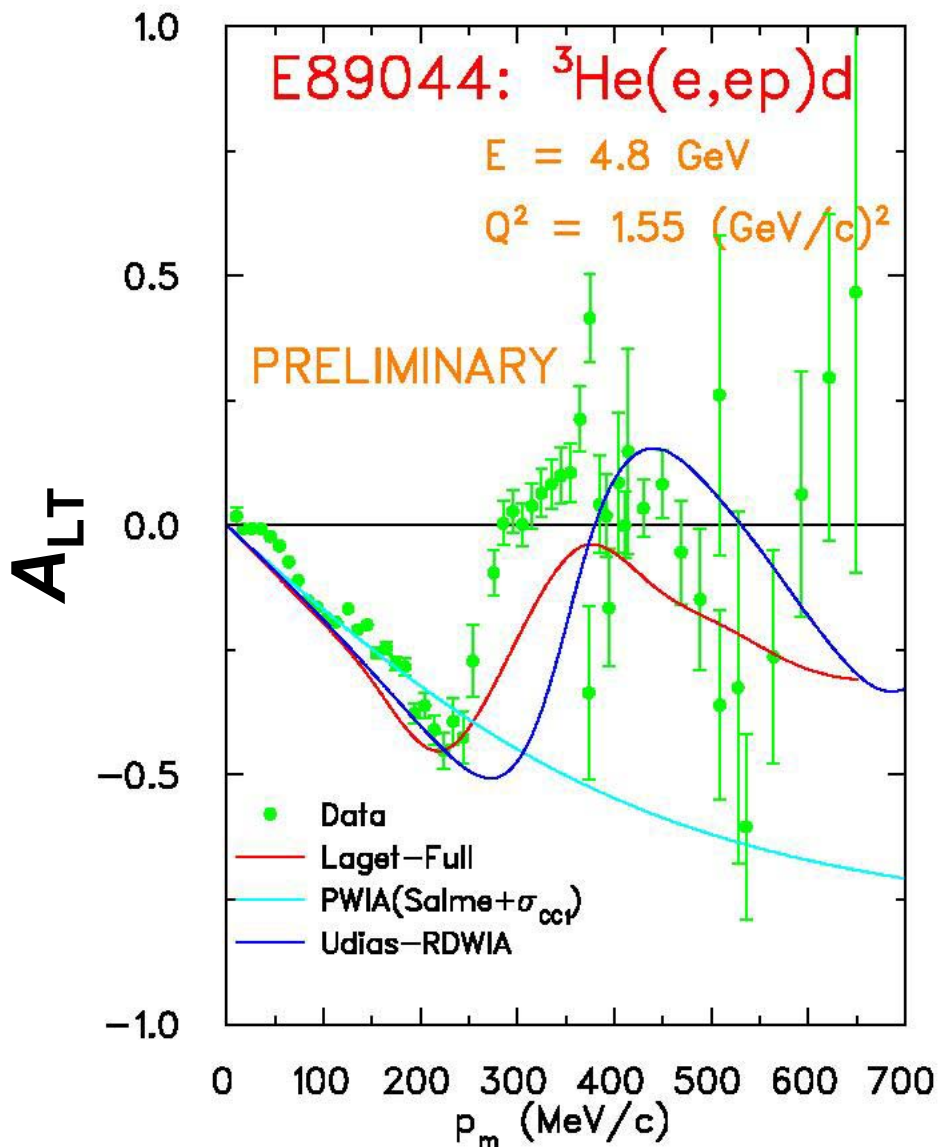
C. Marchand *et al.*, Phys. Rev. Lett. **60**, 1703 (1988).



Large effects
from FSI and
non-nucleonic
currents.

Highest p_m
shows excess
strength.

JLab
Hall A



General features reproduced but not at correct values of p_m .

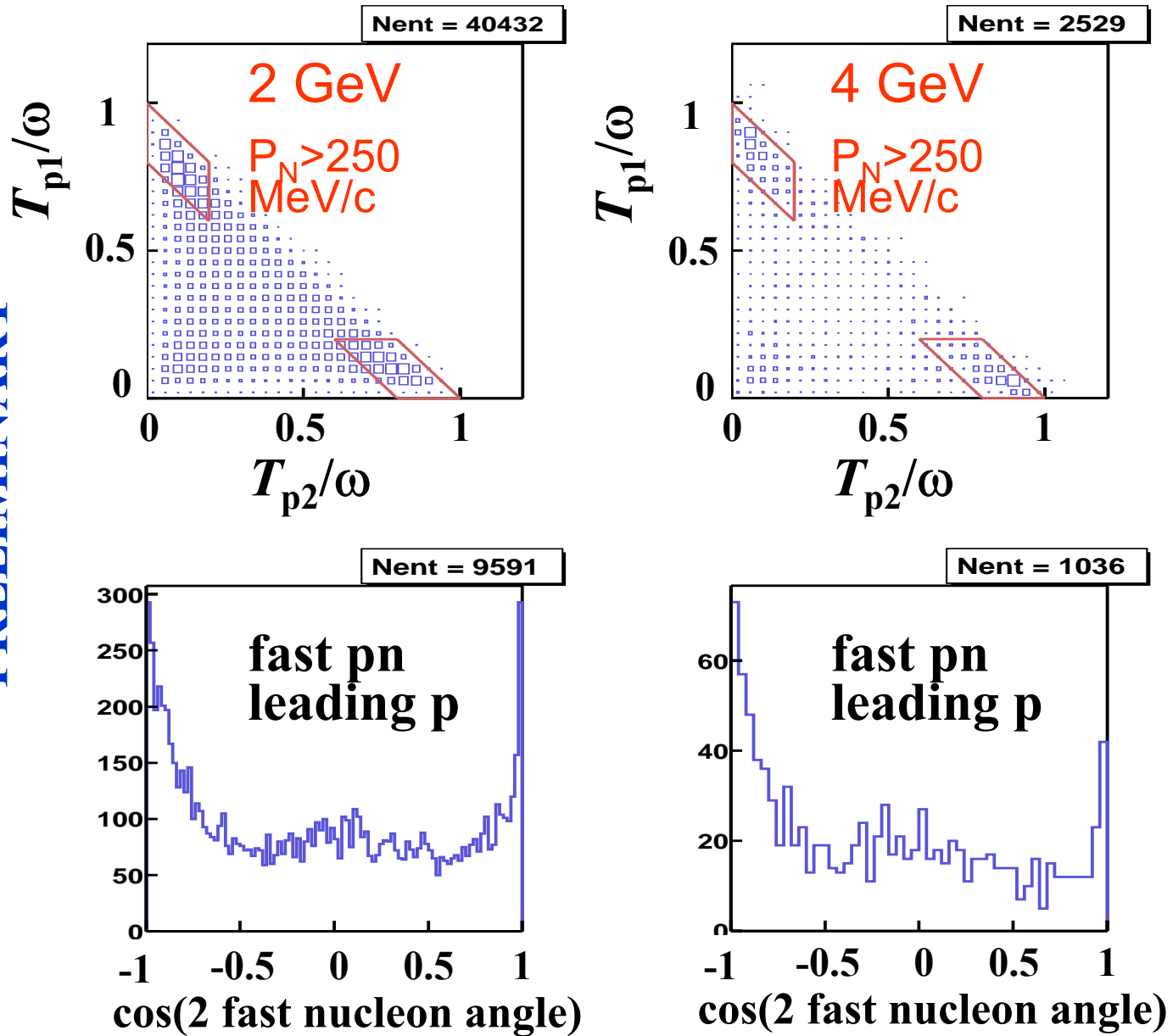
JLab
Hall A

The most direct way
to look for correlated
nucleons?

Detect both of them
→ JLab Hall B

PRELIMINARY

${}^3\text{He}(e,e'pp)n$ Hall B

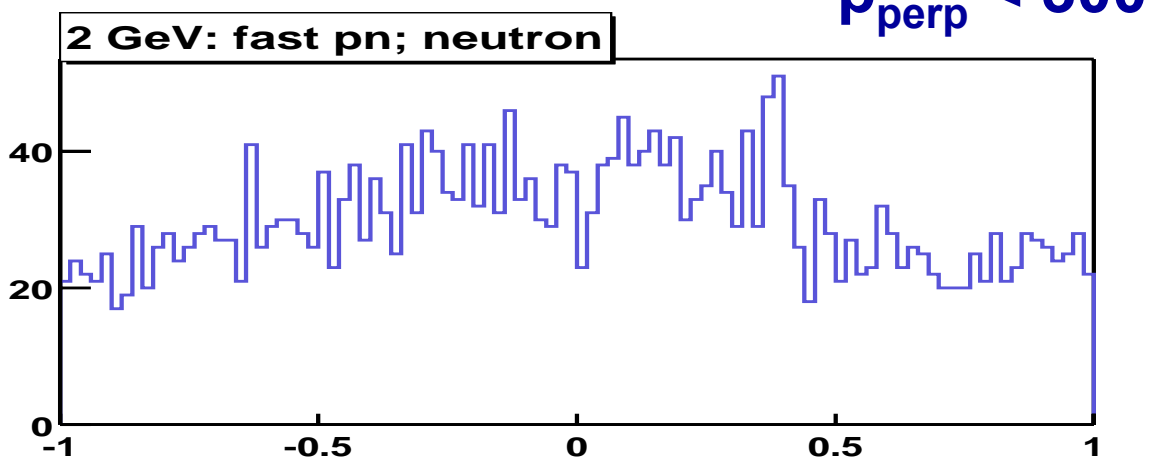


Hall B

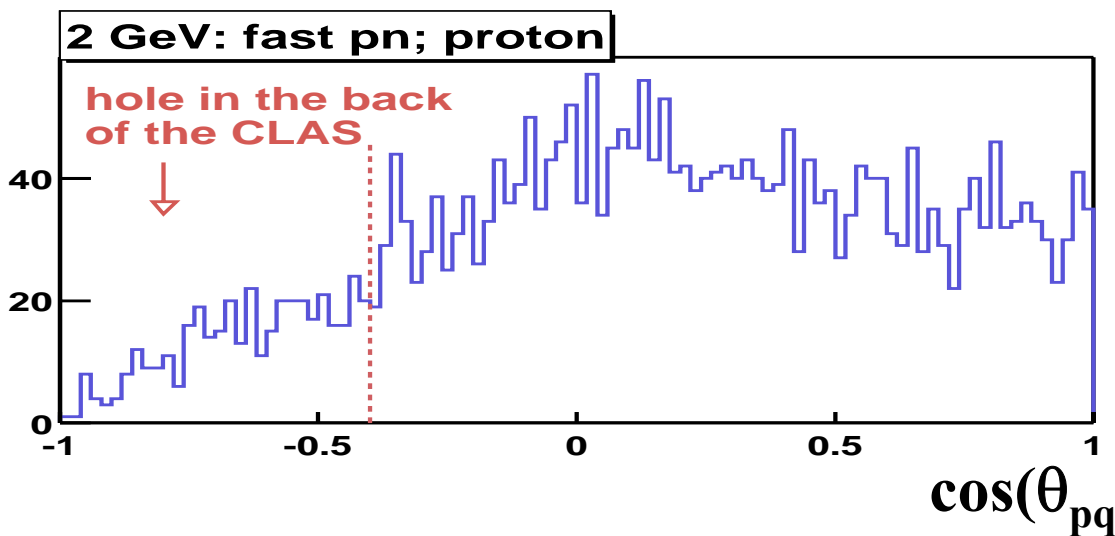
${}^3\text{He}(e,e'pp)n$ 2 GeV

$p_{\text{perp}} < 300 \text{ MeV}/c$

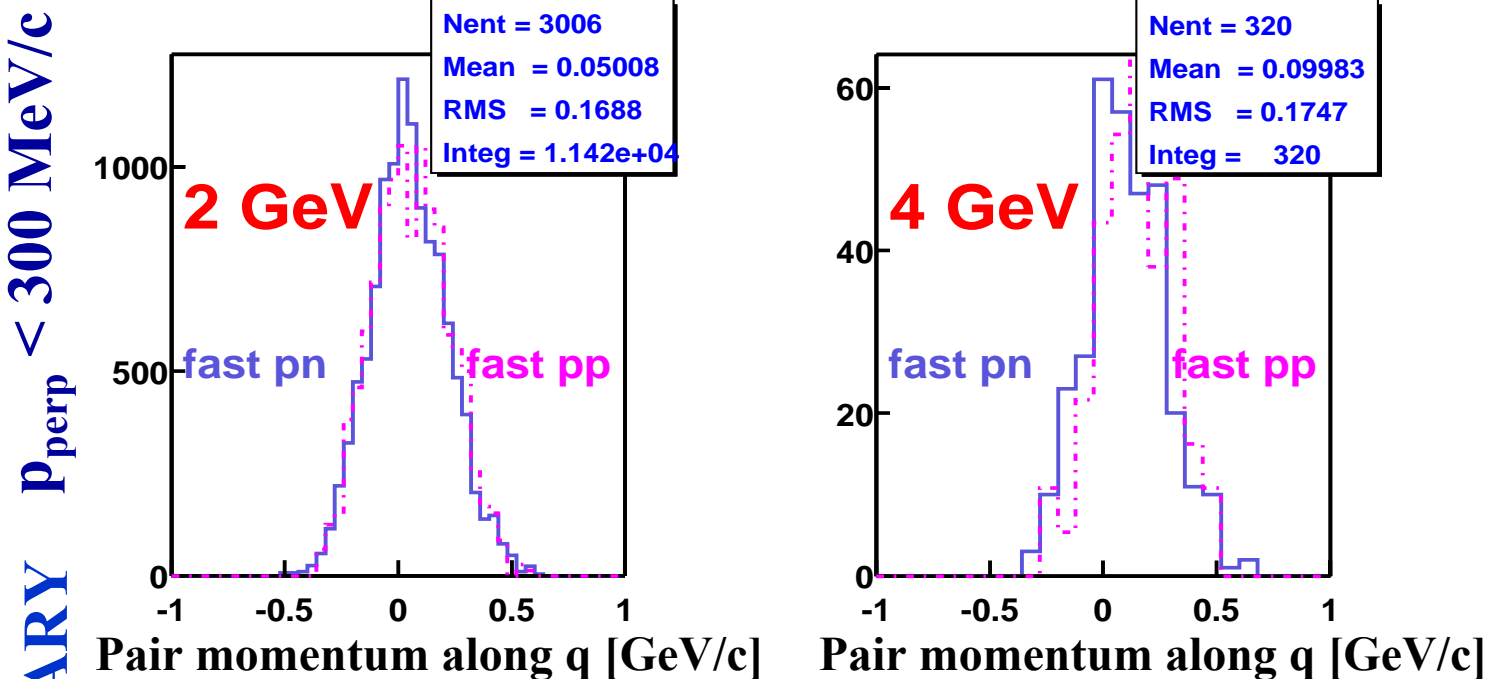
PRELIMINARY



Isotropic fast pairs $\cos(\theta_{nq})$
→ pair not involved in reaction.



Hall B



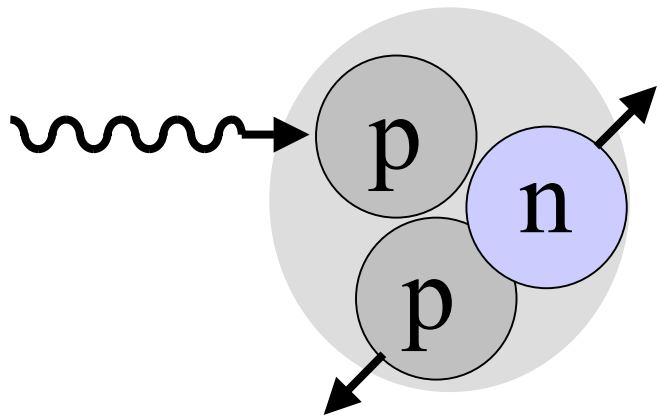
Small momentum along q
→ pair not involved in reaction.

Little Q^2 or isospin dependence.

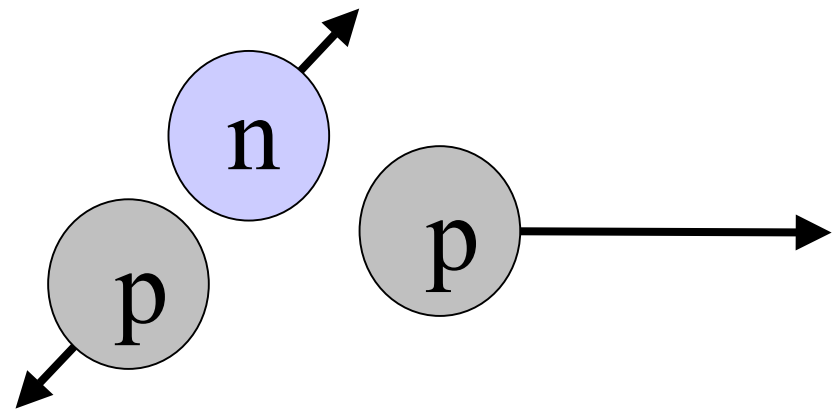
2 GeV has acceptance corrections

Direct evidence of NN correlations

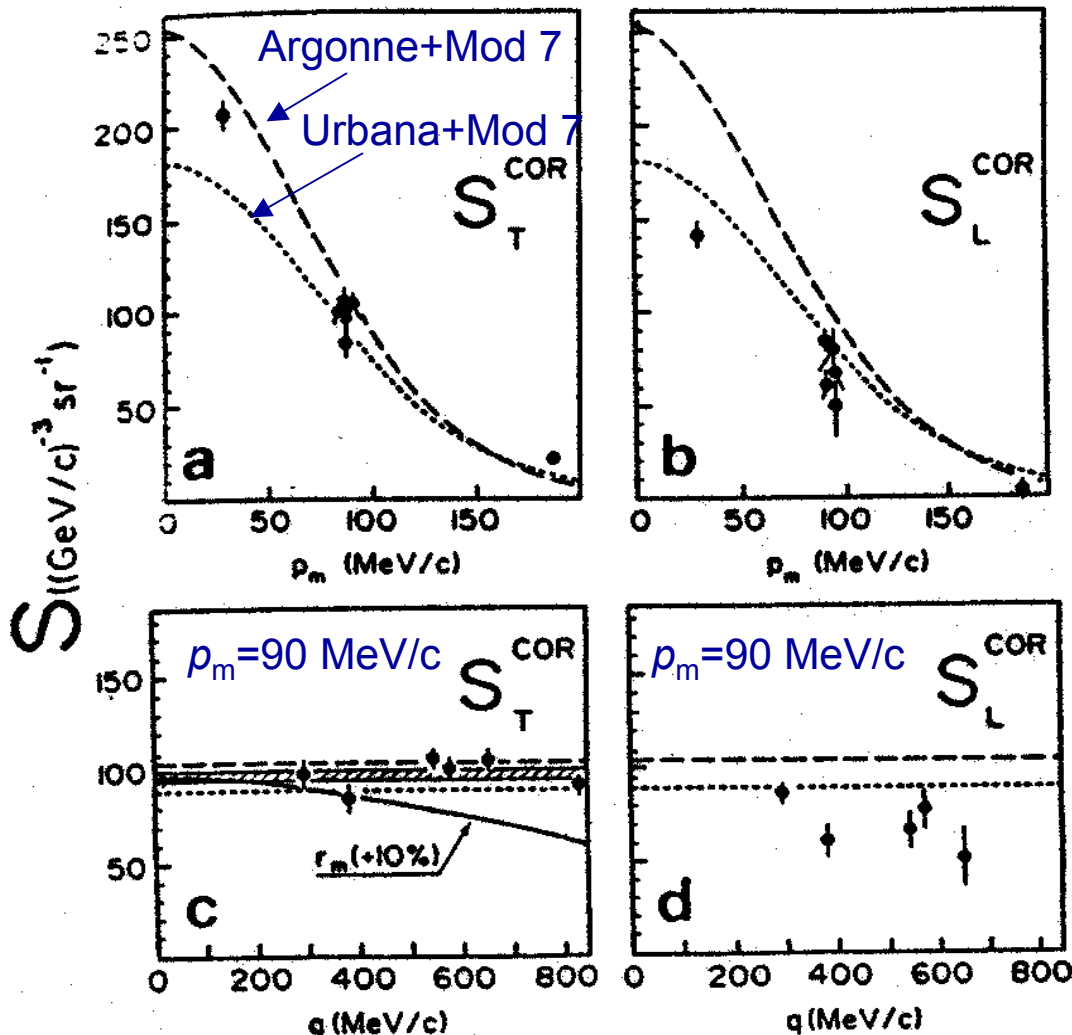
Before



After



${}^4\text{He}(\text{e}, \text{e}'\text{p}){}^3\text{H}$



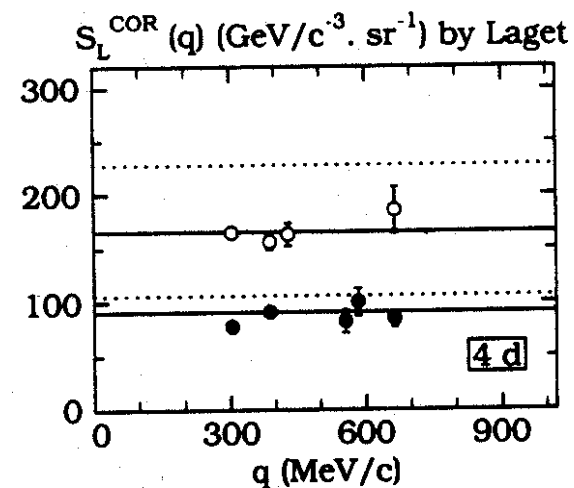
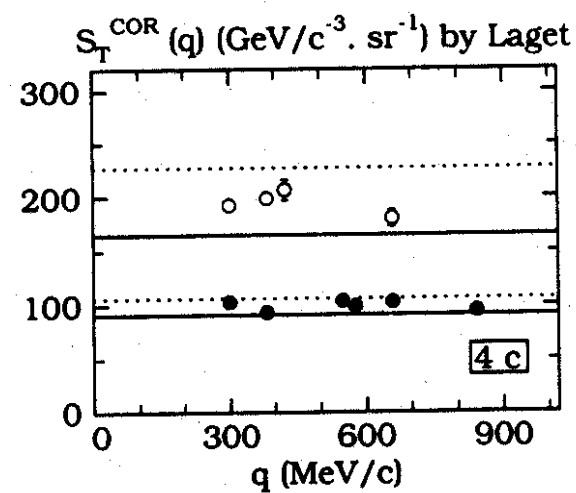
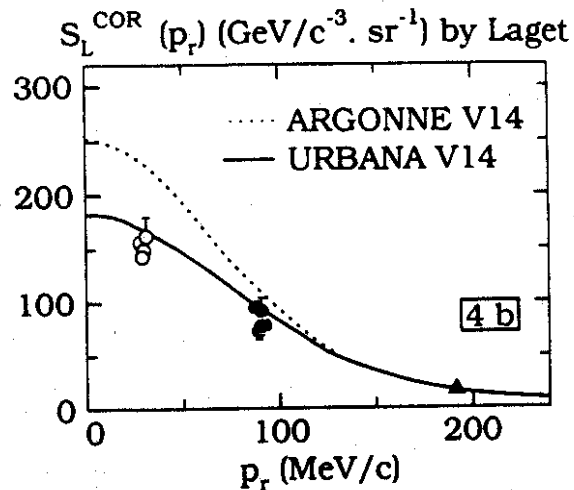
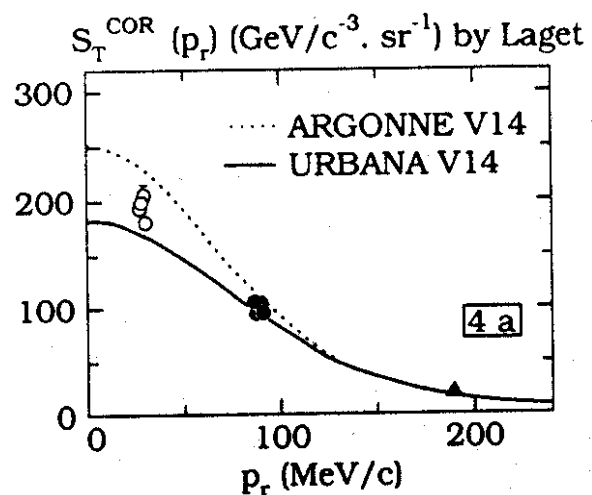
Data and calculations
“corrected” for
MEC+IC
(Laget).

Longitudinal
overpredicted.

Saclay

A. Magnon *et al.*, Phys. Lett. B **222**, 352 (1989).

$^4\text{He}(\text{e}, \text{e}'\text{p})^3\text{H}$

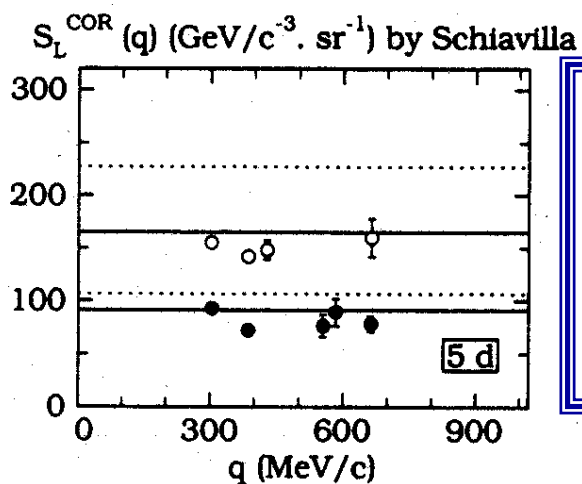
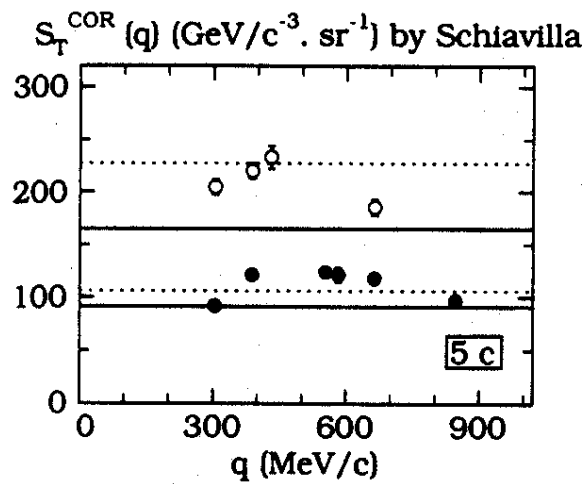
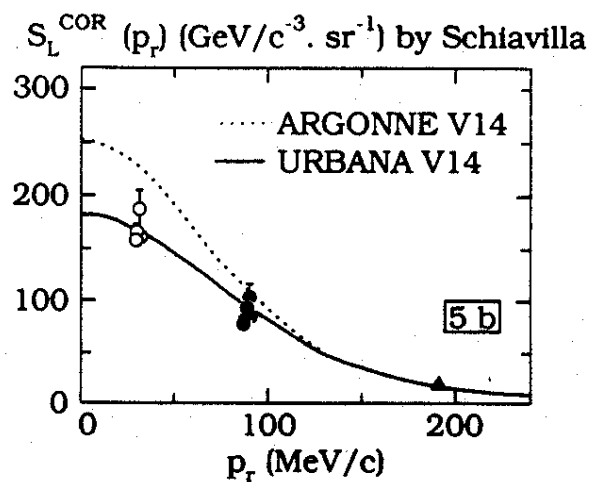
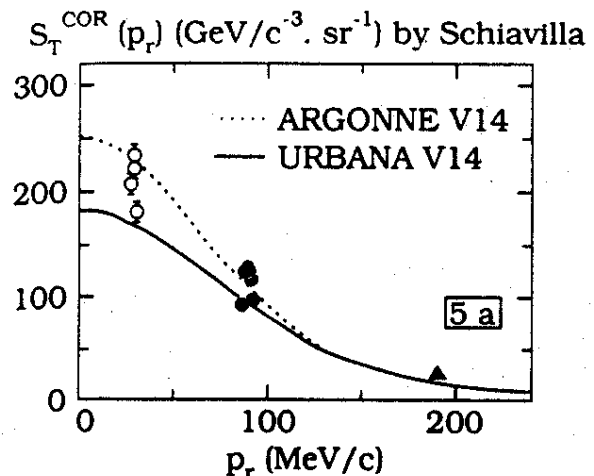


Calculations
predict q
dependence.

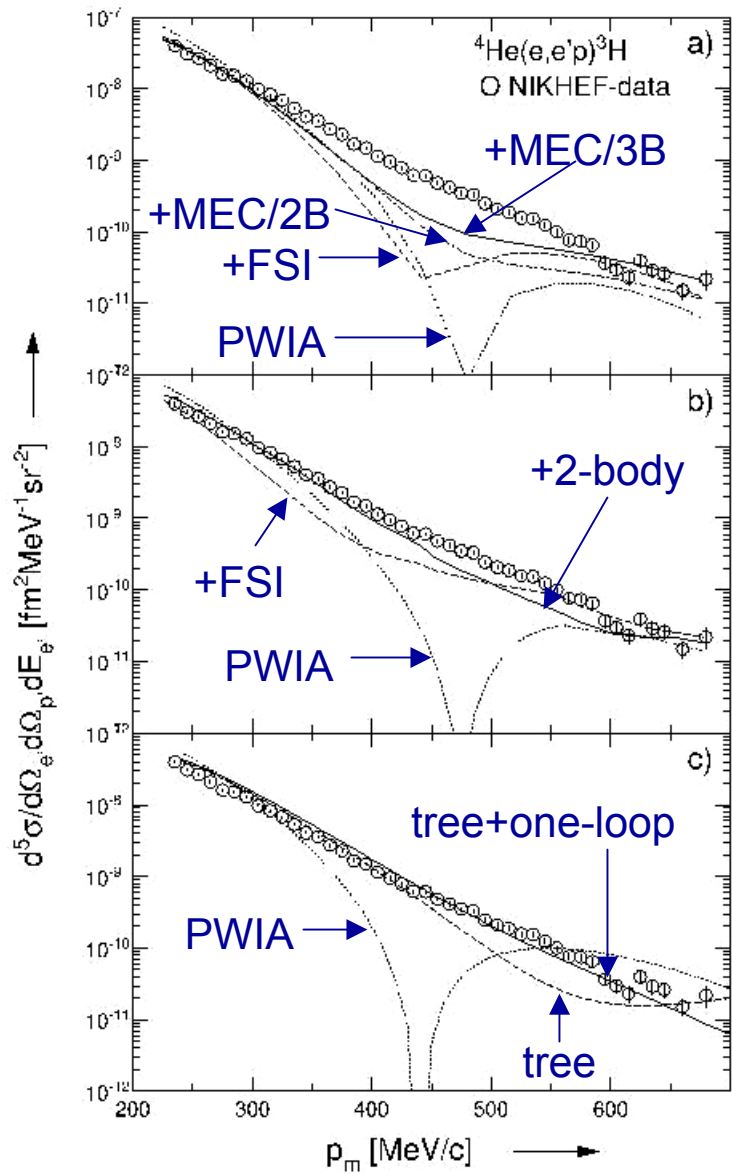
Saclay

J.E. Ducret *et al.*, Nucl. Phys. **A556**, 373 (1993).

${}^4\text{He}(\text{e}, \text{e}'\text{p}){}^3\text{H}$



Again,
calculations
predict q
dependence.



${}^4\text{He}(e, e'p){}^3\text{H}$

Laget

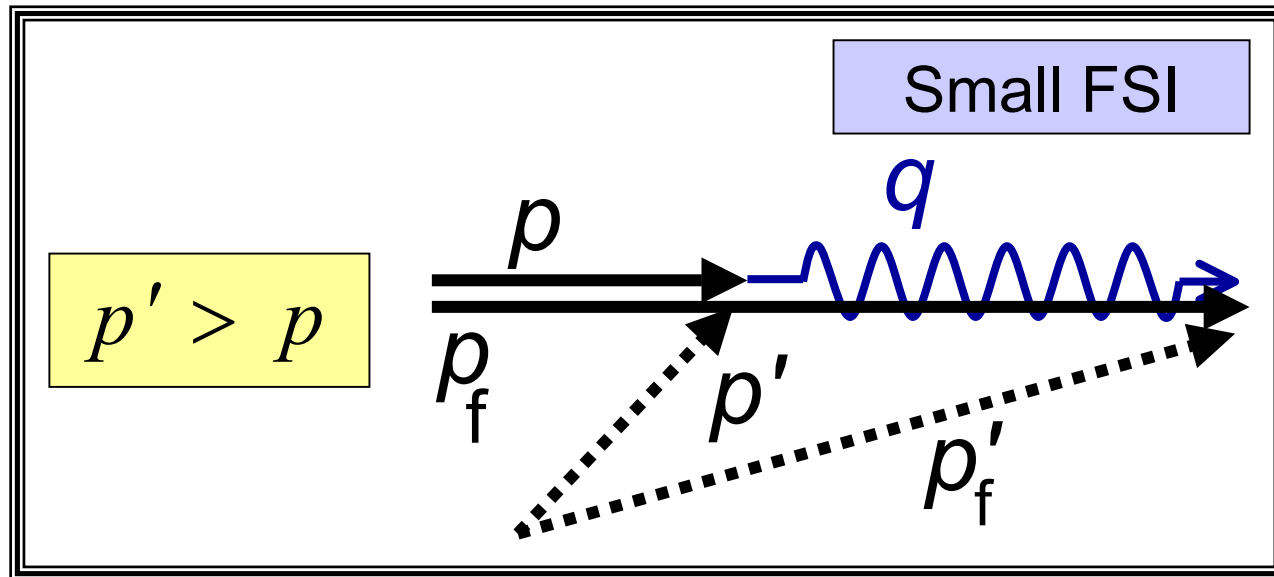
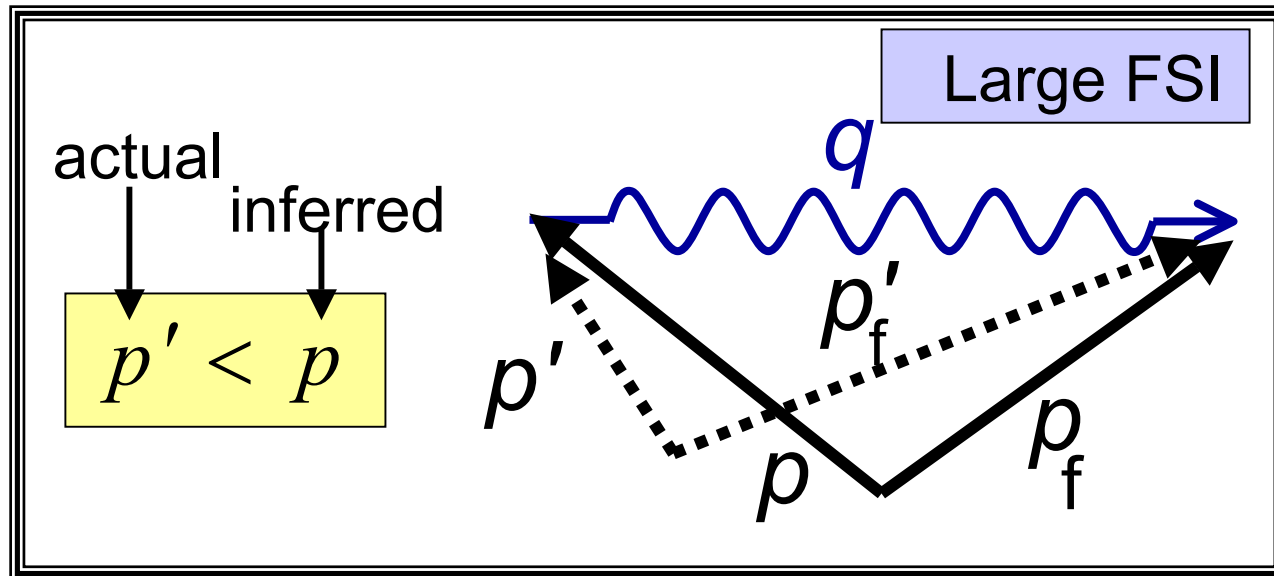
Minimum filled in by
FSI and
2&3-body
currents.

Schiavilla

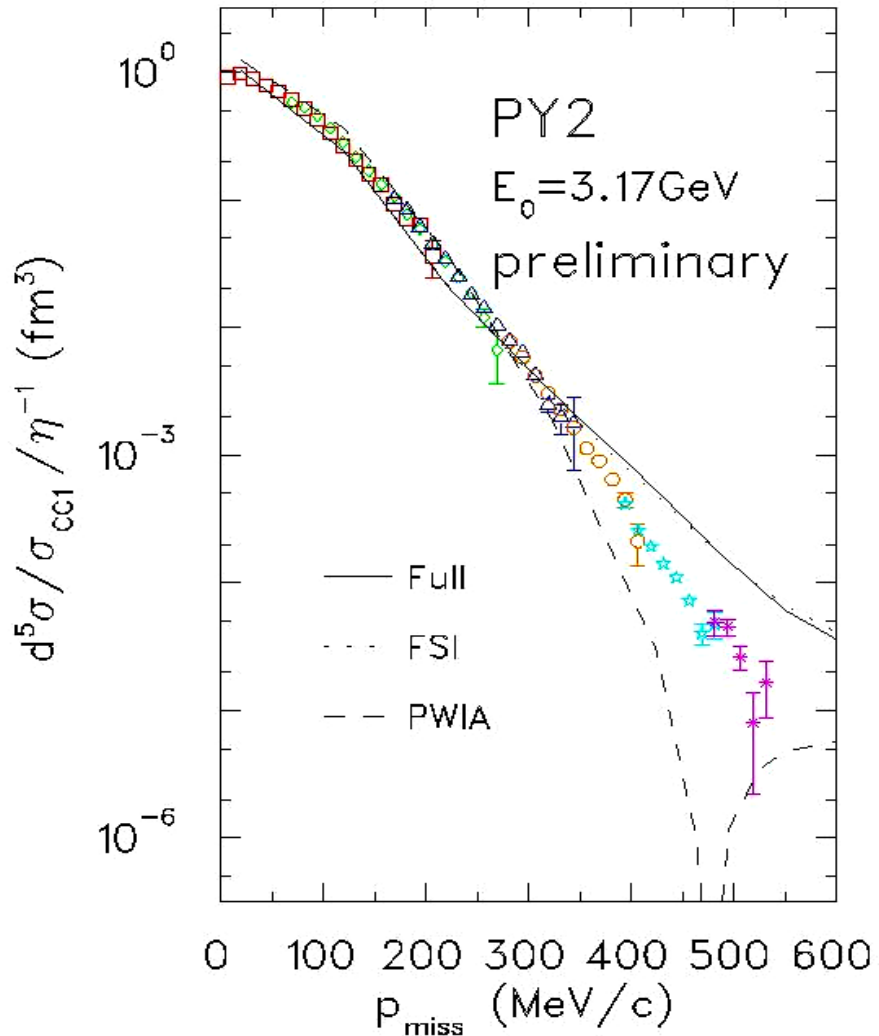
Nagorny

AmPS
NIKHEF-K
Amsterdam

FSI: dependence on kinematics



$^4\text{He}(\text{e},\text{e}'\text{p})^3\text{H}$



It looks like
the minimum
is filled in
here as well.

JLab Hall A Experiment E97-111, J. Mitchell, B. Reitz,
J. Templon, cospokesmen

Summary

- $(e,e'p)$ sensitive to single-particle aspects of nucleus, but ...
- More complicated physics is clearly important.
- Spectroscopic factors reduced compared to naïve shell model (including FSI corrections).
- Missing strength at least partly due to interaction currents: direct interaction with exchanged mesons or interaction with correlated pairs (spreads strength over ε_m).

Summary cont'd.

- After several decades of experimental and theoretical effort, there are still unanswered questions.
- What is the nature of the interaction of the virtual photon with the “nucleon”: medium and offshell effects?
- Handling FSI and other reaction currents still problematic, though realistic calculations are now available for the lighter systems.
- High energy program is underway, pushing to shorter distance scales, emphasizing relativistic effects, ...